DEVELOPMENT AND VALIDATION OF TWO-DIMENSIONAL DEPTH-AVERAGED FREE SURFACE FLOW SOLVER

A THESIS SUBMITTED TO
THE GRADUATE SCHOOL OF NATURAL AND APPLIED SCIENCES
OF
THE MIDDLE EAST TECHNICAL UNIVERSITY

BY

BURAK YILMAZ

IN PARTIAL FULFILLMENT OF THE REQUIREMENTS FOR THE DEGREE OF

MASTER OF SCIENCE

IN

THE DEPARTMENT OF CIVIL ENGINEERING

SEPTEMBER 2003

ABSTRACT

DEVELOPMENT AND VALIDATION OF TWO-DIMENSIONAL DEPTH-AVERAGED FREE SURFACE FLOW SOLVER

Yılmaz, Burak
M.Sc., Department of Civil Engineering
Supervisor: Assoc. Prof. Dr. İsmail AYDIN

September 2003, 101 pages

A numerical solution algorithm based on finite volume method is developed for unsteady, two-dimensional, depth-averaged shallow water flow equations. The model is verified using test cases from the literature and free surface data obtained from measurements in a laboratory flume. Experiments are carried out in a horizontal, rectangular channel with vertical solid boxes attached on the sidewalls to obtain free-surface data set in flows where three-dimensionality is significant. Experimental data contain both subcritical and supercritical states. The shallow water equations are solved on a structured, rectangular grid system. Godunov type solution procedure evaluates the interface fluxes using an upwind method with an exact Riemann solver. The numerical solution reproduces analytical solutions for the test cases successfully. Comparison of the numerical results with the experimental two-dimensional free surface data is used to illustrate the limitations of the shallow water equations and improvements necessary for better simulation of such cases.

Keywords: Free surface flows, shallow flows, depth-averaged equations, Godunov type solution, Riemann solvers

ÖZ

SERBEST YÜZEYLİ AKIMLARDA İKİ-BOYUTLU DERİNLİK ORTALAMALI DENKLEMLERİN ÇÖZÜMÜ İÇİN YAZILIM GELİŞTİRİLMESİ VE DOĞRULANMASI

Yılmaz, Burak
Yüksek Lisans, İnşaat Mühendisliği Bölümü
Tez Danışmanı: Doç. Dr. İsmail AYDIN

Eylül 2003, 101 sayfa

Zamanla değişen, iki boyutlu, derinlik-ortalamalı sığ su akım denklemleri için sonlu hacim metodunu temel alan sayısal çözüm algoritması geliştirilmiştir. Model, literatürden test problemleri ve laboratuar kanalından elde edilen serbest yüzey verileri kullanılarak sınanmıştır. Deneyler üç boyutluluğu öne çıkan serbest yüzeyli akımlardan veri elde etmek için yan duvarlarına düşey kutular yerleştirilmiş dikdörtgen kesitli, yatay bir kanalda gerçekleştirilmiştir. Deneysel veriler hem kritiküstü hem de kritikaltı durumları içermektedir. Sığ su denklemleri; sıralı, dikdörtgen ızgara sistemi üzerinde çözülmüştür. Godunov tipi çözüm prosedürü ara-yüzey akılarını rüzgar yönü metodu kullanarak tam Riemann çözücüsüyle hesaplamaktadır. Mevcut sayısal yaklaşım analitik çözümlü test problemlerini başarıyla çözmektedir. Sayısal çözümlerin iki-boyutlu deney verileri ile karşılaşırılması yapılarak sığ su denklemlerinin kullanımındaki sınırlamalara ve bu durumlar için gerekli iyileştirmelere işaret edilmiştir.

Anahtar Kelimeler: Serbest yüzeyli akımlar, sığ akımlar, derinlik-ortalamalı denklemler, Godunov tipi çözümler, Riemann çözücüler

ACKNOWLEDGEMENTS

I express my sincere appreciation to my supervisor Assoc. Prof. Dr. İsmail Aydın for his wise supervision throughout the research.

I am appreciative to the research assistants of the Hydromechanics Laboratory, especially Onur Dündar, İlker T. Telci and Özgür Uğraş Baran for their valuable comments and suggestions. Not being a hydraulics researcher Baran Yıldırım deserves thanks for his contribution and companion during overnight studies.

I am also grateful to the staff of the Hydromechanics Laboratory, Necla Çankaya, Turan Güney, Cengiz Tufaner, and the late Hüseyin Değirmenci, for their helps.

Very special thanks goes to F. Muazzez Şimşir for keeping me sane during this study and being concerned with me.

I would like to thank to my family for their moral support.

I shall be telling this with a sigh
Somewhere ages and ages hence:
Two roads diverged in a wood, and I—
I took the one less traveled by,
And that has made all the difference…
Robert Frost

TABLE OF CONTENTS

LIST OF FIGURES

LIST OF TABLES

LIST OF SYMBOLS

a	: Celerity
b	: Bottom coordinate
g	: Acceleration due to gravity
h	: Water depth
i	: Subscript for node number in x direction
j	: Subscript for node number in y direction
n	: Manning's roughness coefficient, superscript for time level
t	: Time
u	: Velocity component in x direction
v	: Velocity component in y direction
w	: Velocity component in z direction
x	: Coordinate direction, distance along the channel
y	: Coordinate direction, distance across the channel
z	: Coordinate direction, surface elevation or the depth
A	: Cross sectional area, Jacobian matrix of the flux vector
B	: Channel width
F	: Flux vector in x direction
$F_{i+1/2}$	: Flux vector in x direction at the cell interface
G	: Flux vector in y direction
L	: Subscript for left data state.
R	: Subscript for right data state.
S	: Source vector

S_f	: Friction term due to the bed roughness
S_o	: Friction term due to the bed slope
U	: Vector of conserved variables
W	: Vector of primitive variables
Δt	: Time step
Δx	: Spatial step
Δy	: Spatial step
ρ	: Density
*	: Subscript used for denoting star region

CHAPTER 1

INTRODUCTION

1.1 Introduction and Problem Statement

For many hydraulic engineering problems, the analysis of flow in open channels is required. Analytical and numerical solutions of the one-dimensional, open channel flow equations are very common and have been in use for many years. However, most of the flows in nature are three-dimensional and must be treated as three dimensional or at least two-dimensional for accurate predictions. Kuipers and Vreugdenhill (1973) developed one of the first mathematical models on two dimensional, depth-averaged equations using the finite difference scheme and since then several researchers focused on this concept using different techniques.

Successful simulation of flow requires numerical methods capable of taking into account rapidly varying topography, bed roughness of different scales, vegetation, arbitrarily shaped flow obstructions, free surface and variations of bed boundaries which must be determined as a part of the solution.

Flows with a free surface constitute a large scale of problems of scientific and practical interest, but computationally these problems are very challenging. The main difficulty of solving the whole problem is related with the free surface. Free surface is a boundary to satisfy boundary conditions but location of the boundary itself is unknown and so the domain on which the equations solved is unknown.

In the literature, there is considerable amount of publications on the solution of free surface problems considering many effects, such as bottom friction, viscous effects, side friction, Coriolis effect, etc. Numerical studies are conducted with finite difference methods, finite element methods, finite volume methods or other methods.

The shallow water wave equations have become a common tool for modeling many problems involving unsteady flows. The shallow water wave equations have their origins in the 19th century work of the French mathematician de Saint Venant (Cunge *et.al.*,1994). The most challenging feature of these equations is the permission of the equations to discontinuous solutions even the initial data are smooth. The non-linearity of the equations causes the analytical solution of the equations limited to special cases. As a result, numerical methods must be used to obtain solutions to practical problems, which include discontinuities in the solution. Until the last decade, widely used methods were the finite difference and finite element methods, but these methods created several problems. Finite difference methods do not conserve mass and require special techniques to overcome discontinuities and finite element methods conserve mass over the domain but not at each node; both methods produce oscillations at discontinuities. Finite volume methods solve the integral form of the equations in computational cells. In other words, mass and momentum are conserved in each cell even there is a discontinuity. Fluxes can be evaluated at cell faces that allow capturing wave propagation. These finite volume schemes have been developed for general hyperbolic conservation laws and have been used widely in gas dynamics with Euler equation. Recently, these techniques have been applied (Toro, 2001) to the solution of shallow water wave equations.

1.2 Scope and Objectives of the Thesis

The purpose of this study is to develop a basic solver for two-dimensional unsteady free surface flows and to test it in respect to numerical accuracy and satisfying different types of boundary conditions in flows where three-dimensionality is significant. The study consists of three stages; experimental measurement of surface profiles in a laboratory model, development of a numerical code and numerical computation of the surface profiles for the experimental cases and several test cases for which analytical solutions are available in the literature.

1.3 Description of the Thesis

This thesis is composed of five chapters. In Chapter 1, an introduction is given. In Chapter 2, the experimental setup is described. Experimental procedure and conducted experiments are presented. The numerical data of the experimental study are also provided in appendices.

In Chapter 3, the mathematical formulation of the problem and approaches to solve the system of equations are given. The governing equations that will be used in this study are derived in this section and the numerical methods used and the code developed are discussed.

In Chapter 4, the results from experimental and numerical studies are compared. Also the results of the numerical study with some test cases are given. In Chapter 5, the study is finalized by summarizing the basic conclusions of the work and recommendations for future studies.

CHAPTER 2

EXPERIMENTAL SET-UP AND MEASUREMENTS

2.1 Experimental Set-up

A horizontal rectangular water flume available in the Hydromechanics Laboratory of Civil Engineering Department of Middle East Technical University is modified (Fig. 2.1) to collect free surface data. The sidewalls are made of glass and the channel bottom is made of fiberglass. The channel is 0.67 m wide and 12 m long. In the working section, rectangular boxes of 0.10x0.25 m dimensions were attached on the sidewalls of the channel to create a three-dimensional flow field. When there is no control from the tail water, flow is supercritical and three-dimensional. When the tail water is raised to keep the flow as subcritical, two-dimensional treatment becomes more justified. The rectangular boxes are arranged in a staggered manner to generate asymmetrical, rapidly-varying water surface profiles. Strong vortex structures on horizontal plane around the sharp corners are observed. Water depth in the channel is affected by the tail-water control mechanism located at the end of the channel. A rectangular weir controls the flowrate given into the channel. Photographs showing different views of flow patterns in the channel are printed in Appendix A.

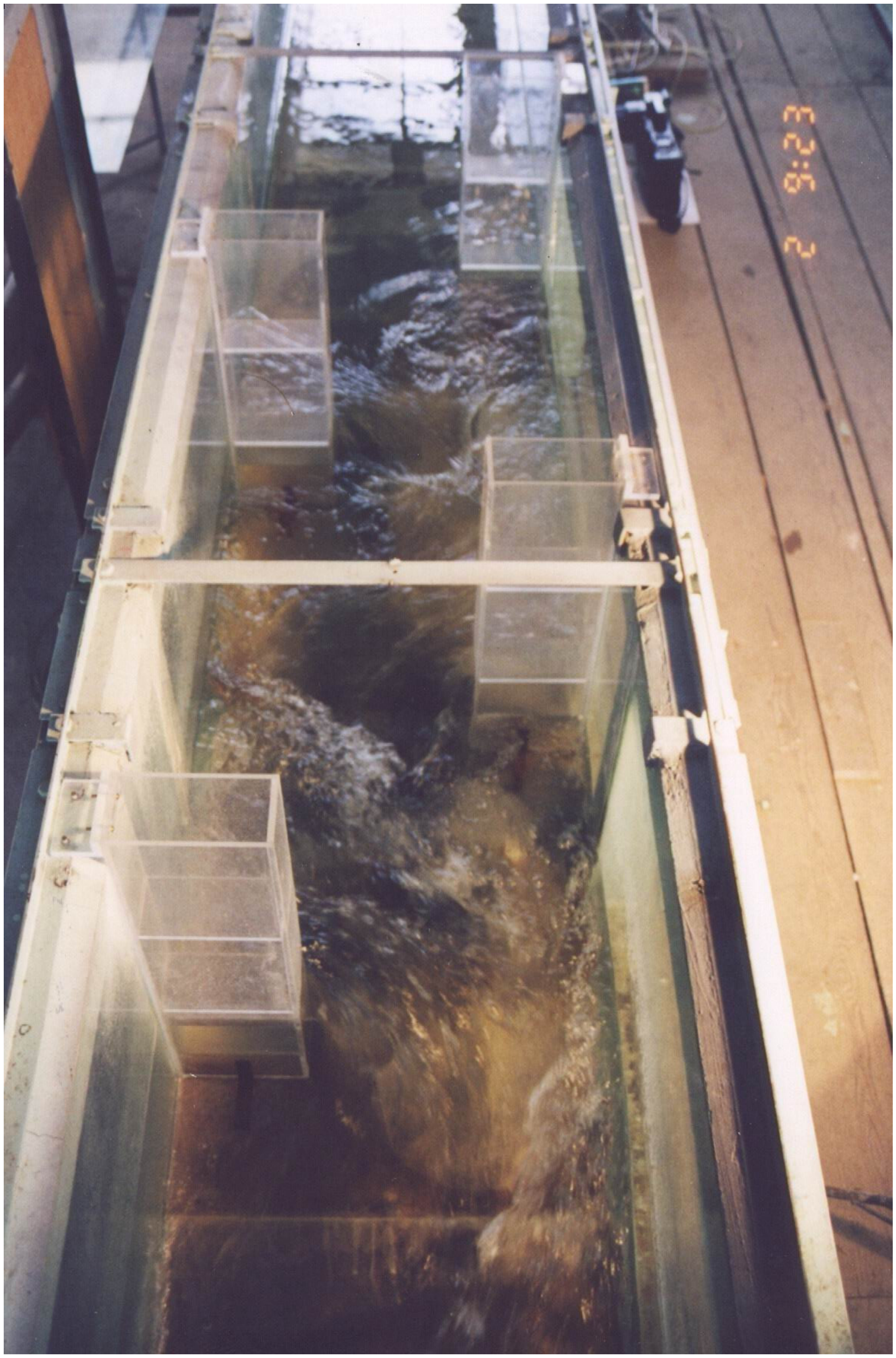

Figure 2.1. Experimental set-up

2.2 Determination of flowrate

A sharp crested rectangular weir made of fiberglass is used in the determination of flowrate. The discharge is computed from the equation (Henderson, 1966):

$$Q = C_d \cdot \frac{2}{3} \cdot \sqrt{2g} \cdot L_l \cdot H^{3/2} \tag{2.1}$$

where Q is discharge, C_d is the discharge coefficient, L_l is the effective length of the crest and H is the measured water head over the crest, excluding the velocity head. The discharge coefficient, C_d, in Equation (2.1) is determined by the equation given by Rehbock in 1929. (Addison, 1954 and King, 1954):

$$C_d = 0.605 + \frac{1}{1000 \cdot H} + 0.08 \cdot \frac{H}{P} \tag{2.2}$$

where P is the weir height.

2.3 Velocity profile at the inlet section

The channel length is not enough to obtain uniform flow conditions in the channel. However, symmetry of flow on horizontal plane at the inlet section is needed to simplify the boundary conditions for numerical studies. Flow conditions at the inlet of the working section was investigated by measuring the velocity distributions on vertical and horizontal planes. Pitot-Prandtl tube was used to measure the point velocity of water in the channel. Vertical velocity distribution shown in Fig. 2.2 shows that the measurement at 60 % of the depth gives the average velocity and the horizontal measurements are done at this depth. Measured velocity profiles shown in Fig. 2.3 demonstrate that the flow at the inlet of the working section is symmetrical .

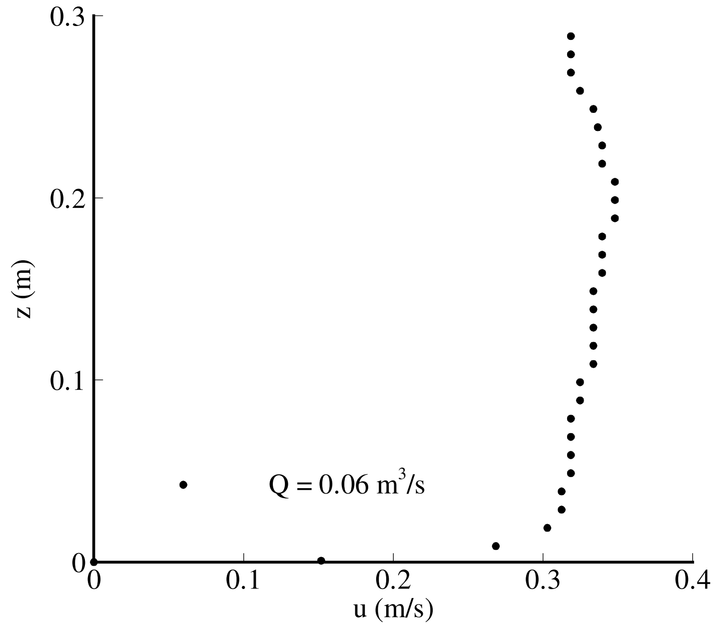

Figure 2.2. Vertical velocity distribution at the midpoint of inlet section

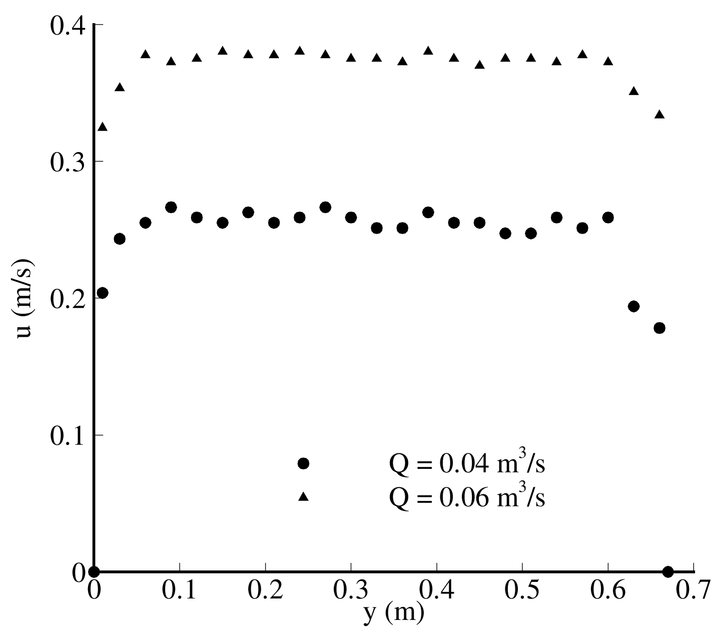

Figure 2.3. Velocity profile at the inlet section across the cross-section

2.4 Measurement of water surface profiles

Water surface profile measurements are done with a point gauge that is mobile in horizontal plane. The surface measurements are conducted for three reference flowrates of 0.02, 0.04, 0.06 m^3/s in the channel. The reference discharges are chosen by considering the experimental conditions and workability in the channel.

Surface measurements are taken at 28 measuring stations located at 0.1 m spacing along the channel axis (Fig.2.4). At each measurement station 23 measurement points were located at 0.03 m spacing. All together 644 point gauge measurements were done to describe the surface profile in the working section for a given test case. A test case is defined by a fixed discharge and a fixed tailwater configuration. When a test case is maintained, water depths are measured with a point gauge paying attention on the fluctuations of the free surface. Two readings of water surface level at each measuring point were taken as the minimum and the maximum. The mean surface level was defined as the average of the minimum and maximum readings by assuming normal distribution holds for the variation of surface profile.

Downstream or tail water conditions play a great role on the flow patterns in the channel as it has a horizontal bed. Two kinds of tail water conditions are obtained by the tailgate configurations. The first case is obtained by completely lowering the tailgate, with no control on the flow. And the second case is obtained by rising the tailgate so that the upstream is submerged. The position of the tailgate for the second case is arranged so that the flow in the whole channel remains subcritical. The conditions of the test cases considered in this thesis are described in Table 2.1. Measured surface profiles for the six test cases are presented in Figures 2.5~2.10.

Table 2.0-1. Experimental cases

Test Case	Discharge (m^3/s)	Tailgate control
A1	0.02	No control
A2	0.02	Submerged
B1	0.04	No control
B2	0.04	Submerged
C1	0.06	No control
C2	0.06	Submerged

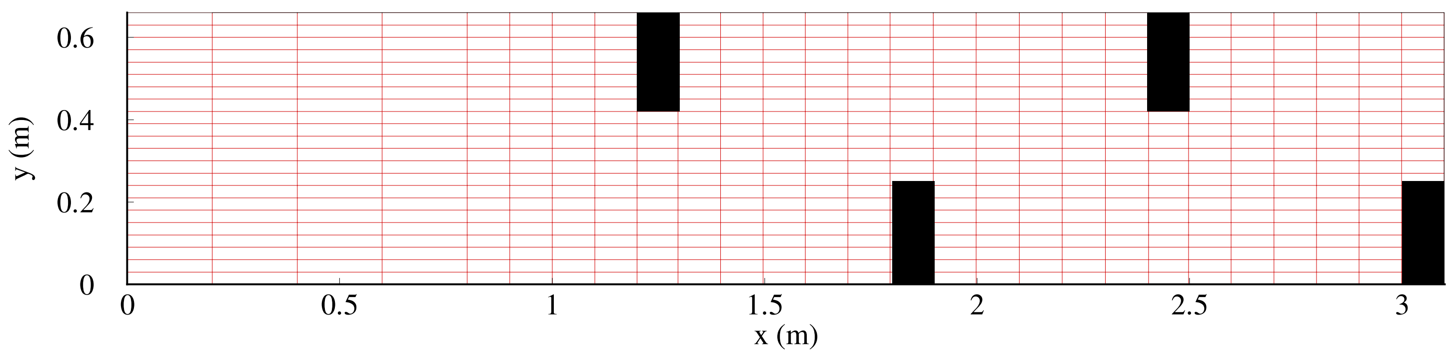

Figure 2.4. Plan view of the measuring channel with measuring points indicated by intersections of the gridlines

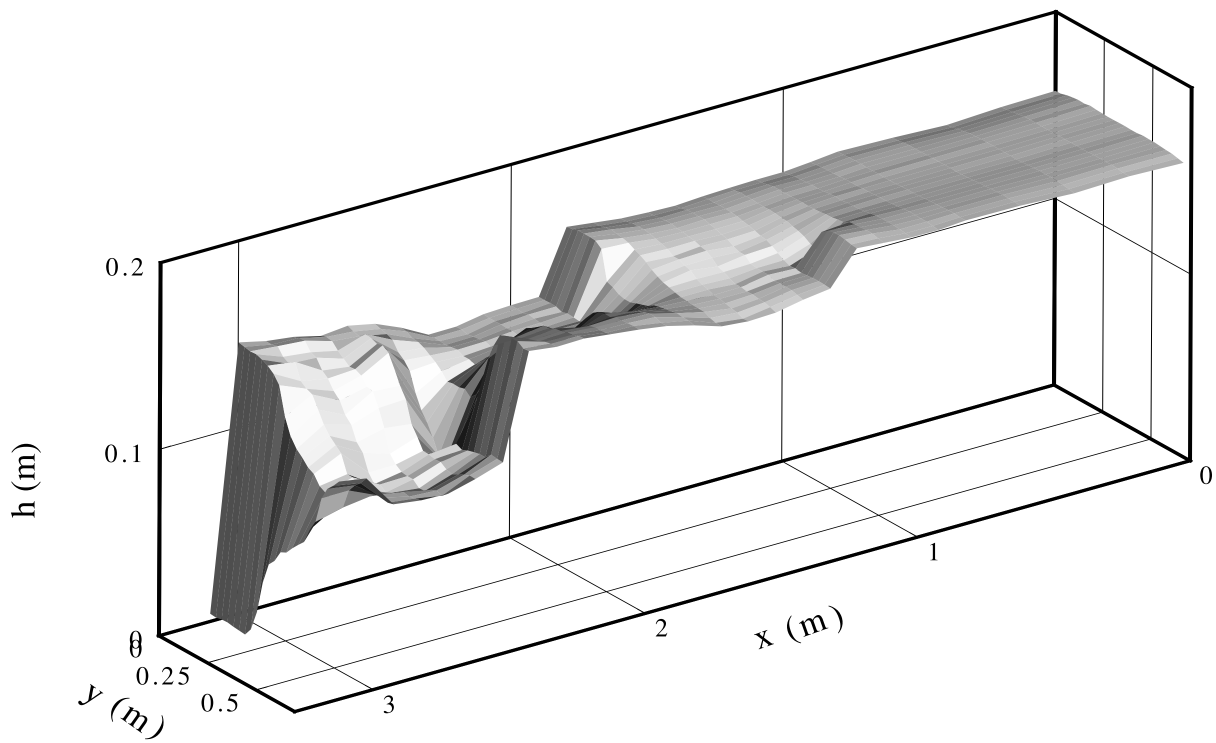

Figure 2.5. Water surface profile of experimental case A1

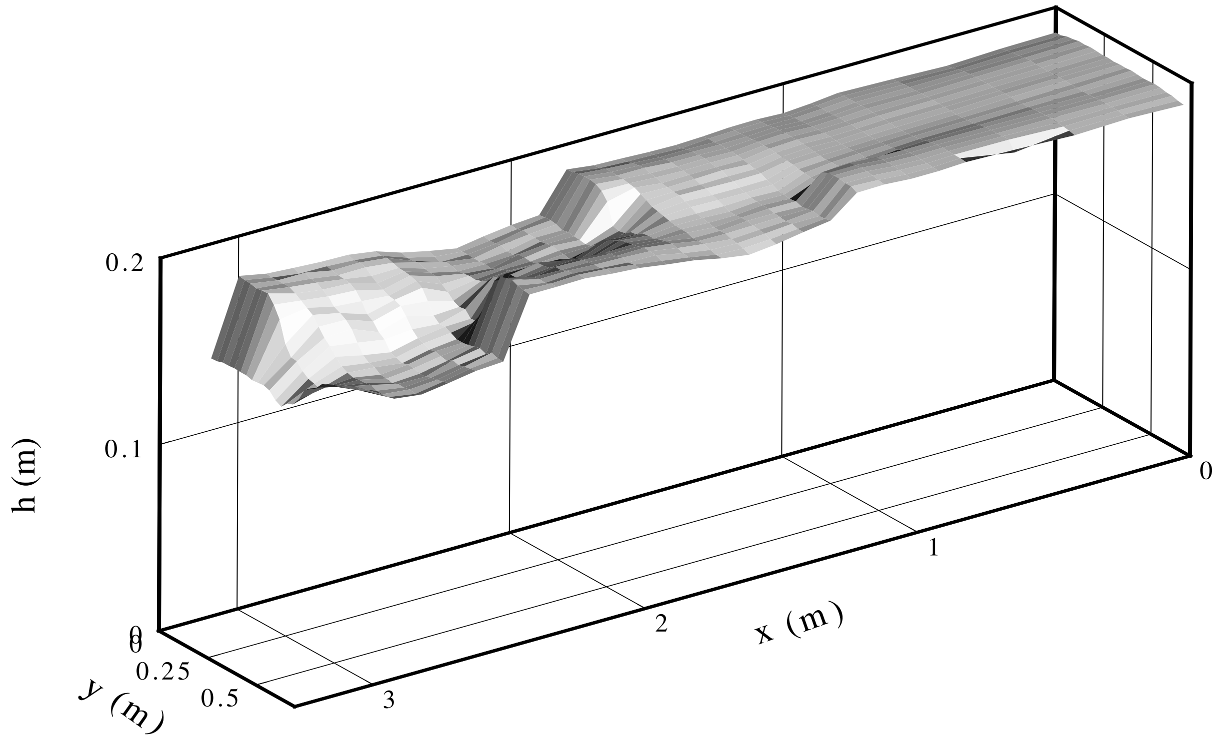

Figure 2.6. Water surface profile of experimental case A2

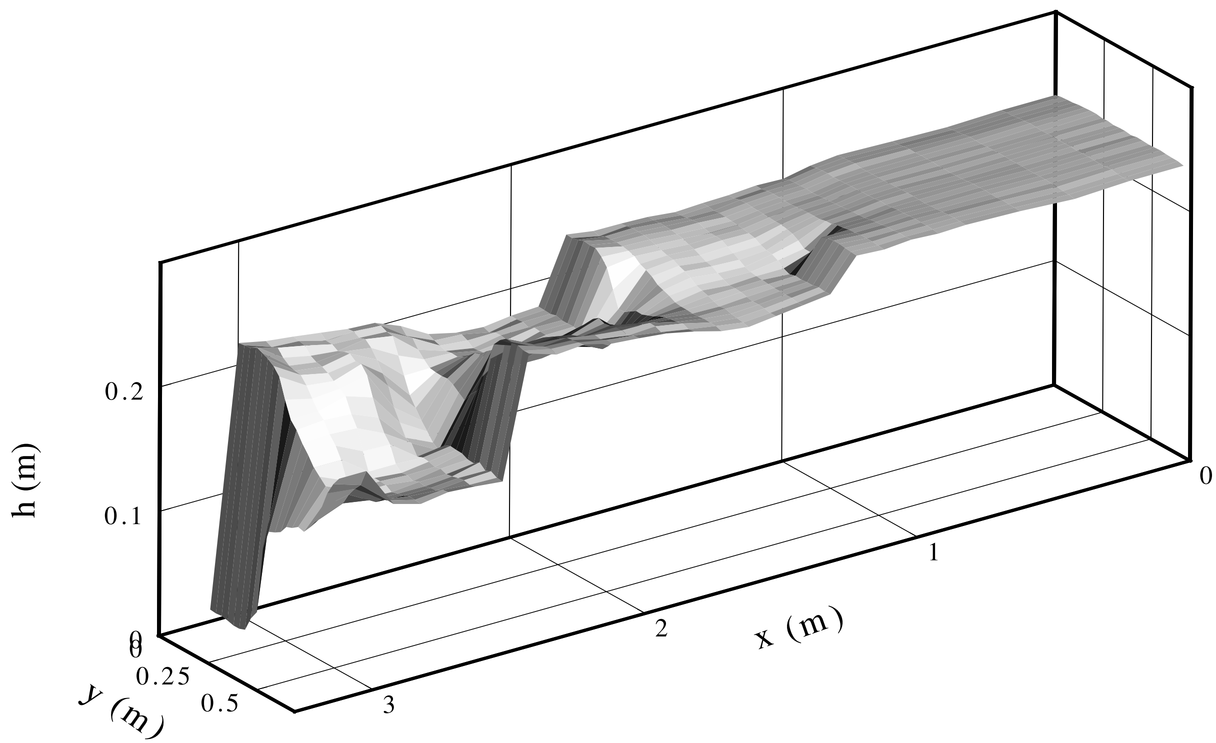

Figure 2.7. Water surface profile of experimental case B1

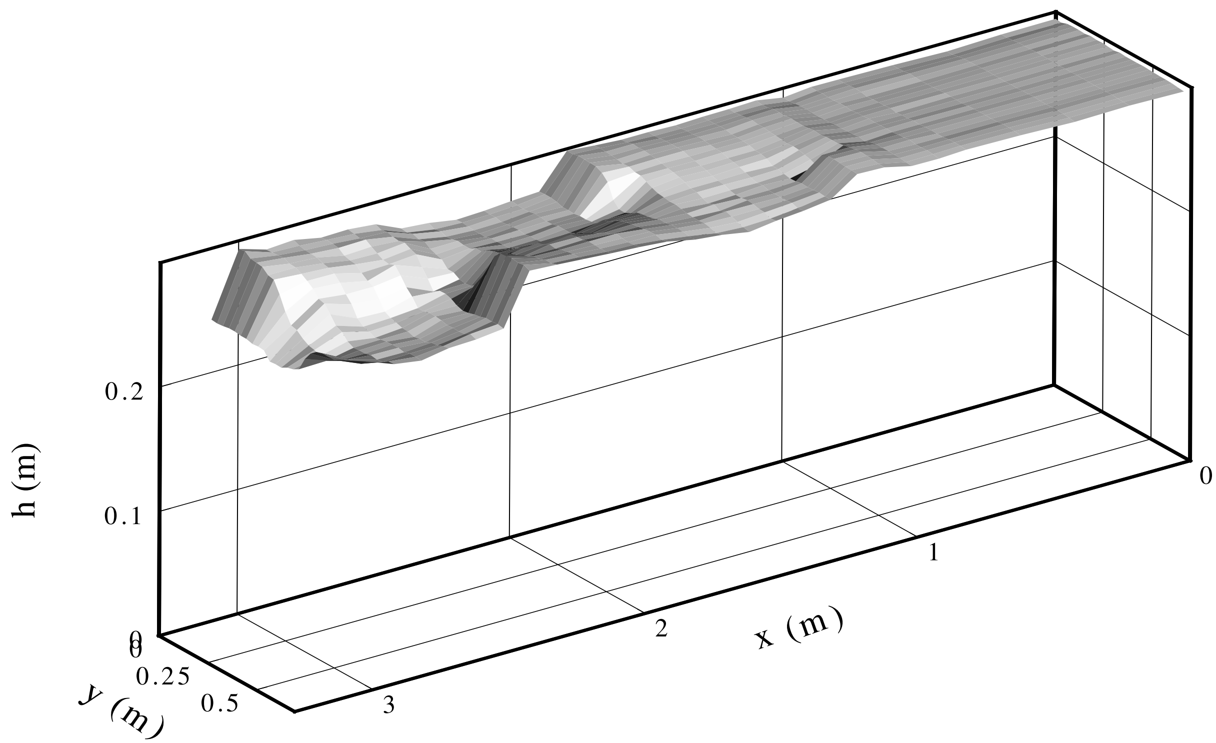

Figure 2.8. Water surface profile of experimental case B2

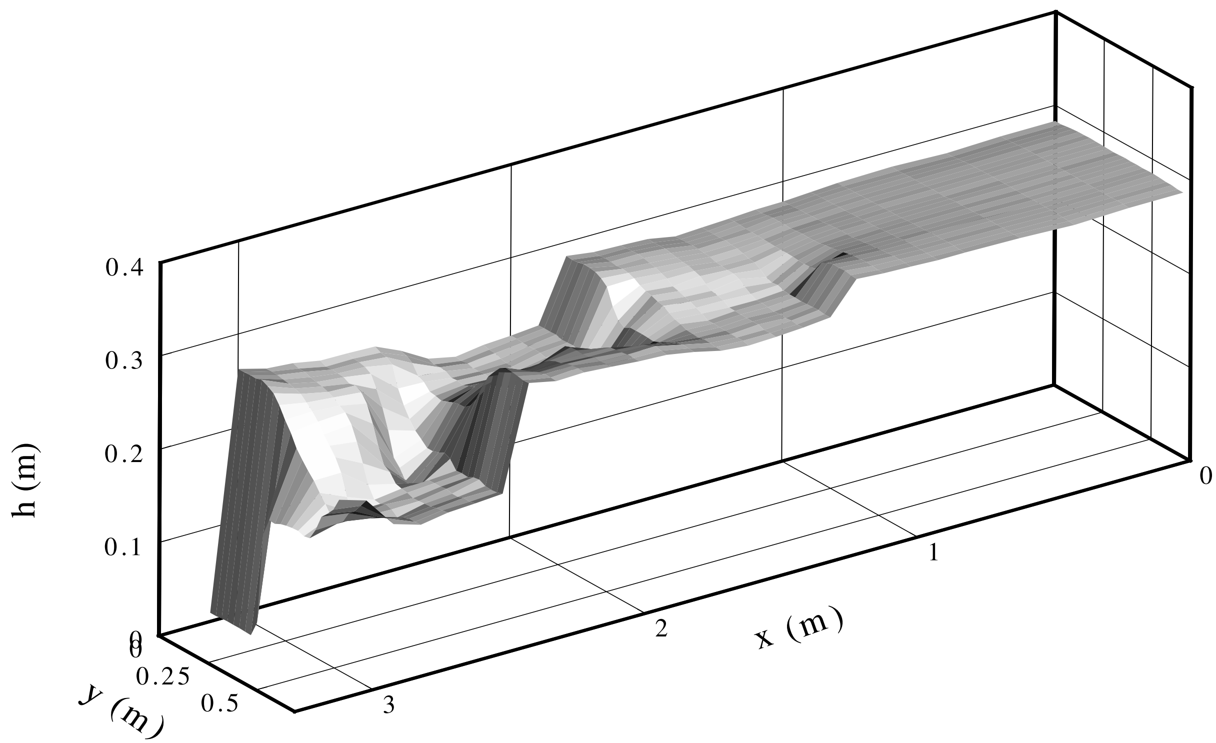

Figure 2.9. Water surface profile of experimental case C1

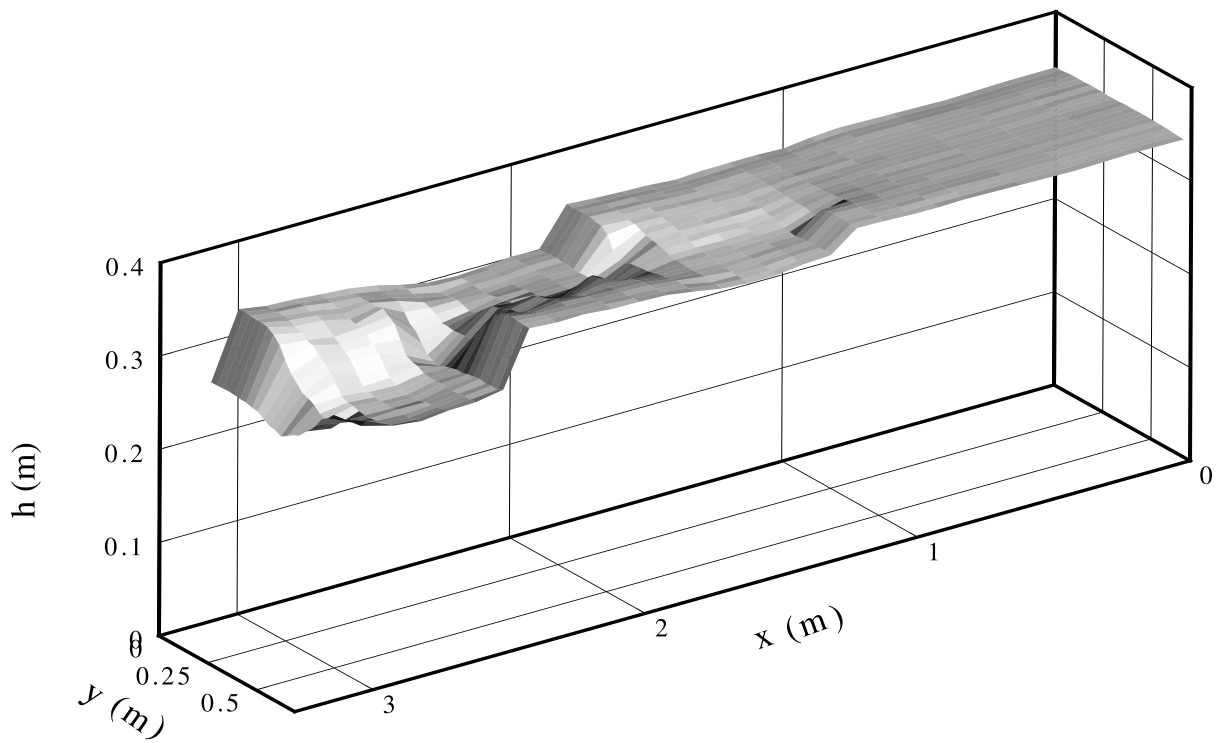

Figure 2.10. Water surface profile of experimental case C2

CHAPTER 3

GOVERNING EQUATIONS

Mathematical models to describe fluid motion in certain practical problems are based on Reynolds Averaged Navier-Stokes (RANS) equations. In practice when forming a mathematical model, many assumptions are made to simplify the problem under consideration, and the most basic equations that will capture the required phenomena are used. In open channel flow the most commonly used models fall under the classification of shallow water equations, in which it is assumed that the flow is shallow relative to the dimensions of the problem considered and the fluid is incompressible. As with all fluid flow models, the basis for forming a shallow water model is to form a continuity equation, corresponding to conservation of mass, and to apply the laws governing classical physics which results in equation of motion. Depending on the construction, such equations can often be written as conservation laws representing the conservation of a particular quantity such as momentum or energy. Additional terms may be included to add other effects such as friction, geometry variation, viscosity, etc. and these are referred as source terms which generally correspond to some form of loss or gain from the system.

3.1 Two-dimensional Depth-Averaged Shallow Flow Equations

Mathematical models called as shallow flow equations, govern a wide variety of physical phenomena. An important class of problems of practical interest involves water flows with a free surface under the influence of gravity. This class includes tides in oceans, breaking of waves on shallow beaches, roll waves in open channels, flood waves in rivers, surges and dam-break wave modeling. The shallow flow approximation can also be applied to obtain mathematical models for flows of heterogeneous mixtures and for the modeling of atmospheric flows.

The development of the two-dimensional depth-averaged free surface flow equations require some simplifying assumptions:

- Depth-averaged values are sufficient to describe the flow properties which vary over the depth.
- Vertical velocity and acceleration are negligible.
- Density is constant.
- Pressure distribution is hydrostatic.

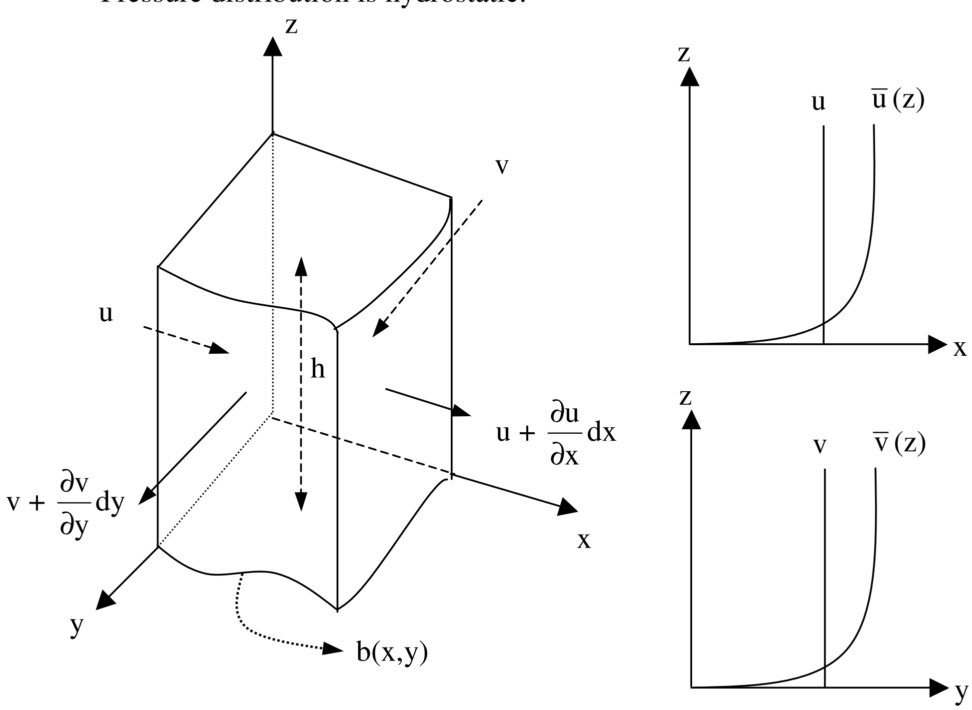

Figure 3.1. Flow with a free surface under gravity

In Fig. 3.1, x,y and z denote the axis directions, h denotes the water surface height from bottom, b denotes the channel bottom function, $\overline{u}(z)$ and $\overline{v}(z)$ denote the local time-averaged velocity components, u and v denote the depth-averaged values where;

$$u = \frac{1}{h}\int_{b}^{b+h} \overline{u}(z)\,dz \ , \tag{3.1}$$

$$v = \frac{1}{h}\int_{b}^{b+h} \overline{v}(z)\,dz \tag{3.2}$$

There are two boundaries with respect to vertical axis on which implicit equations of surface can be written as:

Free surface boundary:

$$\phi = z - h(x,y,t) - b(x,y) = 0 \tag{3.3.a}$$

Bottom boundary:

$$\phi = z - b(x,y) = 0 \tag{3.3.b}$$

The condition that the fluid at the boundary flows along the boundary and never leaves the boundary that there exists no flux across the boundary namely the kinematic condition is,

$$\frac{D\phi(x,y,z,t)}{Dt} = 0 \tag{3.4.a}$$

If the kinematic condition is applied to the boundaries,

$$\frac{D\phi(x,y,z,t)}{Dt} = \frac{\partial \phi}{\partial t} + u\frac{\partial \phi}{\partial x} + v\frac{\partial \phi}{\partial y} + w\frac{\partial \phi}{\partial z} = 0 \tag{3.4.b}$$

for the free surface;

$$-\frac{\partial h}{\partial t} - u\frac{\partial h}{\partial x} - v\frac{\partial h}{\partial y} - u\frac{\partial b}{\partial x} - v\frac{\partial b}{\partial y} + w = 0 \tag{3.5.a}$$

$$w_{z=h+b} = \left(\frac{\partial h}{\partial t} + u\frac{\partial h}{\partial x} + v\frac{\partial h}{\partial y} + u\frac{\partial b}{\partial x} + v\frac{\partial b}{\partial y}\right)_{z=h+b} \tag{3.5.b}$$

for bottom;

$$-u\frac{\partial b}{\partial x} - v\frac{\partial b}{\partial y} + w = 0 \tag{3.6.a}$$

$$w_{z=b} = (u\frac{\partial b}{\partial x} + v\frac{\partial b}{\partial y})_{z=b} \quad (3.6.b)$$

Conservation laws; conservations of mass, x-momentum, y-momentum and z-momentum, are written in terms of time-averaged quantities.

$$\frac{\partial \bar{u}}{\partial x} + \frac{\partial \bar{v}}{\partial y} + \frac{\partial \bar{w}}{\partial z} = 0 \quad (3.7)$$

$$\begin{aligned} &\frac{\partial \bar{u}}{\partial t} + \bar{u}\frac{\partial \bar{u}}{\partial x} + \bar{v}\frac{\partial \bar{u}}{\partial y} + \bar{w}\frac{\partial \bar{u}}{\partial z} + \frac{1}{\rho}\frac{\partial \bar{p}}{\partial x} = \frac{\mu}{\rho}\left(\frac{\partial^2 \bar{u}}{\partial x^2} + \frac{\partial^2 \bar{u}}{\partial y^2} + \frac{\partial^2 \bar{u}}{\partial z^2}\right) \\ &-\left(\frac{\partial \overline{u'^2}}{\partial x} + \frac{\partial \overline{u'v'}}{\partial y} + \frac{\partial \overline{u'w'}}{\partial z}\right) \end{aligned} \quad (3.8)$$

$$\begin{aligned} &\frac{\partial \bar{v}}{\partial t} + \bar{u}\frac{\partial \bar{v}}{\partial x} + \bar{v}\frac{\partial \bar{v}}{\partial y} + \bar{w}\frac{\partial \bar{v}}{\partial z} + \frac{1}{\rho}\frac{\partial \bar{p}}{\partial y} = \frac{\mu}{\rho}\left(\frac{\partial^2 \bar{v}}{\partial x^2} + \frac{\partial^2 \bar{v}}{\partial y^2} + \frac{\partial^2 \bar{v}}{\partial z^2}\right) \\ &-\left(\frac{\partial \overline{u'v'}}{\partial x} + \frac{\partial \overline{v'^2}}{\partial y} + \frac{\partial \overline{v'w'}}{\partial z}\right) \end{aligned} \quad (3.9)$$

$$\begin{aligned} &\frac{\partial \bar{w}}{\partial t} + \bar{u}\frac{\partial \bar{w}}{\partial x} + \bar{v}\frac{\partial \bar{w}}{\partial y} + \bar{w}\frac{\partial \bar{w}}{\partial z} + \frac{1}{\rho}\frac{\partial \bar{p}}{\partial z} = -g \\ &+\frac{\mu}{\rho}\left(\frac{\partial^2 \bar{w}}{\partial x^2} + \frac{\partial^2 \bar{w}}{\partial y^2} + \frac{\partial^2 \bar{w}}{\partial z^2}\right) - \left(\frac{\partial \overline{u'w'}}{\partial x} + \frac{\partial \overline{v'w'}}{\partial y} + \frac{\partial \overline{w'^2}}{\partial z}\right) \end{aligned} \quad (3.10)$$

where μ, ρ and g are the dynamic viscosity, density and gravitational acceleration, respectively. Last terms in momentum equations are Reynolds stresses arise from the averaging. Vertical components of velocity and acceleration are negligible. Eq. 3.10 results in,

$$\frac{1}{\rho}\frac{\partial \bar{p}}{\partial z} = -g \quad (3.11.a)$$

$$\bar{p} = \rho g.(b + h - z) \quad (3.11.b)$$

from which,

$$\frac{\partial \bar{p}}{\partial x} = \rho g\frac{\partial (b+h)}{\partial x} \quad (3.12)$$

$$\frac{\partial \bar{p}}{\partial y} = \rho g\frac{\partial (b+h)}{\partial y} \quad (3.13)$$

Integrating continuity equation (Eq. 3.7) with respect to depth

$$\int_{b}^{b+h}\left(\frac{\partial\overline{u}}{\partial x}+\frac{\partial\overline{v}}{\partial y}+\frac{\partial\overline{w}}{\partial z}\right)dz=0 \tag{3.14}$$

$$\int_{b}^{b+h}\frac{\partial\overline{u}}{\partial x}dz+\int_{b}^{b+h}\frac{\partial\overline{v}}{\partial y}dz+w_{z=b+h}-w_{z=b}=0 \tag{3.15}$$

Using Leibniz's rule;

$$\int_{b}^{b+h}\frac{\partial\overline{u}}{\partial x}dz=\frac{\partial}{\partial x}\int_{b}^{b+h}\overline{u}.dz-u_{z=b+h}\frac{\partial(b+h)}{\partial x}+u_{z=b}\frac{\partial b}{\partial x} \tag{3.16}$$

$$\int_{b}^{b+h}\frac{\partial\overline{v}}{\partial y}dz=\frac{\partial}{\partial y}\int_{b}^{b+h}\overline{v}.dz-v_{z=b+h}\frac{\partial(b+h)}{\partial y}+v_{z=b}\frac{\partial b}{\partial y} \tag{3.17}$$

Substituting equations 3.5.b, 3.6.b, 3.16 and 3.17 into equation 3.15 results in,

$$\frac{\partial h}{\partial t}+\frac{\partial uh}{\partial x}+\frac{\partial vh}{\partial y}=0 \tag{3.18}$$

Integrating x-momentum equation with respect to depth,

$$\int_{b}^{b+h}\left(\frac{\partial\overline{u}}{\partial t}+\frac{\partial\,\overline{u}^{2}}{\partial x}+\frac{\partial\,\overline{uv}}{\partial y}+\frac{\partial\,\overline{uw}}{\partial z}+\frac{1}{\rho}\rho g\frac{\partial(b+h)}{\partial x}\right)dz=\int_{b}^{b+h}\frac{\mu}{\rho}\left(\frac{\partial^{2}\overline{u}}{\partial x^{2}}+\frac{\partial^{2}\overline{u}}{\partial y^{2}}+\frac{\partial^{2}\overline{u}}{\partial z^{2}}\right)dz \tag{3.19}$$

Applying closure hypotheses;

$$\int_{b}^{b+h}\overline{u}^{2}\,dz=hu^{2} \tag{3.20}$$

$$\int_{b}^{b+h}\overline{uv}\,dz=huv \tag{3.21}$$

$$\int_{b}^{b+h}\overline{v}^{2}\,dz=hv^{2} \tag{3.22}$$

results in approximate x-momentum equation

$$\frac{\partial uh}{\partial t}+\frac{\partial(hu^{2}+gh^{2}/2)}{\partial x}+\frac{\partial(huv)}{\partial y}=-gh\frac{\partial b}{\partial x}+\frac{h\mu}{\rho}\left(\frac{\partial^{2}u}{\partial x^{2}}+\frac{\partial^{2}u}{\partial y^{2}}+\frac{\partial^{2}u}{\partial z^{2}}\right) \tag{3.23}$$

Rewriting equation 3.23 in terms of stresses,

$$\frac{\partial uh}{\partial t}+\frac{\partial(hu^2+gh^2/2)}{\partial x}+\frac{\partial(huv)}{\partial y}= \\ -gh\frac{\partial b}{\partial x}-\frac{\tau_{bx}}{\rho}+\frac{1}{\rho}\frac{\partial h\tau_{xx}}{\partial x}+\frac{1}{\rho}\frac{\partial h\tau_{xy}}{\partial y} \tag{3.24}$$

Similarly, y direction momentum equation is arranged as,

$$\frac{\partial vh}{\partial t}+\frac{\partial(huv)}{\partial x}+\frac{\partial(hv^2+gh^2/2)}{\partial y} \\ =-gh\frac{\partial b}{\partial y}-\frac{\tau_{by}}{\rho}+\frac{1}{\rho}\frac{\partial h\tau_{xy}}{\partial x}+\frac{1}{\rho}\frac{\partial h\tau_{yy}}{\partial y} \tag{3.25}$$

The shallow water equations can be written in matrix form as;

$$U_t+F(U)_x+G(U)_y=S(U) \tag{3.26}$$

where,

$$U=\begin{bmatrix} h \\ uh \\ vh \end{bmatrix},\quad F=\begin{bmatrix} uh \\ hu^2+gh^2/2 \\ huv \end{bmatrix},\quad G=\begin{bmatrix} vh \\ huv \\ hv^2+gh^2/2 \end{bmatrix} \\ S=\begin{bmatrix} 0 \\ -gh\frac{\partial b}{\partial x}-\frac{\tau_{bx}}{\rho}+\frac{1}{\rho}\frac{\partial h\tau_{xx}}{\partial x}+\frac{1}{\rho}\frac{\partial h\tau_{xy}}{\partial y} \\ -gh\frac{\partial b}{\partial y}-\frac{\tau_{by}}{\rho}+\frac{1}{\rho}\frac{\partial h\tau_{xy}}{\partial x}+\frac{1}{\rho}\frac{\partial h\tau_{yy}}{\partial y} \end{bmatrix} \tag{3.27}$$

If equation (3.26) is written in quasi-linear form, the characteristics of the equations can be determined.

$$U_t+A(U)U_x+B(U)U_y=S(U)$$

$$A(U)=\begin{bmatrix} \partial f_1/\partial u_1 & \partial f_1/\partial u_2 & \partial f_1/\partial u_3 \\ \partial f_2/\partial u_1 & \partial f_2/\partial u_2 & \partial f_2/\partial u_3 \\ \partial f_3/\partial u_1 & \partial f_3/\partial u_2 & \partial f_3/\partial u_3 \end{bmatrix}= \\ \begin{bmatrix} 0 & 1 & 0 \\ gh-u^2 & 2u & 0 \\ -uv & v & u \end{bmatrix} \tag{3.28}$$

$$B(U)=\begin{bmatrix} \partial g_1/\partial u_1 & \partial g_1/\partial u_2 & \partial g_1/\partial u_3 \\ \partial g_2/\partial u_1 & \partial g_2/\partial u_2 & \partial g_2/\partial u_3 \\ \partial g_3/\partial u_1 & \partial g_3/\partial u_2 & \partial g_3/\partial u_3 \end{bmatrix}= \begin{bmatrix} 0 & 0 & 1 \\ -uv & v & u \\ gh-v^2 & 0 & 2v \end{bmatrix} \tag{3.29}$$

The time dependent two-dimensional shallow water equations are hyperbolic for a wet bed as they have real and distinct eigenvalues. The eigenvalues of A and B are given as,

$$\lambda_{1A}=u-\sqrt{gh} \quad , \quad \lambda_{2A}=u \quad , \quad \lambda_{3A}=u+\sqrt{gh}$$

and

$$\lambda_{1B}=v-\sqrt{gh} \quad , \quad \lambda_{2B}=v \quad , \quad \lambda_{3B}=v+\sqrt{gh}$$

The solution methods described are based on the wet bed assumption, when the bed is specified as dry bed, h =0, the problem needs special treatment and can be understood from the eigenvalues that unless the water height is zero, there are distinct and real values of eigenvalues..

3.2 Solution Methods

Prior to the development of computers and their application to CFD, analytical techniques had to be used for solving partial differential equations. However their application even to the simplest problem require extensive hand computation. One particular method suited to solving problems based on conservation laws is the method of characteristics. One-dimensional St. Venant equations can be formulated with this method, but for most of the problems of practical interest it is not possible to find exact solutions by using analytical techniques. As a result, this has lead to the development of numerical methods.

3.3 Numerical Solution Methods

3.3.1 General Classification of numerical methods

Many techniques are available for numerical simulation work; finite difference, finite element and finite volume methods are the widely used methods for solving general fluid flow problems. There is no strict definition as how to identify a method. The following general descriptors are taken from Hirsch (1988).

A finite difference method represents the problem through a series of values at particular points or nodes. Expressions for the unknowns are derived by replacing the derivative terms in the model equations with truncated Taylor series expansions. The earliest numerical schemes are based upon finite difference methods and it is the one of the easier methods to implement.

The basis of the finite element method is to divide the domain into elements such as triangles or quadrilaterals and to place nodes to each element at which the numerical solution is determined. The solution at any position is then represented by a series expansion of the nodal values. Spectral methods can be considered as a subset of the finite element methods.

The finite volume method is based upon forming a discretisation from an integral form of the model equations, and subdividing the domain into finite volumes. Within each volume, the integral relationships are applied locally so exact conservation at each cell is achieved. The resulting expressions for the unknowns often appear similar to finite difference approximations and may be considered as a special case of finite difference or finite element techniques depending on the method used. For most of the fluid modeling problems based on conservation principles, the finite volume method has become the most popular approach for general fluid flow problems. Within the context of open channel flows, earlier works focused on the application of finite difference and finite element schemes, however recently finite volume methods are used widely.

In order to quantify how well a particular numerical scheme performs in generating a solution to a problem, there are some criteria to be satisfied. These concepts are accuracy, consistency, stability and convergence. In theory these criteria apply to any form of numerical method though they are easily formulated for finite difference schemes. A brief introduction to these concepts based on Hirsch (1988) and Smith (1985) is given below.

Accuracy is a measure of how well the discrete solution represents the exact solution of the problem. Two quantities exist to measure this, the local error or the truncation error, which measures how well the difference equations match the differential equations, and the global error which reflects the overall error which cannot be computed unless the exact solution is known. Mathematically, for a method to be consistent the truncation error must decrease as the step size is reduced. For a scheme to be used practically, it must be consistent.

If a scheme is said to be stable then any errors in the solution will remain bounded. In practice if an unstable method is used the solution will tend to infinity. Most methods have stability limits which place restrictions on the size of grid spacing (i.e. Δx, Δt) usually in terms of a limit on the CFL (Courant-Friedrichs-Lewy) number.

Another requirement is that the numerical scheme should be convergent, which by definition means the numerical solution should approach to the exact solution as the grid spacing is reduced. It is usually not easy to prove the convergence of a scheme, instead Lax's Equivalence theorem is used which states that, ' for a well posed initial value problem and a consistent method, stability implies convergence.' A well-posed problem must have the following conditions;

- A solution must exist.
- The solution should be unique.
- The solution should depend on the initial and boundary data.

In this work the numerical solution is achieved by using finite volume method, so the finite volume methods will be explained in more detail in the following sections.

3.3.2 Finite Volume Methods

The fundamental difference between finite volume and finite difference methods is that in finite difference methods the differential form of the equations are discretised, whereas for finite volume methods the discretisation is performed on an integral formulation of the equations. The resulting discretisation often resembles the ones obtained in finite difference methods. The basis of the finite volume methods is to construct an integral form of the governing equations which is valid for any arbitrary closed volume.

3.3.2.1 Godunov type methods

Godunov methods use the wave propagation information to construct the numerical schemes. This is achieved in various approaches, at the highest level local Riemann problem is solved exactly and at the lowest level just the sign of a single wave at intercell boundary is given. Centred methods do not use any propagation information so it is easier to construct the scheme.

One of the first attempts to develop an upwind scheme suitable for solving systems of conservation laws was by Courant, Isaacson and Rees (Courant *et.al.*,1952) introduced as CIR method. The CIR method was based on tracing the characteristics from one time level to the next and employed the characteristic form of the equations. Originally this technique was considered for the Euler equations, however as the construction was not based on the conservation form of the equations, the method was not succesful in solving problems containing discontinuities. In 1959, Godunov published a new technique which differed from previous schemes in that it assumed the numerical solution was constant within each cell, instead of considering nodal values. The basis of the method was to solve a series of Riemann problems between each of the cell interfaces and this led to an expression for the numerical flux. The method was explicit and required that the time step was limited in such a way that neighboring Riemann problems would not interact. It was the starting point for the Riemann based schemes with which this thesis is concerned.

If the one-dimensional system of conservation laws is considered, Eq. 3.26 takes the following form;

$$U_t + F(U)_x = 0 \tag{3.30}$$

This is called the differential form of the conservation laws and is valid only for the case in which the solution is smooth throughout the system. In the presence of discontinuities integral form of the equations must be used.

$$\oint (U\,dx - F(U)\,dt) = 0 \tag{3.31}$$

where the line integration is performed along the boundary of the domain. By choosing a quadrilateral control volume in x-t plane of dimensions $[x_{i-1/2}, x_{i+1/2}]\,X\,[t^n, t^{n+1}]$, another expression of the integral form of the conservation laws can be written as;

$$\int_{x_{i-1/2}}^{x_{i+1/2}} U(x, t^{n+1})\,dx = \int_{x_{i-1/2}}^{x_{i+1/2}} U(x, t^n)\,dx - \left[\int_{t^n}^{t^{n+1}} F(U(x_{i+1/2}, t))\,dt - \int_{t^n}^{t^{n+1}} F(U(x_{i-1/2}, t))\,dt\right] \tag{3.32}$$

The integral averages of U(x,t) at t = t^n and t = t^{n+1} over the length Δx_i are defined as ;

$$U_i^n = \frac{1}{\Delta x_i}\int_{x_{i-1/2}}^{x_{i+1/2}} U(x, t^n)\,dx \tag{3.33.a}$$

and,

$$U_i^{n+1} = \frac{1}{\Delta x_i}\int_{x_{i-1/2}}^{x_{i+1/2}} U(x, t^{n+1})\,dx \tag{3.33.b}$$

where $\Delta x_i = x_{i+1/2} - x_{i-1/2}$

Also the integral averages of the flux at positions $x_{i-1/2}$ and $x_{i+1/2}$ are defined as;

$$F_{i-1/2} = \frac{1}{\Delta t}\int_{t^n}^{t^{n+1}} F(U(x_{i-1/2}, t)\,dt \qquad (3.34.a)$$

and,

$$F_{i+1/2} = \frac{1}{\Delta t}\int_{t^n}^{t^{n+1}} F(U(x_{i+1/2}, t)\,dt \qquad (3.34.b)$$

Using these definitions the integral form of the conservation laws becomes,

$$U_i^{n+1} = U_i^n - \frac{\Delta t}{\Delta x}\left[F_{i+1/2} - F_{i-1/2}\right] \qquad (3.35)$$

where intercell fluxes are calculated at the boundaries of the cell. The upwind method of Godunov is a scheme that utilises the solution of local Riemann problem whether exactly or approximately. Scheme is first order in space and time, and higher order extensions are possible. It is assumed that the initial data U^n at the time $t = t^n$ is a set of integral averages U_i over the control volume and this results in a piece-wise constant distribution of data as shown in Fig.3.2.

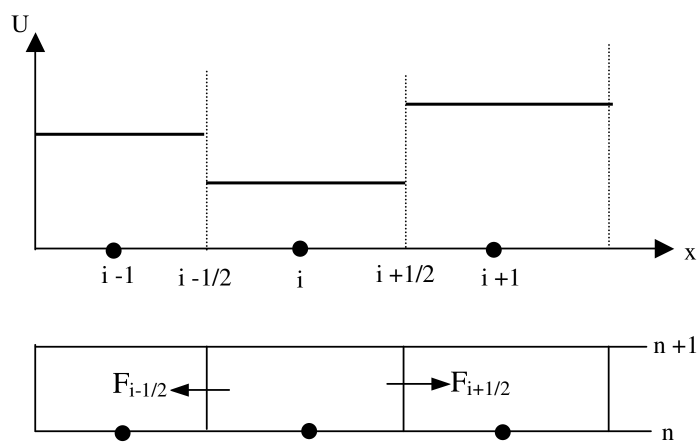

Figure 3.2. Upwind method for one-dimensional flow

This piece-wise distribution requires a solution of Riemann problem with left and right data states to find the intercell set of primary variables. Godunov flux at the boundaries can be defined as the physical flux function evaluated with intercell solution of primary variables.

$$F_{i+1/2} = F(U_{i+1/2}(0)) \text{ and } F_{i-1/2} = F(U_{i-1/2}(0))$$

Two items are needed to evaluate the Godunov flux:

- The solution of the Riemann problem, with given initial data, U_L=U_i and U_R=U_{i+1}
- A solution sampling procedure to identify the required value at x/t = 0.

To simulate transmissive boundaries, $h^n_{m+1} = h^n_m$, $un^n_{m+1} = un^n_m$, $ut^n_{m+1} = ut^n_m$ are set and for solid reflective boundaries, $h^n_{m+1} = h^n_m$, $un^n_{m+1} = -un^n_m$, $ut^n_{m+1} = ut^n_m$ where un denotes the normal, ut denotes the tangential velocity component with respect to the boundary and subscripts m and m+1 denote boundary cell and imaginary cell, respectively. Fig. 3.3 shows the orientation of these nodes.

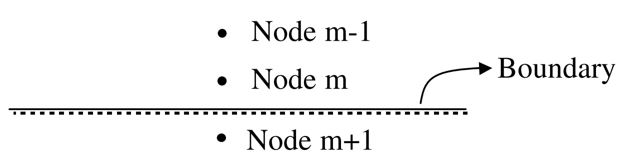

Figure 3.3. Orientation of boundary nodes

3.3.2.2 Riemann problem and Riemann Solvers

Having introduced Godunov's method and obtained the update formula which is based on the solution of a Riemann problem, it is necessary to explain what a Riemann problem is. The Riemann problem is defined as an initial value problem of the form given in Eq. 3.30 with the initial conditions shown in Fig. 3.2 where the initial values may be discontinuous across x_o. The solution of the Riemann problem has different approaches but all have certain properties in common. The constant states U_L and U_R are linked by waves, where the number of the waves present in the solution is the same as the number of equations in the conservation law. The region between the waves is referred as star region and within this section variables are constant. The types of waves present depend on the system being considered and for shallow water equations the waves are either shock or rarefaction waves.

3.3.2.3 Exact Solution of Riemann Problem

The Riemann problem is a generalisation of the dam break problem. Toro (1992) presented an exact Riemann solver based on which his earlier work for compressible gas dynamics. This method reduces the problem to the solution of a non-linear equation for the water depth by an iterative technique. The remaining flow variables follow directly through the complete structure of the solution of the Riemann problem.

There are several reasons for studying the exact solution of the Riemann problem. First, it is the simplest initial value problem for the full set time-dependent non-linear equations, the solution of which may include simultaneously both smooth and discontinuous solutions. The information provided by the Riemann problem solution is fundamental to the understanding of basic features of wave propagation in shallow water models. Exact solution can be used locally in Godunov-type methods and just a bit expensive than the approximate Riemann solvers.

For the x-split two-dimensional shallow water equations, if the exact solution of the Riemann problem is concerned shown in Figure 3.2; the structure of the general solution looks like in Fig. 3.4, three waves seperate four constant states, subscripts $_{*,L,R}$ show the variable's region as star region, left of the waves and right of the waves, respectively.

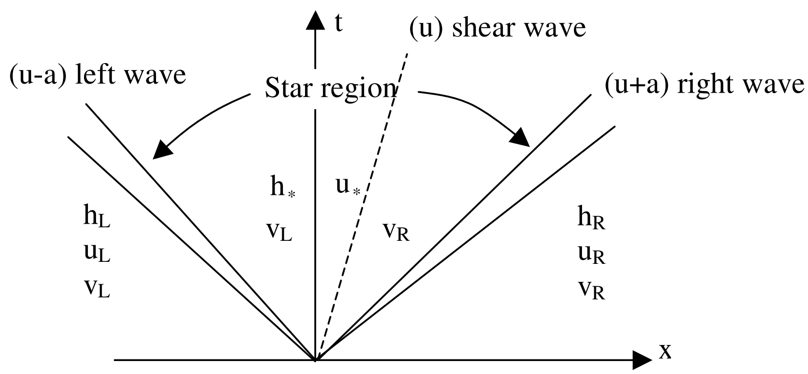

Figure 3.4. Structure of the general solution of the Riemann problem

If we denote , $W = [h, u, v]^T$ primitive variables, these four states are W_L (left data), W_R (right data), W_{*L} , W_{*R} . W_{*L} and W_{*R} are the unknown quantities of the problem in the star region. The left and the right waves are either shock or rarefaction waves and the middle wave is always a shear wave. Part of the solution is to determine the types of the waves for the given initial conditions. Across the left and right waves both h and u change but v remains constant, across the shear wave v changes discontinuously and both h and u remain constant. If we denote the depth and velocity in the star region as h_* and u_*, types of non-linear left and right waves are determined by;

$h_* > h_L$: left wave is a shock wave

$h_* \leq h_L$: left wave is a rarefaction wave

$h_* > h_R$: right wave is a shock wave

$h_* \leq h_L$: right wave is a rarefaction wave

Left and right waves are not affected by the tangential velocity component, so by a single algebraic, non-linear equation for the water depth h_* is obtained connecting left and right data states.

3.3.2.3.1 Solution for h_* and u_*

The solution h_* for the described Riemann problem is given by the roots of the following algebraic equation;

$$f(h) = f_L(h, h_L) + f_R(h, h_R) + (u_R - u_L) \qquad (3.36)$$

where the functions f_L and f_R are defined as;

$$f_L = \begin{cases} 2(\sqrt{gh} - \sqrt{gh_L}) & \text{if } h \le h_L \text{ (rarefaction)} \\ (h - h_L)\sqrt{\frac{1}{2}g\left(\frac{h + h_L}{hh_L}\right)} & \text{if } h > h_L \text{ (shock)} \end{cases} \qquad (3.37)$$

$$f_R = \begin{cases} 2(\sqrt{gh} - \sqrt{gh_R}) & \text{if } h \le h_R \text{ (rarefaction)} \\ (h - h_R)\sqrt{\frac{1}{2}g\left(\frac{h + h_R}{hh_R}\right)} & \text{if } h > h_R \text{ (shock)} \end{cases} \qquad (3.38)$$

The solution for the particle velocity u_* in the star region is given by:

$$u_* = \frac{1}{2}(u_L + u_R) + \frac{1}{2}\left(f_R(h_*, h_R) - f_L(h_*, h_L)\right) \qquad (3.39)$$

There are four possible cases to consider connecting u_* to the data states across the left and right waves and each wave is analysed seperately. If the left wave is a rarefaction wave,

$$u_* = u_L - 2(a_* - a_L) \qquad (3.40)$$

since $a = \sqrt{gh}$

$$u_* = u_L - f_L(h_*, h_L) \qquad (3.41.a)$$

$$f_L(h_*, h_L) = 2(\sqrt{gh_*} - \sqrt{gh_L}) \qquad (3.41.b)$$

if the right wave is a rarefaction wave,

$$u_* = u_R - f_R(h_*, h_R) \qquad (3.42.a)$$

$$f_R(h_*, h_L) = 2(\sqrt{gh_*} - \sqrt{gh_R}) \qquad (3.42.b)$$

if the left wave is a shock wave,

$$u_* = u_L - f_L(h_*, h_L) \qquad (3.43.a)$$

$$f_L(h_*,h_L) = (h_* - h_L)\sqrt{\frac{1}{2}g\left(\frac{h_* + h_L}{h_*.h_L}\right)} \tag{3.43.b}$$

if the right wave is a shock wave,

$$u_* = u_R - f_R(h_*,h_R) \tag{3.44.a}$$

$$f_R(h_*,h_R) = (h_* - h_R)\sqrt{\frac{1}{2}g\left(\frac{h_* + h_R}{h_*.h_R}\right)} \tag{3.44.b}$$

Elimination of u_* in all cases gives the equation 3.36;

$$f_L(h_*,h_L) + f_R(h_*,h_R) + u_R - u_L = 0 \tag{3.36}$$

Assuming the root of h_* is available by the iterative solution, velocity in star region is defined as;

$$u_* = \frac{1}{2}(u_L + u_R) + \frac{1}{2}\left(f_R(h_*,h_R) - f_L(h_*,h_L)\right) \tag{3.39}$$

3.3.2.3.2 Iterative solution for h_*

There is no explicit solution of the Equation 3.36. As the derivative of the function is available, the use of Newton-Raphson method is possible;

$$h^{n+1} = h^n - \frac{f(h^n)}{f'(h^n)} \tag{3.45}$$

As a starting value for the iteration, a h^0 value is assumed using two rarefaction approximation to the celerity;

$$h^0 = \frac{1}{g}\left[\frac{1}{2}(a_L + a_R) - \frac{1}{4}(u_R - u_L)\right]^2 \tag{3.46}$$

The iteration is stopped whenever the change in h is smaller than a prescribed tolerance,

$$\Delta h = \frac{\left|h^{n+1} - h^n\right|}{(h^{n+1} + h^n)/2} < \text{ TOL} \tag{3.47}$$

3.3.2.3.3 Sampling the solution

W(x,t) is needed at an arbitrary point (x, t_*), where $x_L < x < x_R$ and t_* is an arbitrary positive time. For a given time t_*, the solution is only dependent on x and gives a profile at the given time. Sampling procedure is just the determination of the solution whether in the left of the shear or right of the shear as shown in Fig. 3.4. There are two possibilities for a given point,

- Point lies in the left of the shear wave.

The solution on the left side of the shear wave is determined by the character of the left wave. If $h_* > h_L$, the left wave is a shock wave and the complete solution is;

$$W(x,t_*) \equiv \begin{cases} W_{*L} = [h_*, u_*, v_L]^T & \text{if } S_L \le x/t_* \le u_* \\ W_L = [h_L, u_L, v_L]^T & \text{if } x/t_* \le S_L \end{cases} \tag{3.48}$$

If $h_* \le h_L$, the left wave is a rarefaction wave and the complete solution is;

$$W(x,t_*) \equiv \begin{cases} W_{*L} & \text{if } S_{TL} \le x/t_* \le u_* \\ W_{L\,FAN} & \text{if } S_{HL} \le x/t_* \le S_{TL} \\ W_L & \text{if } x/t_* \le S_L \end{cases} \tag{3.49}$$

- Point lies in the right of the shear wave.

Similarly like the previous case, if $h_* > h_R$, the right wave is a shock wave and the complete solution is;

$$W(x,t_*) \equiv \begin{cases} W_{*R} = [h_*, u_*, v_R]^T & \text{if } u_* \le x/t_* \le S_R \\ W_R = [h_R, u_R, v_R]^T & \text{if } S_R \le x/t_* \end{cases} \tag{3.50}$$

If $h_* \le h_R$, the right wave is a rarefaction wave and the complete solution is;

$$W(x,t_*) \equiv \begin{cases} W_{*R} & \text{if } u_* \le x/t_* \le S_{TR} \\ W_{R\,FAN} & \text{if } S_{TR} \le x/t_* \le S_{HR} \\ W_R & \text{if } S_{HR} \le x/t_* \end{cases} \tag{3.51}$$

where the variables are given as;

$$S_L = u_L - a_L q_L \tag{3.52}$$

$$S_R = u_R + a_R q_R \tag{3.53}$$

$$q_K = \sqrt{\frac{1}{2}\left[\frac{(h_* + h_K)\,h_*}{h_K^2}\right]} \tag{3.54}$$

$$S_{HL} = u_L - a_L \tag{3.55}$$

$$S_{TL} = u_* - a_* \tag{3.56}$$

$$S_{HR} = u_R + a_R \tag{3.57}$$

$$S_{TR} = u_* + a_* \tag{3.58}$$

$$W_{L\,FAN} \equiv \begin{Bmatrix} a = 1/3(u_L + 2a_L - x/t) \\ u = 1/3(u_L + 2a_L + 2x/t) \end{Bmatrix} \tag{3.59}$$

$$W_{R\,FAN} \equiv \begin{Bmatrix} a = 1/3(-u_R + 2a_L + x/t) \\ u = 1/3(u_R - 2a_R + 2x/t) \end{Bmatrix} \tag{3.60}$$

This exact solution is valid for split two dimensional equations including the solution for the tangential velocity component. This procedure is valid only for the wet bed case in which the water depth is everywhere positive.

3.3.2.4 Approximate Solutions of Riemann Problem

To compute numerical solutions by Godunov type methods, approximate Riemann solvers may be used. Making the choice between exact and approximate solvers is motivated by computational cost, simplicity and correctness. Correctness should be the governing criterion. Widely used approximate solvers can be listed as; HLL, HLLC, Roe's and Osher's approximate Riemann solvers (Toro, 1997)

3.3.3 Application of numerical Methods to open channel flow

Having introduced the ideas and methodologies behind numerical techniques, this section goes on to review the application of computational methods to open channel flow. The purpose of this section is to illustrate the progress of computational hydraulics in recent years and to highlight what has been achieved within the field. In addition, surveying the literature provides a means to identify suitable test cases for analyzing the performance of numerical schemes.

The review is divided into two subsections. The first part includes one-dimensional studies and details of the various methods. The second subsection is intended to give an overview of how the original one-dimensional methods have been extended to higher dimensions.

3.3.3.1 One-dimensional Studies

Fennema and Chaudhry (1986) presented a paper introducing three explicit schemes to the Saint Venant equations and compared the results for problems containing shocks with solutions from the implicit Preissmann scheme. Three methods considered were the McCormack, Lambda and Gabutti schemes, all of which are second order accurate. The paper showed a number of results for flows containing bores and illustrated how the explicit schemes gave rise to numerical oscillations around the discontinuity. By the addition of artificial viscosity, the oscillations were reduced and the profiles became similar to the results produced by the Preissmann scheme. The point highlighted by the paper was the computational simplicity of explicit schemes when compared with implicit ones, and comparing with the Preissmann scheme 10-25 % of CPU time is required.

Alcrudo, Garcia-Navarro and Saviron (1992) extended the application of Roe's scheme to shallow water flows to include prismatic channels of arbitrary cross section. A series of solutions were presented and contrasted with those obtained from the McCormack and Lax-Friedrichs schemes. In particular the examples considered highlighted the shock capturing ability of Roe's scheme. Solutions for the dam-break problem with a depth ratio of 100:1 were shown. The Mc Cormack scheme was used with artificial viscosity and this enabled a solution to be produced, however the results were poor and included an unphysical stationary jump. The Lax-Friedrichs scheme generated a reasonable solution typical of a first order scheme. The two other problems illustrated in the paper considered the case of one bore propagating over another, and a situation in which the bores traveling in opposing directions. The Roe scheme performed well for both of the problems. However McCormack scheme created oscillations near the bores.

Garcia- Navarro and Saviron (1992) applied the McCormack scheme to a variety of discontinuous flow problems in rectangular channels. The paper included details of how to apply the method of characteristics to the boundaries in order to generate appropriate boundary data and also showed how to incorporate discontinuous flows at the upstream boundary. Results were presented for four test problems. The first was the uniform motion of a shock through a smooth rectangular channel. The second problem involved the propagation and reflection of shock waves in a channel which was closed at the downstream boundary. The third case considered was one shock propagating over another to form a larger shock. The conclusion made from this experiment was that comparisons made between this scheme and a third order explicit method showed that ‘it was not worth going further for this kind of problems’. The final example included the effect of source terms and consisted of flow over a ladder of cascades, which were enforced by use of internal weir boundary condition. The steady state numerical solution was shown, which contained small oscillations due to the presence of the weirs.

In another paper Alcrudo *et.al.* (1992) introduced a TVD variant of the McCormack scheme. Results were shown for five different test cases. The first problem was the ladder of cascades problem in the previous paper but with different choices of S_0 and n. Comparing the TVD and non TVD versions of the scheme, small oscillations were seen to be removed when the flux limiters are introduced. The second problem considered was a flood wave in a sloping trapezoidal channel. The TVD version of the program performed much better than the non-TVD version. The final two examples presented the solutions for flow through a converging- diverging channel created by a sinusoidal width variation. Again the TVD version performed better than the other.

Yang, Hsu and Chang (1993) presented results from five different numerical methods for a number of problems. The schemes considered were based on two general formulations, giving rise to a set of finite difference and finite element methods. The schemes selected corresponded to a second order TVD method, a second order ENO (essentially non oscillatory) and a third order ENO scheme with finite difference formulations and second order TVD and ENO schemes by finite element methods. For all five schemes results were shown for the dam break problem. All of the methods produced practically identical results in which the shock was well resolved and no oscillations were present.

Zoppou and Roberts (2003) published their paper on explicit schemes for dam-break simulations. A number of numerical schemes for solving one-dimensional wave equations applied to problems containing discontinuities in the solution have been examined.

3.3.3.2 Two-dimensional Studies

Fennema and Chaudhry (1989) applied the Beam and Warming scheme to the two-dimensional shallow water equations. Using an approximate factorization two-dimensional problem was re-expressed as two one-dimensional problems. The method was applied to the partial dam break problem. The effects of friction and bed slope were included in the study with various boundary conditions, but the paper presented results for a flat frictionless channel. It was noted that McCormack scheme fails for a depth ratio larger than 4:1.

Toro (1992) presented several Riemann solvers within the context of shallow water flows, and considered their application through the Weighted Average Flux method (WAF) to a series of one-dimensional and two-dimensional problems. The paper illustrated how to determine the exact solution of the Riemann problem for the one-dimensional Saint-Venant equations, which led to the development of Toro's exact solver, the two-rarefaction approximate Riemann solver and two-shock approximate Riemann solver. The paper also considered the approximate Riemann solvers of Roe and

Harten,Lax and van Leer (HLL). The WAF method was constructed by considering the solution of a Riemann problem at the cell interfaces; which is explained in previous sections. The resulting scheme is second order so it can produce non-physical oscillations, but a corresponding TVD method can be constructed by applying a flux limiter. Satisfactory results are obtained using approximate solvers for the classical dam break problem and circular dam-break problem.

Fraccarollo and Toro (1995) compared numerical results generated by the WAF scheme with experimental data obtained from a dam-break problem. The HLL Riemann solver was used together with a flux limiter to produce the numerical data. The comparison between the experimental and computational results highlighted certain differences, particularly near the dam location. However the overall the numerical approach was seen to predict the predominant flow features.

Toro (2001) presented his exact solver with various methods to be used including the finite volume method.

Bradford and Sanders (2002) published their study on finite volume model for flooding of arbitrary topography. MUSCL scheme with Roe approximate Riemann solver is used, and reported to be an accurate and robust approach for solving the shallow water equations. Special techniques are introduced to overcome difficulties created by the topography.

Caleffi, Valiani and Zanni (2003) compared physical model data and numerical results with a new explicit TVD algorithm. The solution obtained is based on a Godunov type scheme with HLL approximate Riemann solver. Dam-break, circular dam-break, hydraulic jump and partial dam-break problems gave reasonable results except unusual bed changes in the topography.

3.4 Numerical methods used in this study

Godunov type upwind finite volume method is used to solve unsteady, two-dimensional, depth-averaged shallow flow equations derived in section 3.1. Exact Riemann solver introduced by Toro (2001) is adapted to the solution to compute the primitive variables at the interfaces.

3.4.1 Solution Scheme

Let us recall the two dimensional shallow water equation (Eq. 3.26)

$$U_t + F(U)_x + G(U)_y = S(U)$$

where the terms described in Eq. 3.27 will be as follows, noting that the viscous stresses in source term are neglected,

$$U = \begin{bmatrix} h \\ uh \\ vh \end{bmatrix}, F = \begin{bmatrix} uh \\ hu^2 + gh^2/2 \\ huv \end{bmatrix}, G = \begin{bmatrix} vh \\ huv \\ hv^2 + gh^2/2 \end{bmatrix}, S = \begin{bmatrix} 0 \\ -\dfrac{\tau_{bx}}{\rho} \\ -\dfrac{\tau_{by}}{\rho} \end{bmatrix}$$

As can be seen in the source term, viscous stresses are neglected in the current model. The updating conservative formula becomes;

$$U_{i,j}^{n+1} = U_{i,j}^{n} - \frac{\Delta t}{\Delta x}\left[F_{i+1/2,j} - F_{i-1/2,j}\right] - \frac{\Delta t}{\Delta y}\left[G_{i,j+1/2} - G_{i,j-1/2}\right] - \Delta t S_{i,j} \qquad (3.61)$$

where $F_{i+1/2,j}$ is the intercell flux corresponding to the intercell boundary between cells (i,j) and (i+1,j). There are many choices for evaluating this flux; here the Godunov flux is concerned in which the flux is computed from the values at the interfaces. For any cell considered, there exists a Riemann problem to be solved whose data states are $U_{i,j}$ and $U_{i+1,j}$ and the solution is denoted by $U_{i+1/2,j}$. Godunov flux $F_{i+1/2,j}$ at the intercell boundary is defined in terms of the solution obtained, $U_{i+1/2,j}$. Same procedure is used again for the other direction to compute the flux $G_{i,j+1/2}$.

For a cell to be updated to the next time level, all fluxes at the interfaces are computed using the exact Riemann solver. Considering the cell (i,j), $F_{i+1/2,j}$, $F_{i-1/2,j}$, $G_{i,j+1/2}$, $G_{i,j-1/2}$ are used to compute the next time level.

However, when using Riemann solver, choosing the left and right initial data states affects the convergence of the solution. For this reason, initial data states U_L and U_R for an interface are extrapolated from the neighboring cells called as boundary extrapolated values. By this way, the data states to be included in Riemann solution consists of intercell values instead of center values. In order to avoid the numerical oscillations, a constraint is enforced in data reconstruction step by limiting the slopes when extrapolating. If the slope of any variable between cell centers is denoted by Δ_i, the limited slopes are;

$$\bar{\Delta}_i = \begin{cases} \max\left(0, \min\left(\beta\Delta_{i-1/2}, \Delta_{i+1/2}\right), \min\left(\Delta_{i-1/2}, \beta\Delta_{i+1/2}\right)\right), & \Delta_{i+1/2} > 0 \\ \min\left(0, \max\left(\beta\Delta_{i-1/2}, \Delta_{i+1/2}\right), \max\left(\Delta_{i-1/2}, \beta\Delta_{i+1/2}\right)\right), & \Delta_{i+1/2} < 0 \end{cases} \quad (3.62)$$

Then this value is used instead of the Δ_i. The parameter β is a limiting variable and β=1 reproduces the Minbee limiter, while β=2 produce the Superbee, in this study Minbee is used (Toro, 2001). Using this limited slope, extrapolation is carried out as; $W_{i,j}^{L} = W_{i,j} - \frac{1}{2}\bar{\Delta}_i \Delta x$.

3.4.2 Initial and Boundary Conditions

Initial conditions are specified in the whole domain as the water depth and velocity values of the inflow boundary.

Three types of boundary conditions are specified, inflow, outflow and wall boundaries. Wall boundaries are specified as slip boundary conditions. The values of water depth and velocity component tangent to the boundary are given as the same with the boundary cell and the velocity component normal to the boundary is given reverse. For inflow boundaries surface data obtained from the experiments are given and kept constant during the solution. Velocity is given as uniform which is an acceptable assumption as illustrated in Fig. 2.3. For the outflow boundary, again the experimental surface data is given to the boundary nodes. The other variables (velocity components) are extrapolated from the domain.

3.4.4 Source Terms

Source terms coming from viscous stresses are neglected and since the solution is computed on a horizontal channel bottom slope term automatically vanishes. Bottom friction is modeled according to the following formulas (Kuipers and Vreugdenhil 1973):

$$\tau_{bx} = \rho g h \frac{n^2 u \sqrt{u^2 + v^2}}{h^{4/3}} \text{ and } \tau_{by} = \rho g h \frac{n^2 v \sqrt{u^2 + v^2}}{h^{4/3}}$$

The Manning's coefficient is taken as 0.01 for the plexiglas used.

3.4.5 Convergence and Stability

In practical computations, one chooses a value of CFL close to the maximum allowed. For non-linear systems such as the shallow flow equations, a reliable estimate for time step must be found which is given below. An unreliable estimate may cause the scheme to crash no matter how sophisticated the intercell fluxes are computed. The recommended CFL for two-dimensional shallow flows is CFL<0.5. In the present study CFL = 0.4 is used unless a problem is faced.

$$\Delta t_x = \frac{CFL.\Delta x}{S^x{}_{max}} \quad , \quad \Delta t_y = \frac{CFL.\Delta y}{S^y{}_{max}} \quad , \quad S^k{}_{max} = \max_{i,j} \left\{ \left| u_{i,j} \right| + a_{i,j} \right\}$$

Time step is determined using the minimum of the time steps computed in both directions.

3.4.6 Solution procedure

The cell average values in a cell are updated to next time level with Eq. 3.61. in a single step, involving flux contributions from all intercell boundaries. This conservative formula is the extension of the one-dimensional formulation and it is completely determined once the intercell numerical fluxes are specified. After observing the behavior of the errors with time for all the cases, a maximum of 40 seconds is realized to be sufficient to reach the steady state.

However, computer was run for 90 seconds and the solution was obtained by taking time average of all variables from 60 seconds to 90 seconds to eliminate the noise in the computed values. The algorithm used is as follows;

1. Specify the initial conditions for primitive variables
2. Calculate the time step using CFL condition
3. Specify the boundary conditions
4. Update the Riemann problem variables using a slope limiter
5. Solve the Riemann problem for all interfaces as explained in section 3.3.2.3
6. Compute the primitive variables for next time step using Eq. 3.61
7. Go to step 2, if output time is not reached yet.

CHAPTER 4

RESULTS AND DISCUSSIONS

4.1 Test Cases

The capabilities and performance of the numerical scheme for the solution of the shallow water equations is illustrated by considering several test cases given in the literature. The test cases considered are one-dimensional dam break for different conditions and a two-dimensional dam break case. Since the examples are from literature, all the details of how they are set up are not given here.

4.1.1 Test Case 1 : One –Dimensional Dam Break 1

This example is generally used to illustrate shock-capturing capabilities of the schemes and it is used by several researchers to compare Riemann solvers with each other and to compare schemes with first or higher order accuracies.

The problem is set-up as follows: A dam is initially situated in the middle of the domain. The initial condition is given as 5 m water depth at the upstream of the dam and 0.3 m water depth at the downstream. The dam is removed instantaneously and the model is run for 10 seconds. The computational domain is divided into 300 cells. The size of each cell is 1x1 m

Table 4.0-1. Comparison of one-dimensional dam break results, Test Case 1

Table 4.1. Comparison of one-dimensional dam break results, Test Case 1

Scheme	Velocity at dam site (m/s)	Water depth at dam site (m)
Exact	4.670	2.220
Osher	4.661	2.222
FVS	4.463	2.316
HLL	4.459	2.285
HLLC	4.459	2.285
Roe	4.717	2.212
Roe entropy fixed	4.639	2.233
Current study	4.659	2.221

Comparison of the results of the present model and others taken from Erduran *et.al.*(2002) is shown in Table 4.1. Current model computes the velocity and water depth at the dam site more accurate than the other models except the model using Osher's Riemann solver for velocity. When the water depth is considered current model gives the most accurate result.

4.1.2 Test Case 2 : One –Dimensional Dam Break 2

The problem is set-up as follows; A dam is initially situated in the middle of the domain. The initial flow condition is given as 10 m water upstream of the dam and 0.0 m water depth downstream. The dam is removed instantaneously and the model is run for 50 seconds. The computational domain is 2000 meters. The cell size is varied to observe the mesh size and accuracy relationship. Figure 4.1 shows the solution for two different mesh sizes and the analytical solution. Analytical solution stated in the paper by Zoppou and Roberts(2003) is given in Table 4.2, where h_0 denotes the initial upstream depth and h_1 denotes the initial downstream depth.

Table 4.2. Analytical solution of one-dimensional dam break problem (Zoppou , Roberts (2003)), Test Case 2.

Table 4.2. Analytical solution of one-dimensional dam break problem (Zoppou , Roberts (2003)), Test Case 2.

Range	Analytical solution
$x \leq -t\sqrt{gh_0}$	$u = 0$ $h = h_0$
$-t\sqrt{gh_0} < x \leq 2t\sqrt{gh_0}$	$u = \frac{2}{3}\left(\sqrt{gh_0} + \frac{x}{t}\right)$ $h = \frac{4}{9g}\left(\sqrt{gh_0} - \frac{x}{2t}\right)^2$
$2t\sqrt{gh_0} \leq x$	$u = 0$ $h = h_1$

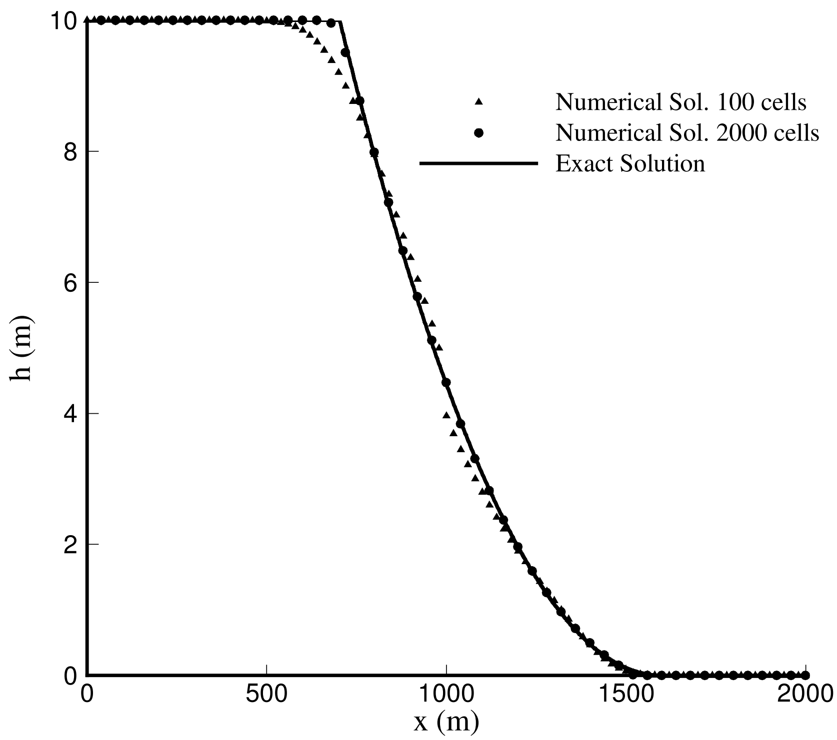

Figure 4.1. Comparison of analytical and numerical solutions of one-dimensional dam break problem, Test Case 2.

This example shows the importance of mesh size on the accuracy of the solution, but the point must be considered is the efficiency of the model. The more accurate results are obtained with the longer computational times. For this test case run time ratio was 1:15 considering the solutions with 100 cells and 2000 cells.

4.1.3 Test Case 3: Two –Dimensional Dam Break

The aim of this test case is to study the code ability to reproduce discontinuous solutions with particular attention to two-dimensionality of the flow field. The problem is set-up as follows; the geometry of the problem consists of a 200 x 200 m basin as illustrated in Figure 4.2. The initial water level of the dam is 10 m and the tail water is 5 m high. At the instant of dam failure, water is released into the downstream side through a breach 75 m wide, forming a wave that propagates while spreading laterally. At the same time a negative wave propagates upstream. The problem domain was discretisized into 1x1 m meshes and the computational model was run for up to 7.2 s after the dam break. Fig. 4.3.a and 4.3.b show the three-dimensional view of the water surface plots for the present study and from Anastasiou and Chan(1997) respectively.

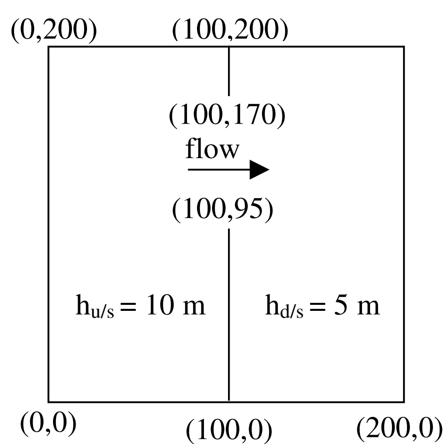

Figure 4.2. Definition of problem domain for two-dimensional dam break, Test Case 3.

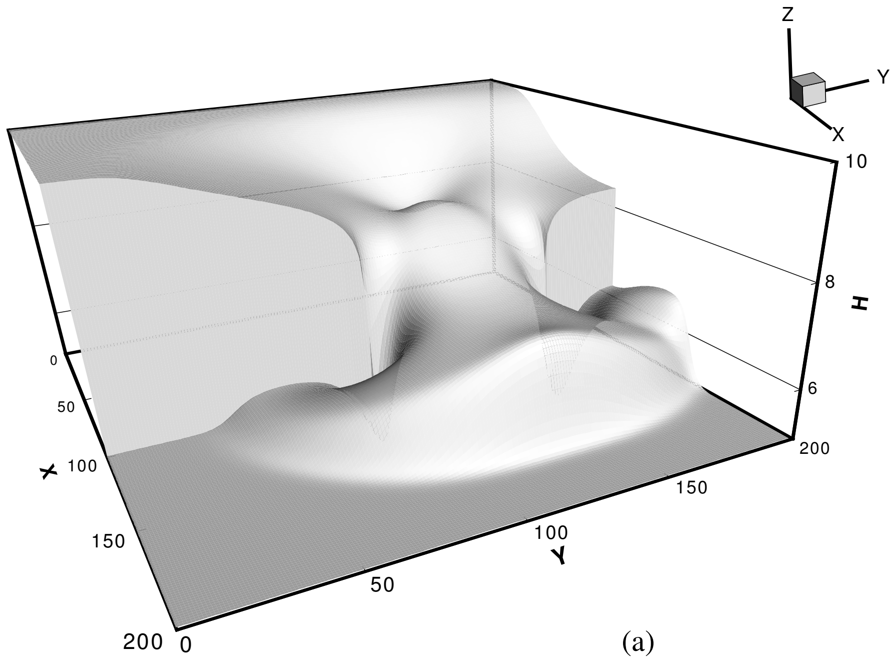

(a)

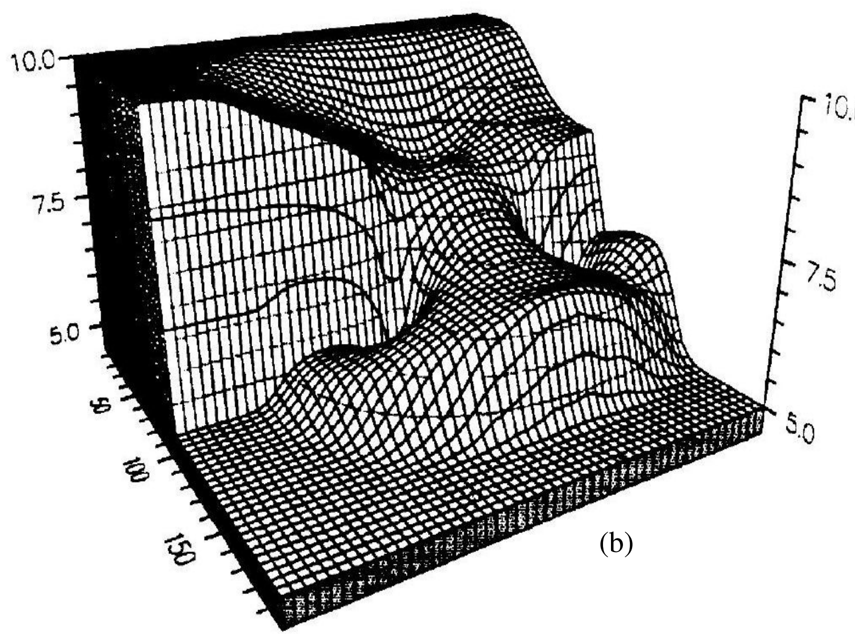

(b)

Figure 4.3. Surface plot of two-dimensional dam break problem, Test Case 3 (a) Solution with the current model. (b) Solution by Anastasiou and Chan (1997).

As illustrated in Fig. 4.3., the flow is characterized by a rarefaction wave traveling upstream and a shock wave traveling downstream, spreading of wave laterally can be easily observed in the figure. Unlike the one-dimensional problem there is no exact results for this test so accuracy cannot be discussed, but the solution given in Figure 4.3.b is taken from accepted results in the literature.

4.2 Free surface Profiles

The computed surface profile plots corresponding to the present experimental cases are given in Figures 4.4.~4.9. In general, computed surface patterns reproduce the measured surface profiles with exception of Case A2 and Case C2. The solutions in these two cases have large numerical oscillations which could not be damped by the selected slope limiter.

To focus on the variation of water depth in the flume, six cross-sectional profiles and one longitudinal profile are plotted for each case described in Table 2.1. For the cross-sectional figures, water levels are shown as minimum, maximum and time-averaged values for the numerical study and minimum and maximum values for the experimental study at the stations x = 0, 1, 1.5, 2, 2.5, 3 meters across the channel. For the longitudinal figures profiles along the centerline (y=0.33 m) of the flume are plotted. These comparisons are given in Figures 4.10~4.21. The differences between minimum and maximum readings of the water levels in the experiments are small, indicating small fluctuations of the water surface. However, in the numerical computations there are very large positive oscillations which cause the time average values to differ from the experimental values.

4.3 Velocity Profiles

The velocity profile from the experimental study is unavailable. For the sake of completeness, velocity profile at a specified case (B1) is plotted as a sample and the two-dimensionality of the velocity field is shown in Fig. 4.22 by giving a plan view of the velocity field.

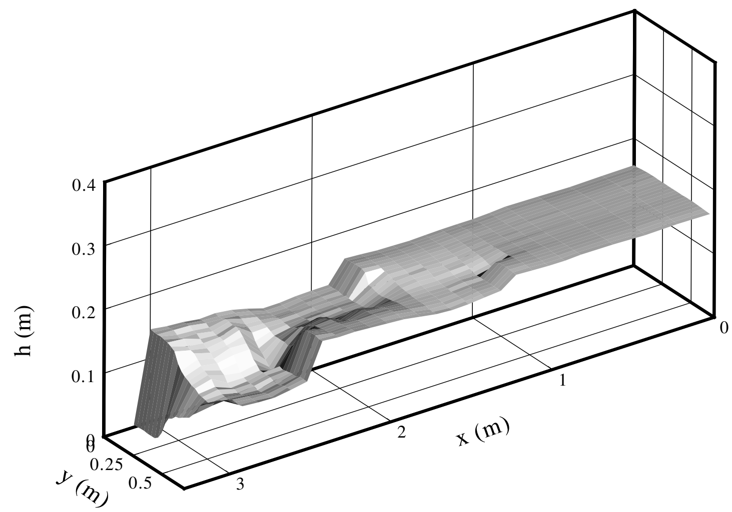

Computed

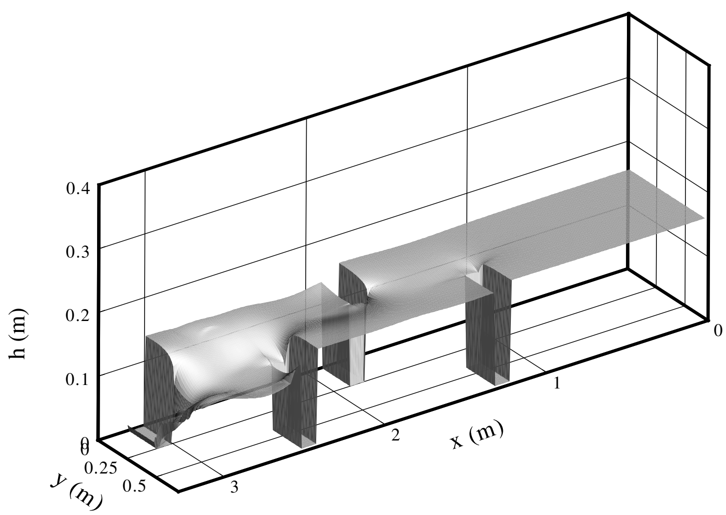

Figure 4.4. Water surface profiles, Case A1

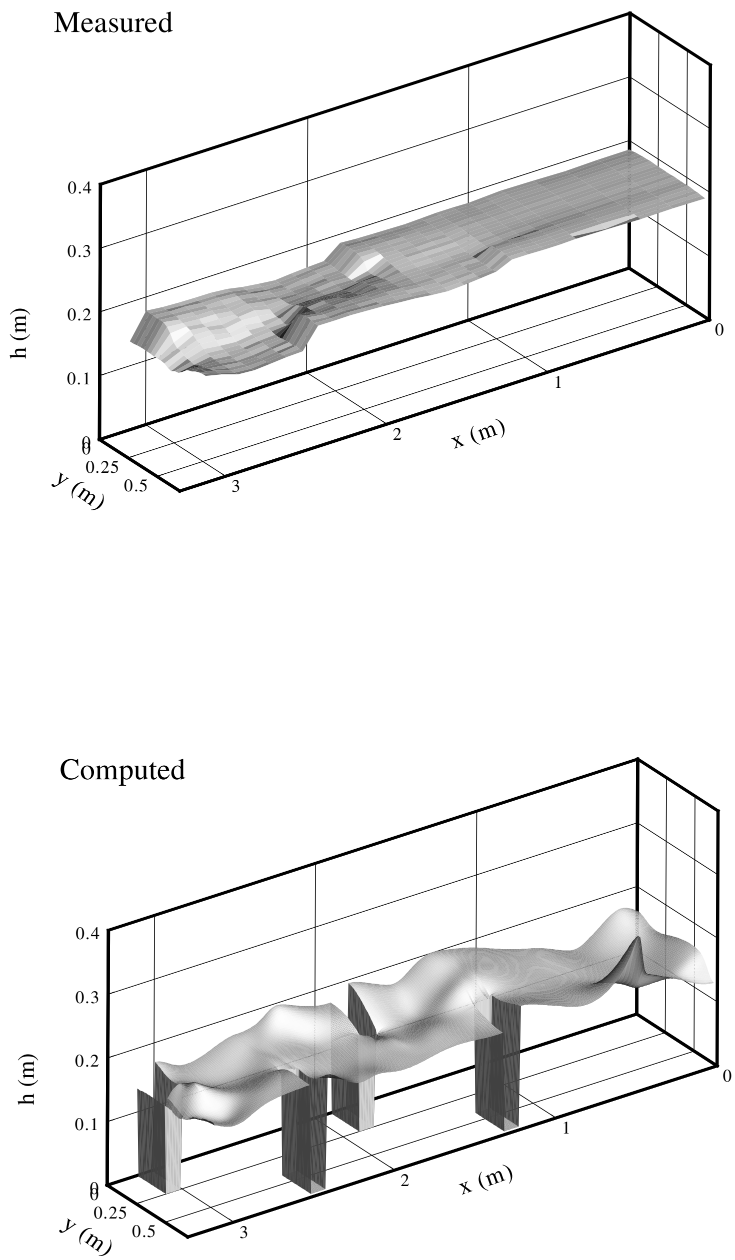

Figure 4.5. Water surface profiles, Case A2

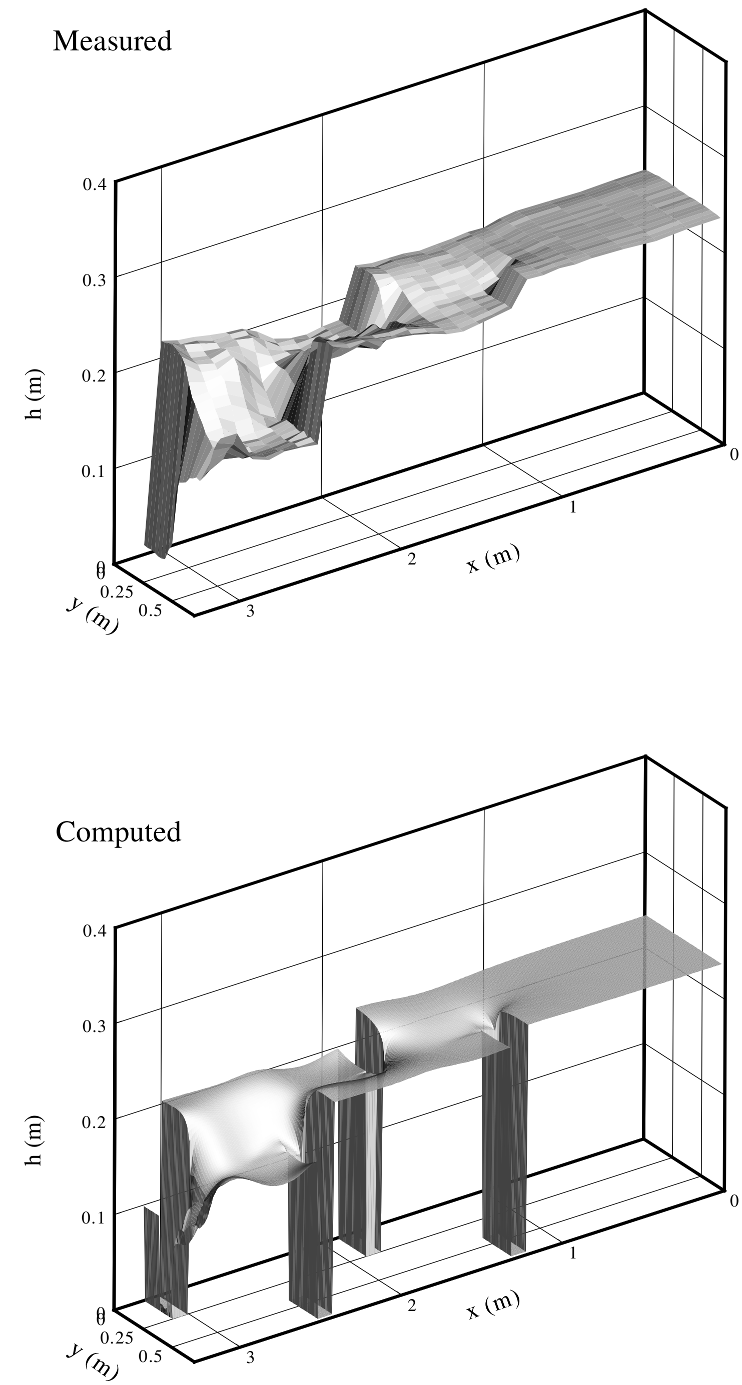

Figure 4.6. Water surface profiles, Case B1

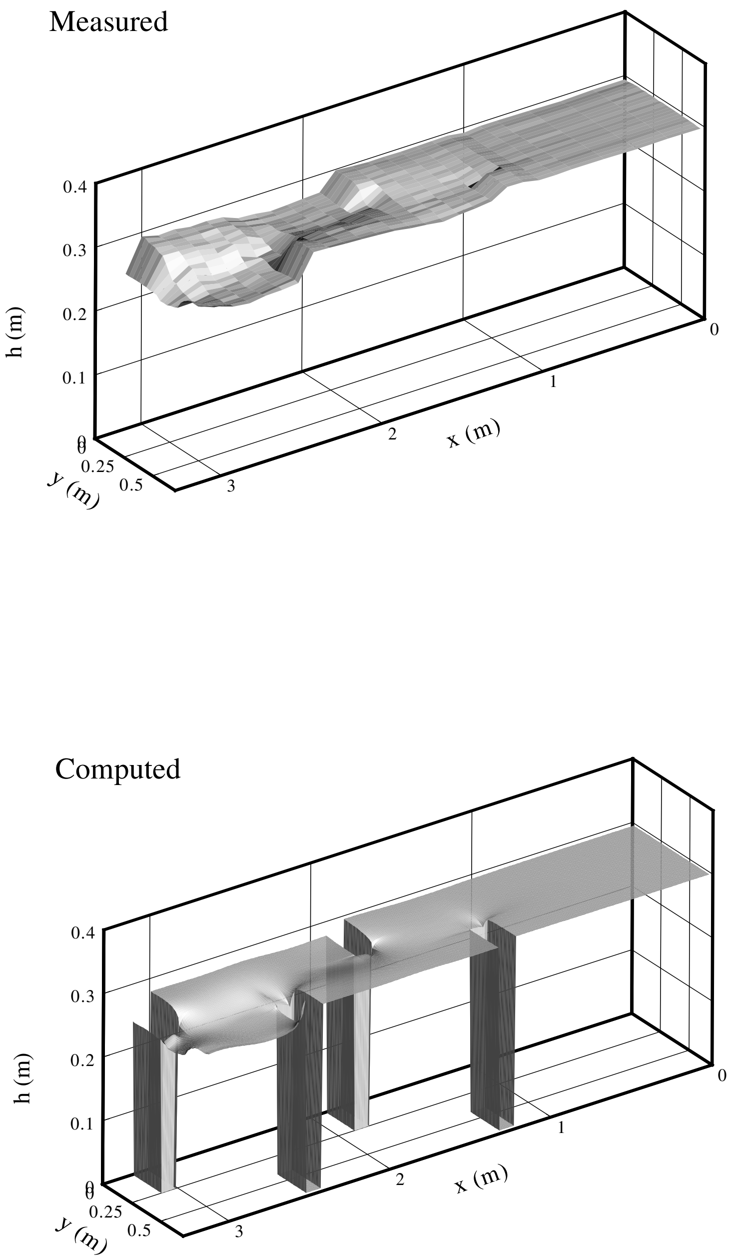

Figure 4.7. Water surface profiles, Case B2

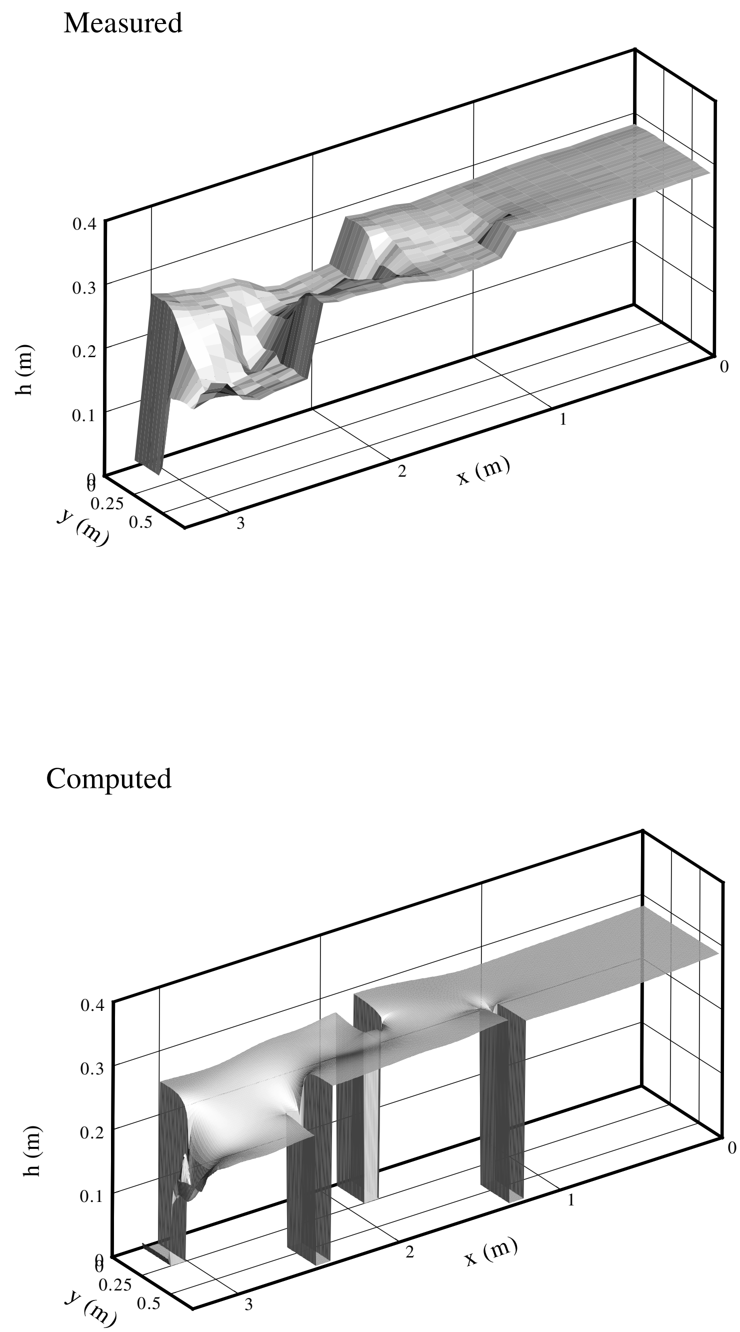

Figure 4.8. Water surface profiles, Case C1

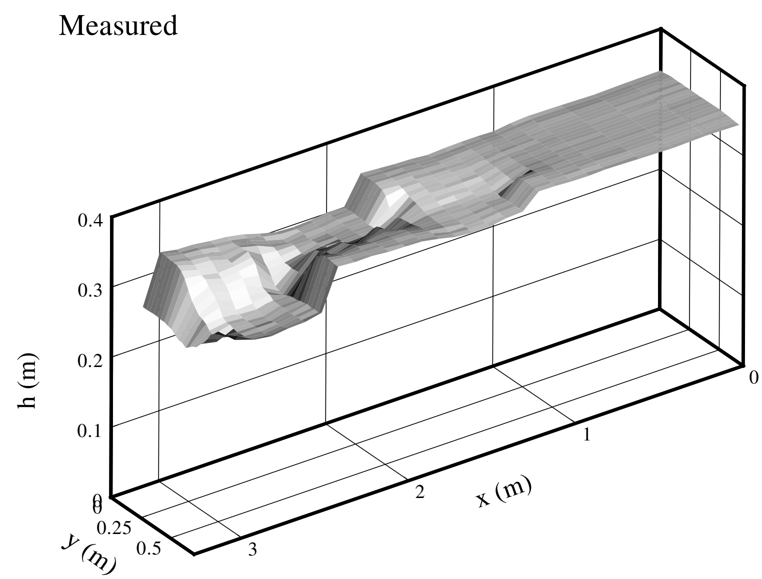

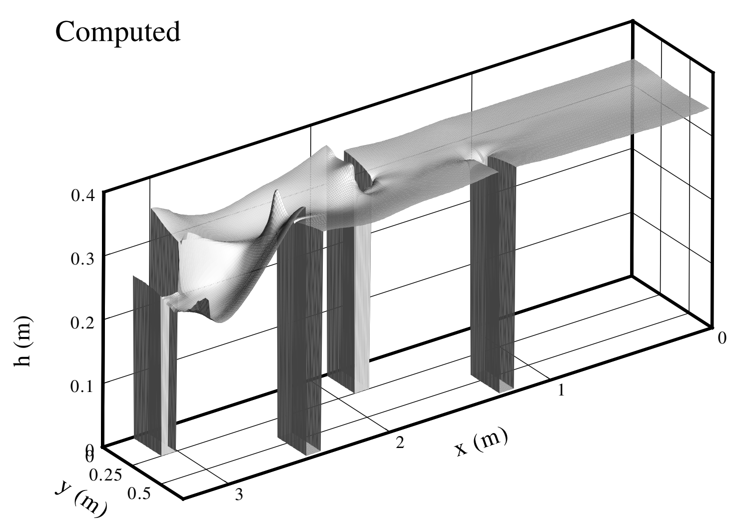

Figure 4.9. Water surface profiles, Case C2

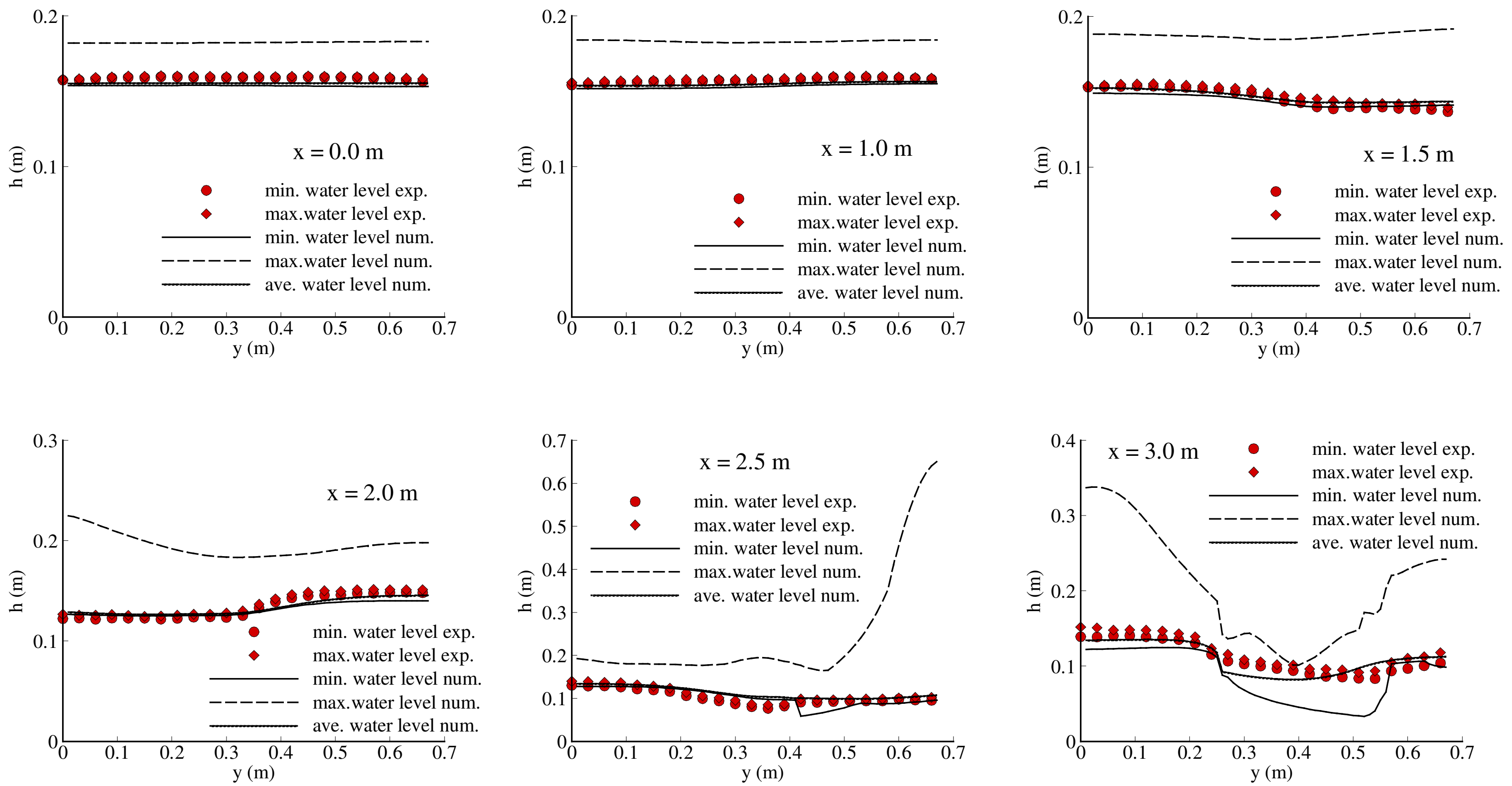

Figure 4.10. Comparison of measured and computed water surface profiles at certain cross-sections, Case A1

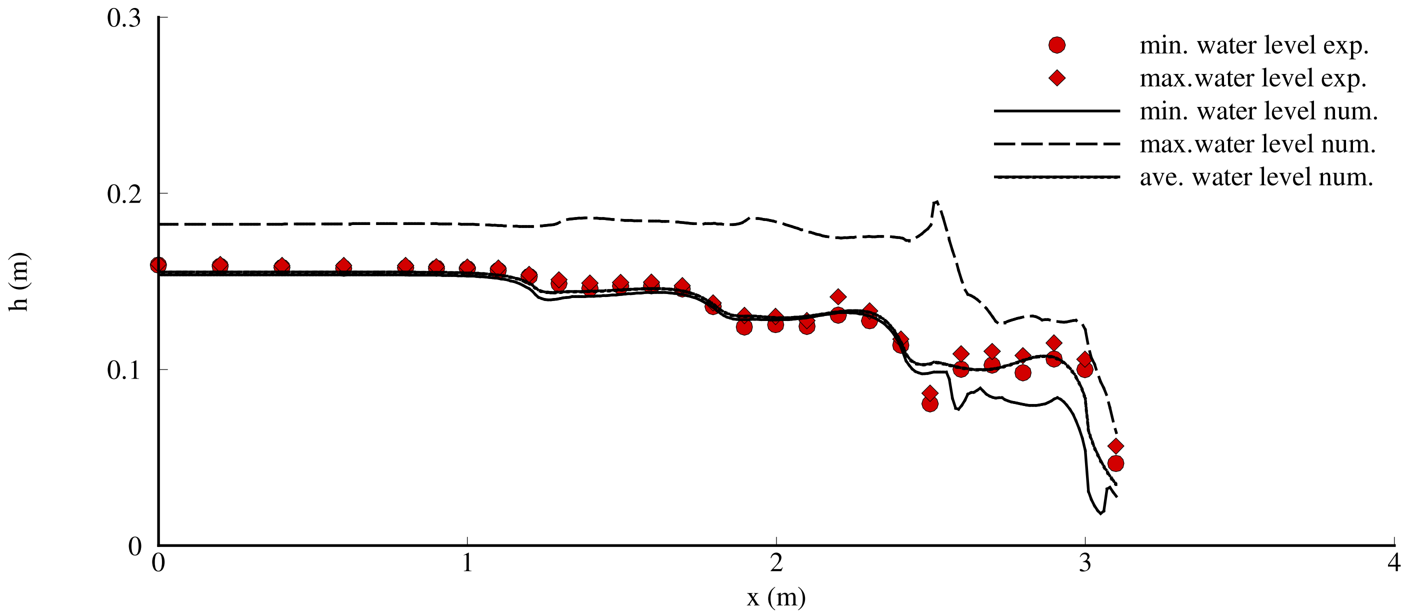

Figure 4.11. Comparison of measured and computed water surface profiles along the channel centerline, Case A1

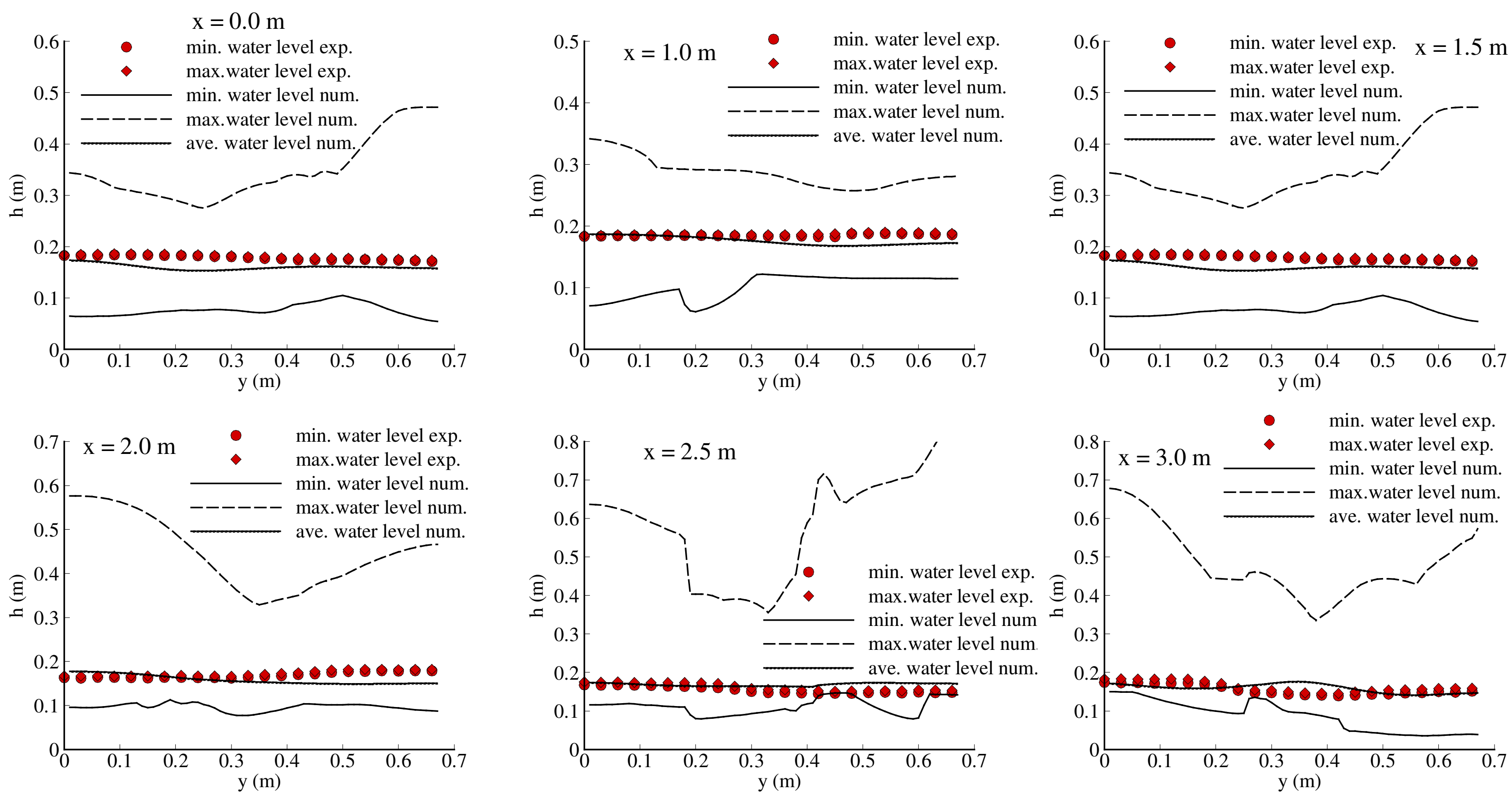

x = 0.0 m
x = 1.0 m
x = 1.5 m
x = 2.0 m
x = 2.5 m
x = 3.0 m
min. water level exp.
max.water level exp.
min. water level num.
max.water level num.
ave. water level num.
h (m)
y (m)

Figure 4.12. Comparison of measured and computed water surface profiles at certain cross-sections, Case A2

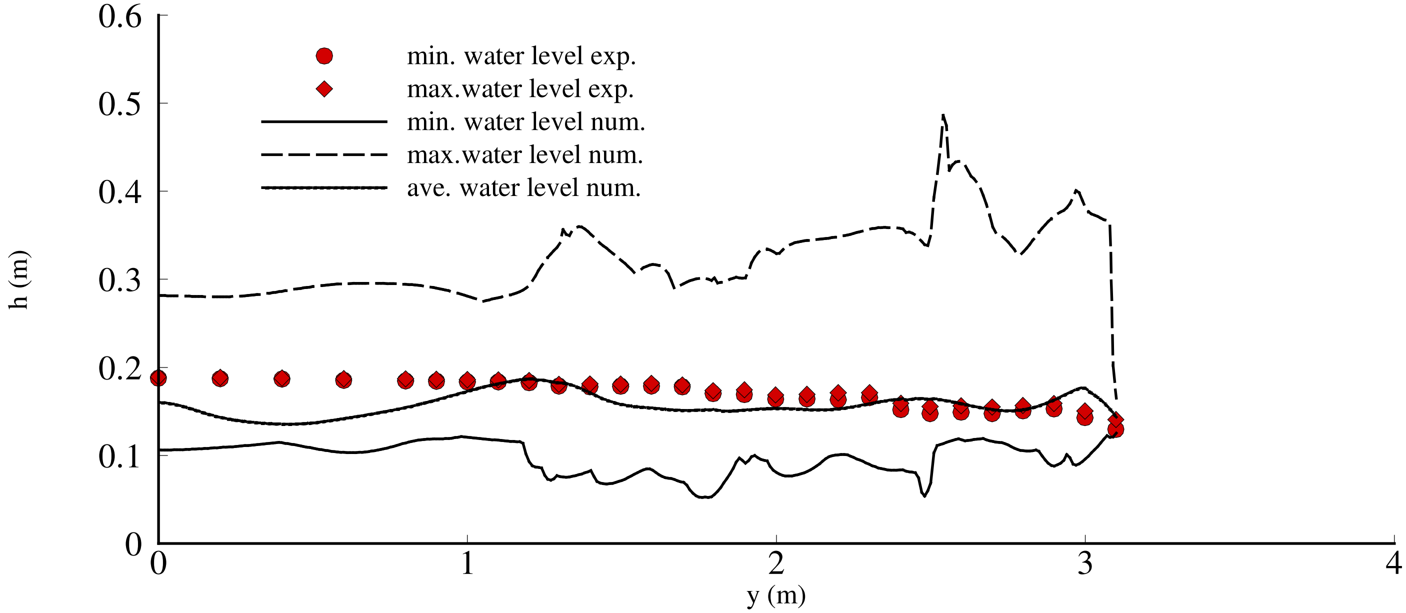

Figure 4.13. Comparison of measured and computed water surface profiles along the channel centerline, Case A2

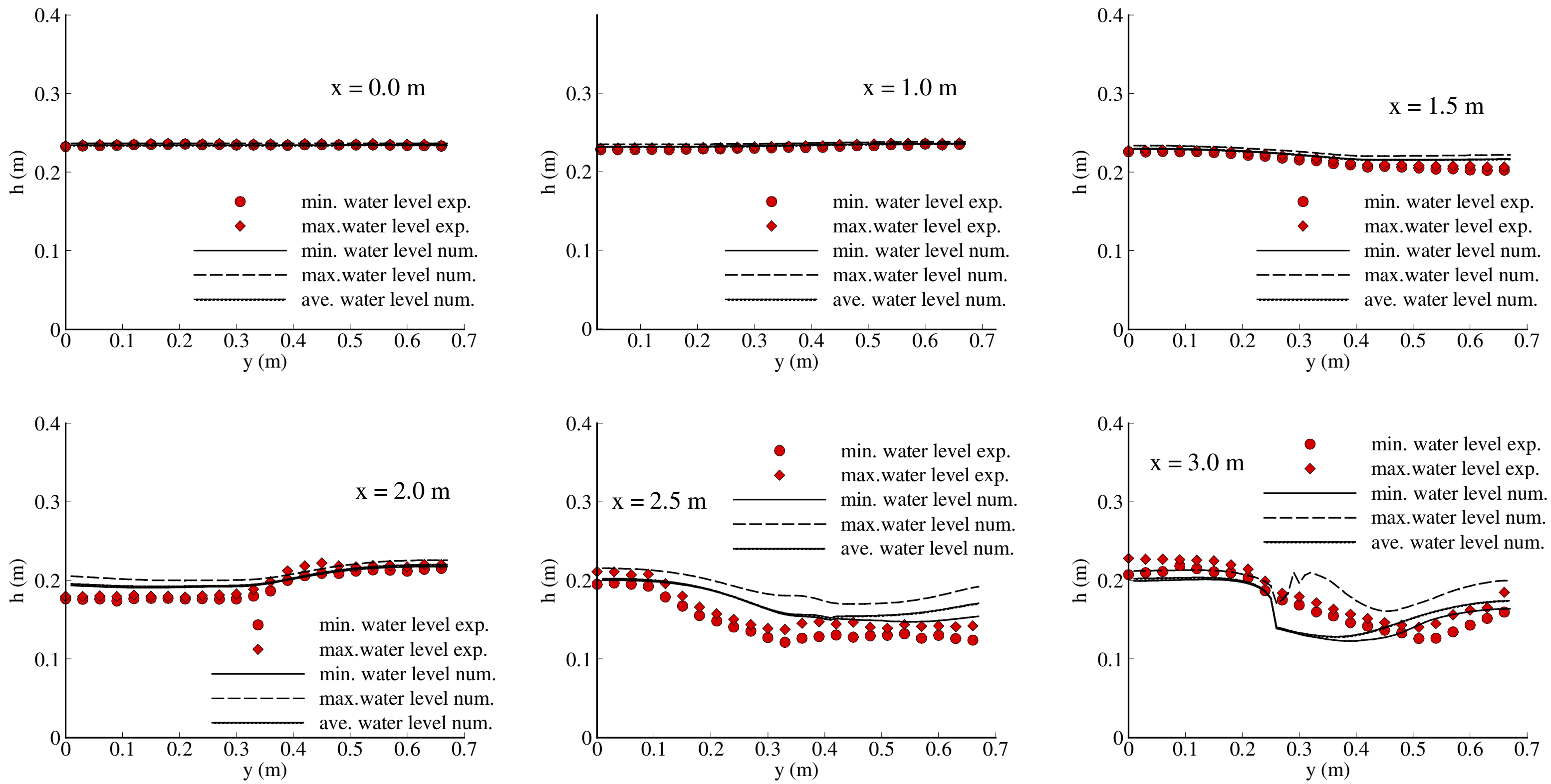
x = 0.0 m
x = 1.0 m
x = 1.5 m
x = 2.0 m
x = 2.5 m
x = 3.0 m
min. water level exp.
max.water level exp.
min. water level num.
max.water level num.
ave. water level num.
h (m)
y (m)

Figure 4.14. Comparison of measured and computed water surface profiles at certain cross-sections, Case B1

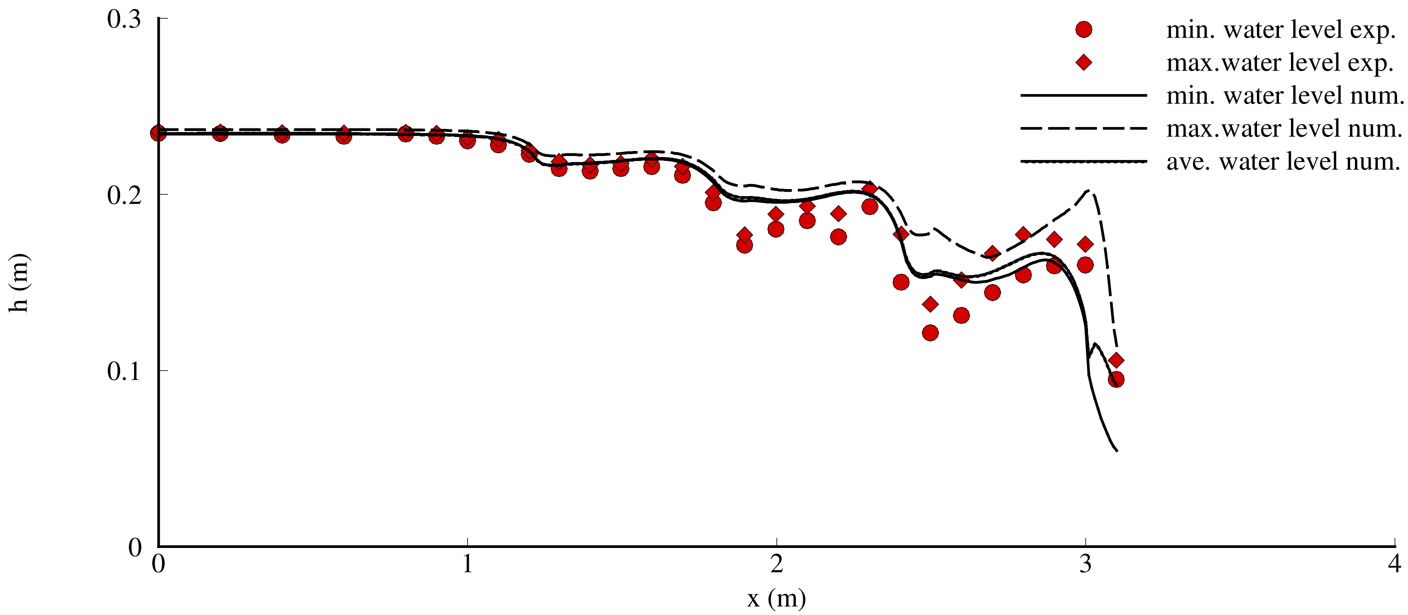

Figure 4.15. Comparison of measured and computed water surface profiles along the channel centerline, Case B1

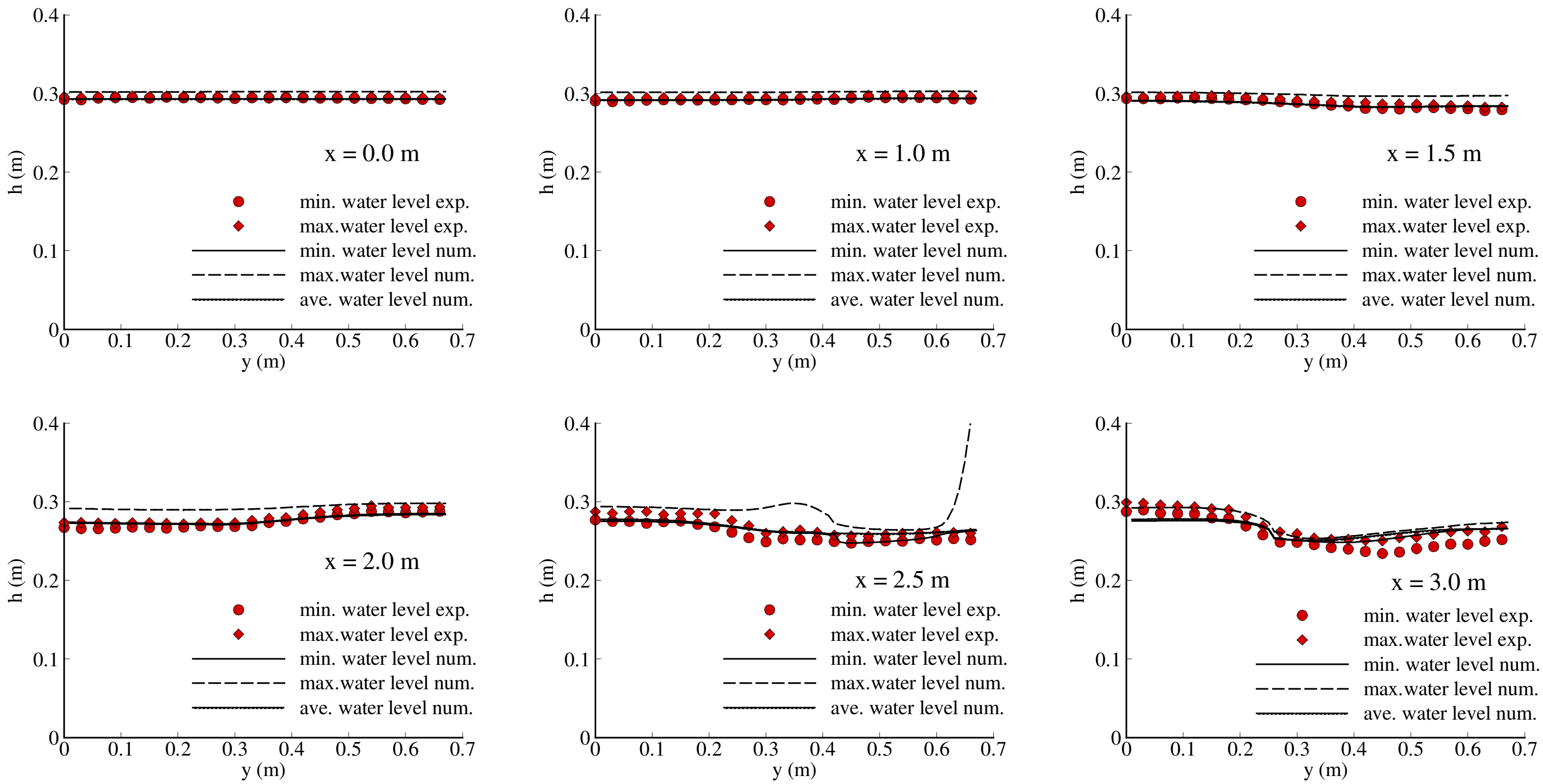

x = 0.0 m
x = 1.0 m
x = 1.5 m
x = 2.0 m
x = 2.5 m
x = 3.0 m
min. water level exp.
max.water level exp.
min. water level num.
max.water level num.
ave. water level num.
h (m)
y (m)

Figure 4.16. Comparison of measured and computed water surface profiles at certain cross-sections, Case B2

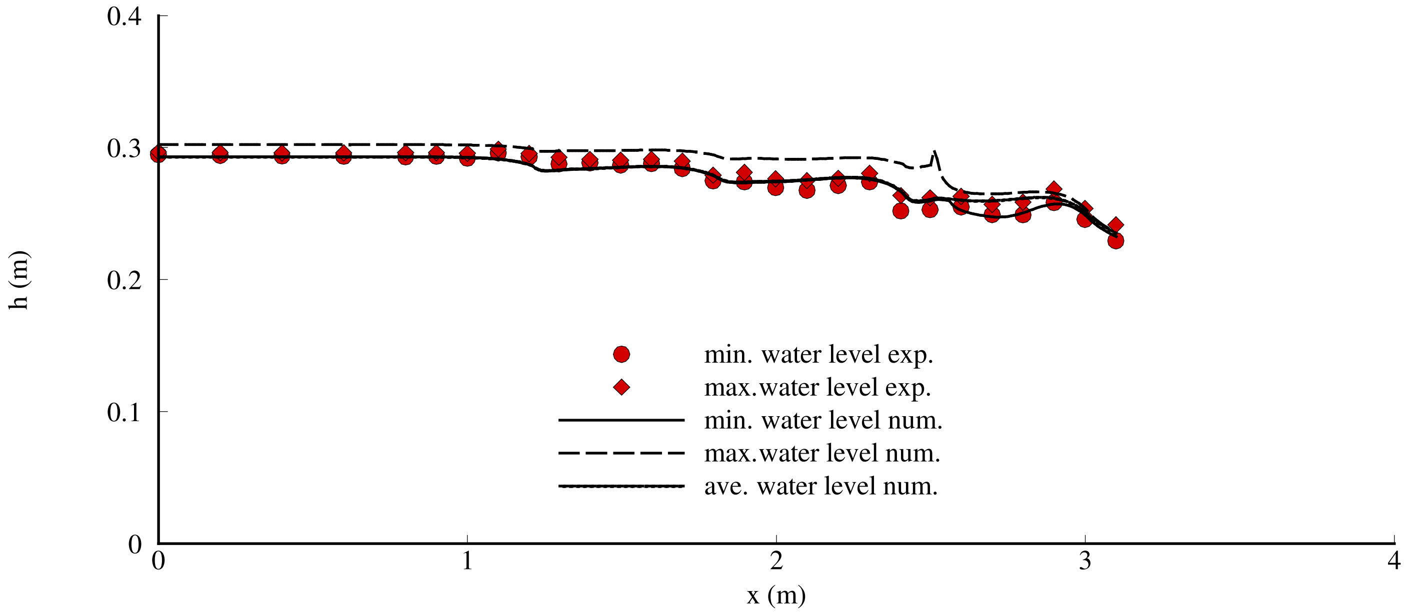

Figure 4.17. Comparison of measured and computed water surface profiles along the channel centerline, Case B2

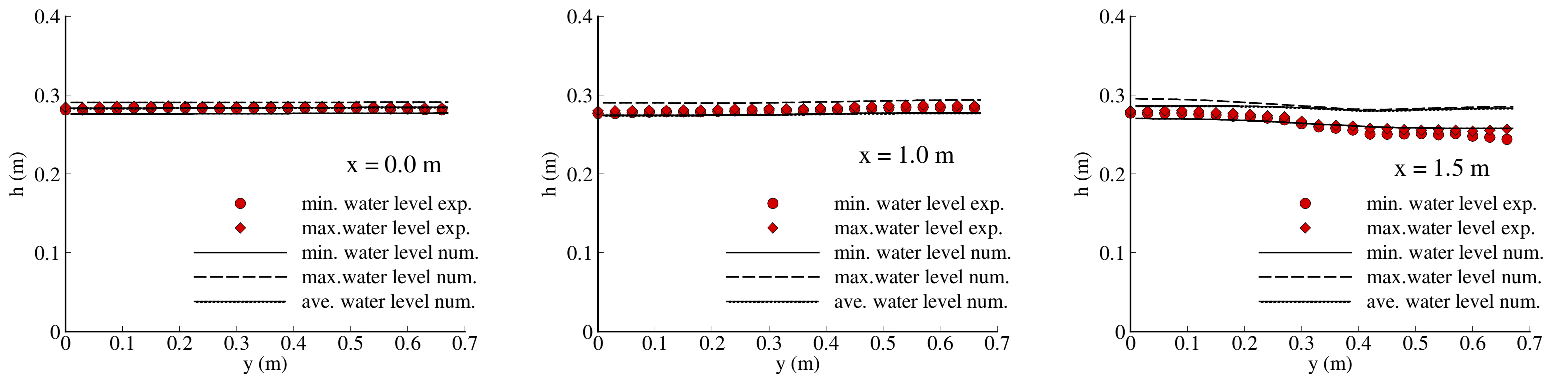

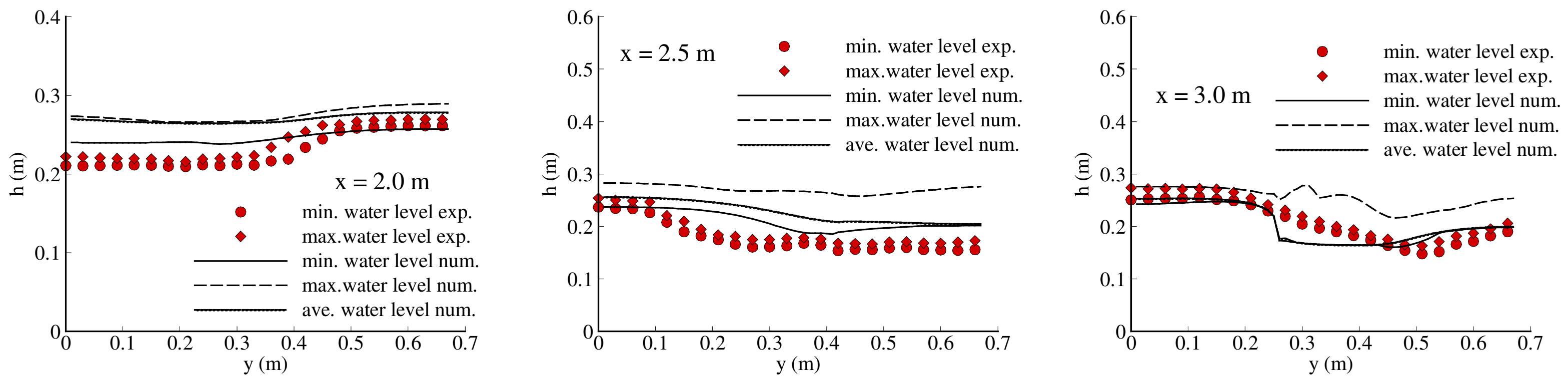

Figure 4.18. Comparison of measured and computed water surface profiles at certain cross-sections, Case C1

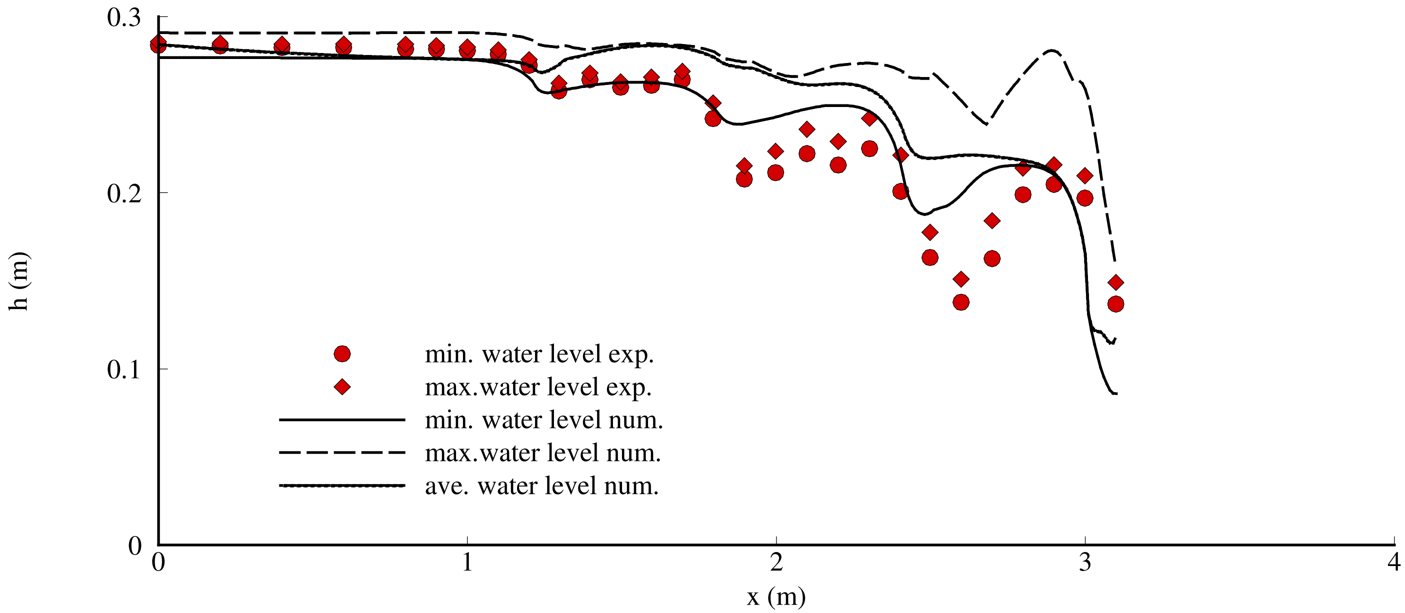

Figure 4.19. Comparison of measured and computed water surface profiles along the channel centerline, Case C1

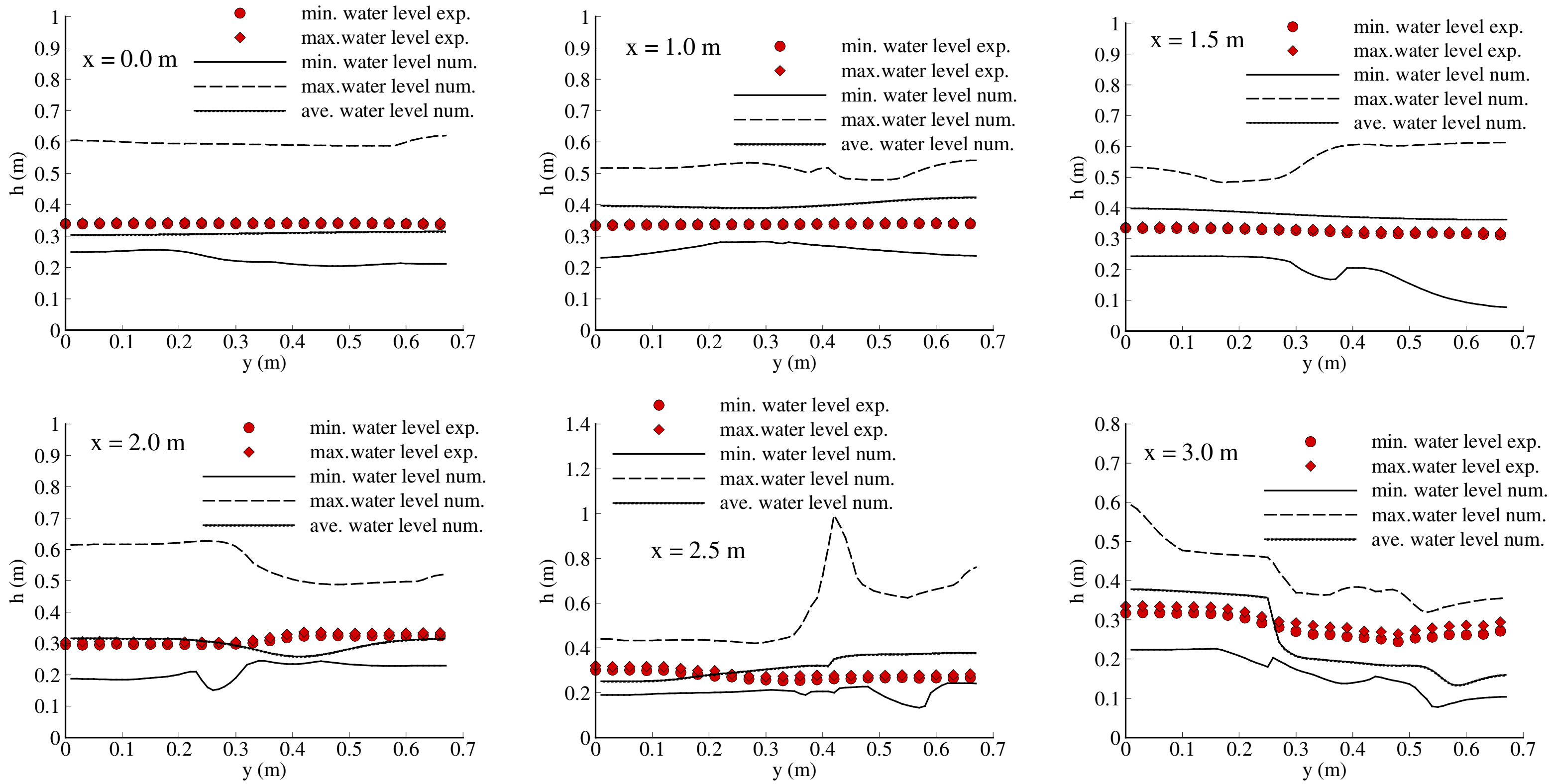

Figure 4.20. Comparison of measured and computed water surface profiles at certain cross-sections, Case C2

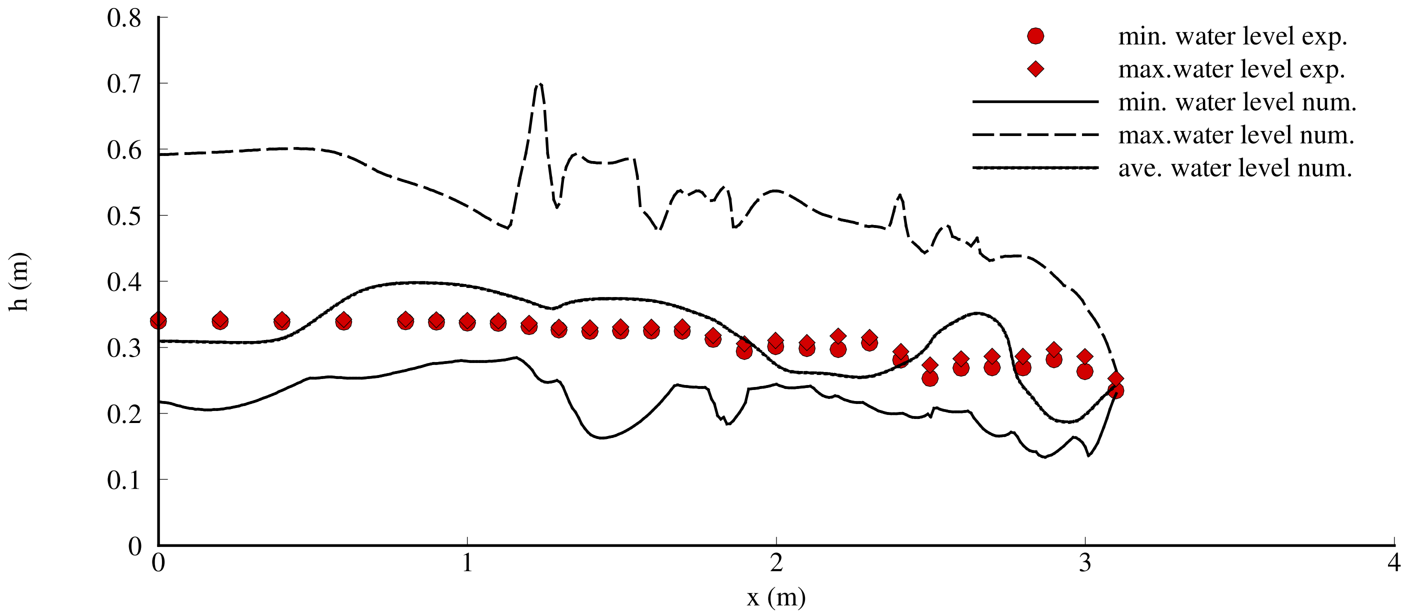

Figure 4.21. Comparison of measured and computed water surface profiles along the channel centerline, Case C2

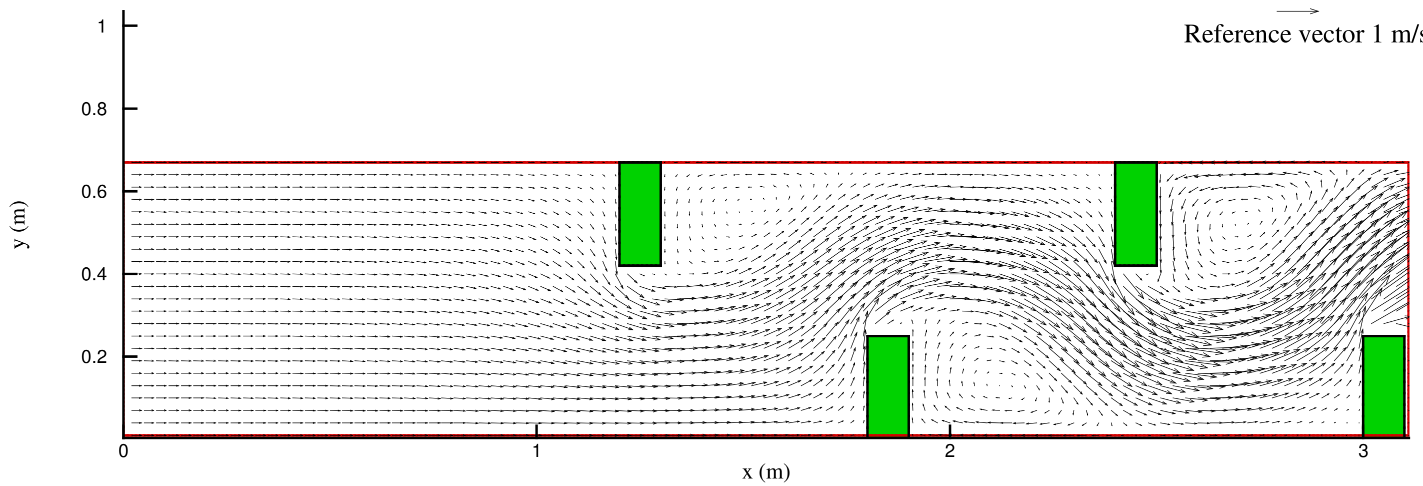

Figure 4.22. Velocity vector field, Case B1

4.4 Final Remarks

As the comparisons of test cases and experimental cases with the numerical results are considered, it can be said that the current model is an acceptable and accurate model for one-dimensional problems and some of the two-dimensional problems. It is observed by Molls and Chaudhry (1995) that viscous stresses do not significantly affect the converged solution excluding recirculating flows. In the present experimental cases the flow is recirculating behind the boxes and there are strong vortex structures. Therefore, the experimental cases may need to be studied using the viscous stresses for more accurate results. In numerical computation of some experimental cases such as case A2 and C2, unacceptable oscillations of water surface levels are present which prevent a converged solution. This result may be due to failure of slope limiter used in extrapolations. On the other hand, viscous dissipation may be necessary to damp such oscillations.

In numerical solutions, water levels on downstream faces of the solid boxes on the sidewalls are usually higher than the measured values. Such differences between measured and computed fields may be a result of energy losses in the real flow due to recirculation around the boxes. It is necessary to include a turbulence model into the computer code to simulate the complicated flow patterns.

CHAPTER 5

CONCLUSIONS

A computer code is developed for Godunov type numerical solution of two-dimensional depth-averaged shallow water equations using exact Riemann solver in finite volume scheme.

- The code produced satisfactory results for the one-dimensional test cases for which analytical solutions are available. It can be used for dam-break analysis and one-dimensional study of flood waves.
- The code can be used to compute the two-dimensional shallow flows. However, when the flow field is affected by sidewalls in a narrow domain , the shallow water assumption is not justified. If the code is to be used in such complicated flow fields for free surface computations, an appropriate turbulence model must be incorporated to account for turbulent stresses.
- Approximate Riemann solvers may be used instead of exact Riemann solver to reduce cpu requirements.

REFERENCES

Addison, H. (1954). “A Treatise On Applied Hydraulics”, New York, John Wiley & Sons Inc.

Alcrudo, F., Garcia-Navarro, P. and Saviron, J. (1992). “Flux Difference Splitting For 1-d Open Channel Flow Equations”, Int. J. Numer. Methods in Fluids, 14, 1009-1018.

Alcrudo, F., Garcia-Navarro, P., Saviron, J. (1992). “1-d Open Channel Flow Simulation Using TVD-McCormack Scheme”, J Hydr. Eng., ASCE, 118, 1359-1372.

Anastasiou, K. and Chan, C., (1997). “Solution of 2d Shallow Water Equations Using Finite Volume Method on Unstructures Triangular Meshes”, Int. J. Numer. Methods in Fluids, 24, 1225-1245.

Bradford, S.F. and Sanders B.F. (2002). “Finite Volume Model for Shallow-Water Flooding of Arbitrary Topography”, J Hydr. Eng., ASCE, 113, 289-298.

Caleffi, V., Valiani, A. and Zanni, A. (2003). “Finite Volume Method for Simulating Extreme Events in Natural Channels”, J Hydr. Res., IAHR, 41-2, 167-177.

Courant R., Isaacson, E., and Rees, M. (1952). “On the Solution of Nonlinear Hyperbolic Differential Equations by Finite Differences”, Comm. Pure App. Math., 5, 243-255.

Cunge, J.A., Holly, F.M. and Verwey, A. (1994). "Practical Aspects of Computational River Hydraulics", New York, Pitman Publishing Ltd.

Erduran, K.S., Kutija, V. and Hewett, C.J.M. (2002). "Performance of Finite Volume Solutions to the Shallow Water Equations with Shock-capturing Schemes", Int. J. Numer. Methods in Fluids, 40, 1237-1273.

Fennema, R. and Chaudhry, M. (1986). "Explicit Numerical Schemes for Unstedy Free-surface Flows with Shocks", Water Resources Research, 22, 1923-1930.

Fennema, R. and Chaudhry, M. (1989). "Implicit Methods For Two-dimensional Free Surface Flows", J. Hydr. Res., 27, 321-332.

Fraccolo, L. and Toro, E., (1995). "Experimental and Numerical Assessment of the Shallow Water Model for Two-dimensional Dam-break Type Problems", J. Hydr. Res., 33, 843-864.

Garcia-Navarro, P. and Saviron, J. (1992). "McCormack's Method For the Numerical Simulation of One-dimensional Discontinuous Unsteady Open Channel Flow", J Hydr. Res., 30, 95-105.

Henderson, F. M. (1966). "Open Channel Flow", New York, Macmillan Publishing Co. Inc.

Hirsch, C. (1988). "Numerical Computation of Internal and External Flows, Vol. 1", Wiley

Hirsch, C. (1990). "Numerical Computation of Internal and External Flows, Vol. 2", Wiley

King, H.W. (1954). “Handbook of Hydraulics”, New York, McGraw Hill Book Company, Inc.

Kuipers, J. and Vreugdenhill, C. B. (1973). “Calculations of two-dimensional horizontal flow.” Rep. S163, Part 1, Delft Hydraulics Lab. Delft, The Netherlands.

Molls, T. and Chaudhry, M.H. (1995). “Depth-averaged Open-Channel Flow Model”, J Hydr. Eng., ASCE, 113, 453-465

Smith, G. (1985). “Numerical Solution of Partial Differential Equations”, Oxford,

Toro, E.F. (1992). “Riemann Problems and the WAF Method for Solving the Two-dimensional Shallow Water Equations”, Phil. Trans. R. Soc. Lond., 338, 43-68.

Toro, E.F. (1997). “Riemann solvers and numerical methods for fluid dynamics:an introduction”, Heidelberg-Berlin, Springer-Verlag.

Toro, E.F. (2001). “Shock-Capturing Methods for Free-Surface Shallow Flows”, Chichester, John Wiley & Sons, Ltd

Yang, J.Y., Hsu, C.A. and Chang S.H. (1993). “Computations of Free Surface Flows, I: One-dimensional dam-break flow”, J Hydr. Res., IAHR, 31(1), 19-34.

Zoppou, C. and Roberts, S. (2003). “Explicit Schemes for Dam-Break Simulations”, J Hydr. Eng., ASCE, 1, 11-34.

APPENDIX A

PHOTOGRAPHS FROM THE EXPERIMENTS

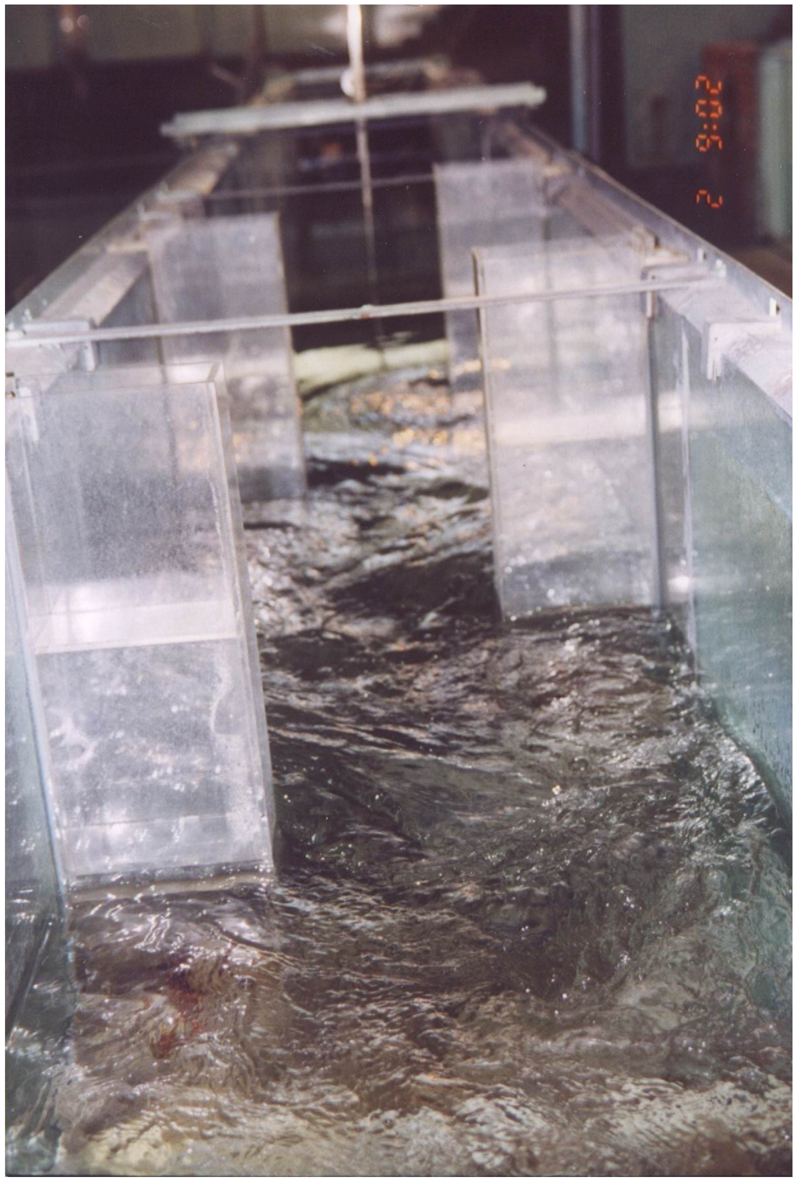

Figure A.1. Downstream view, Case B2

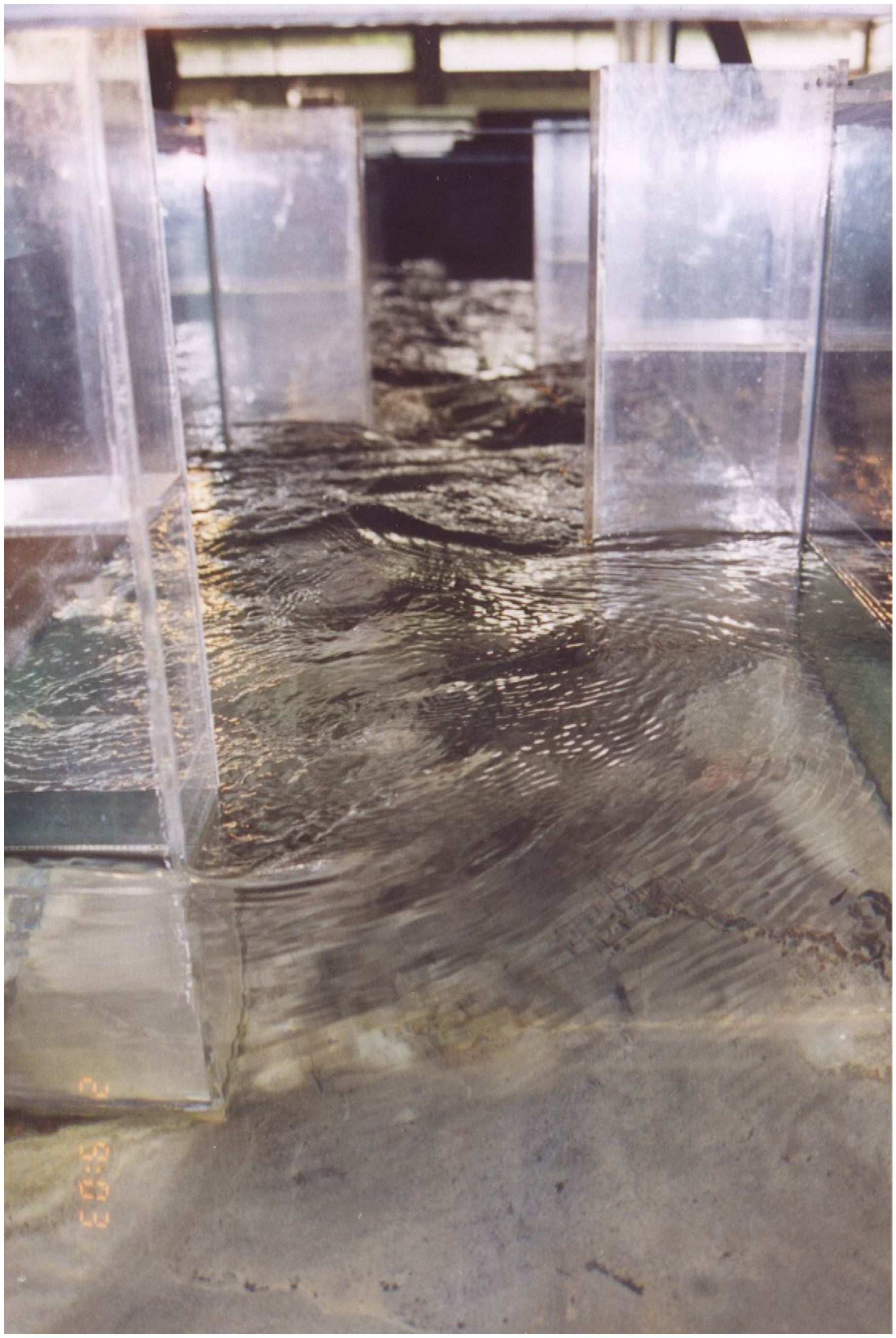

Figure A.2. Upstream view, Case B2

Figure A.3. Downstream view, Case B1

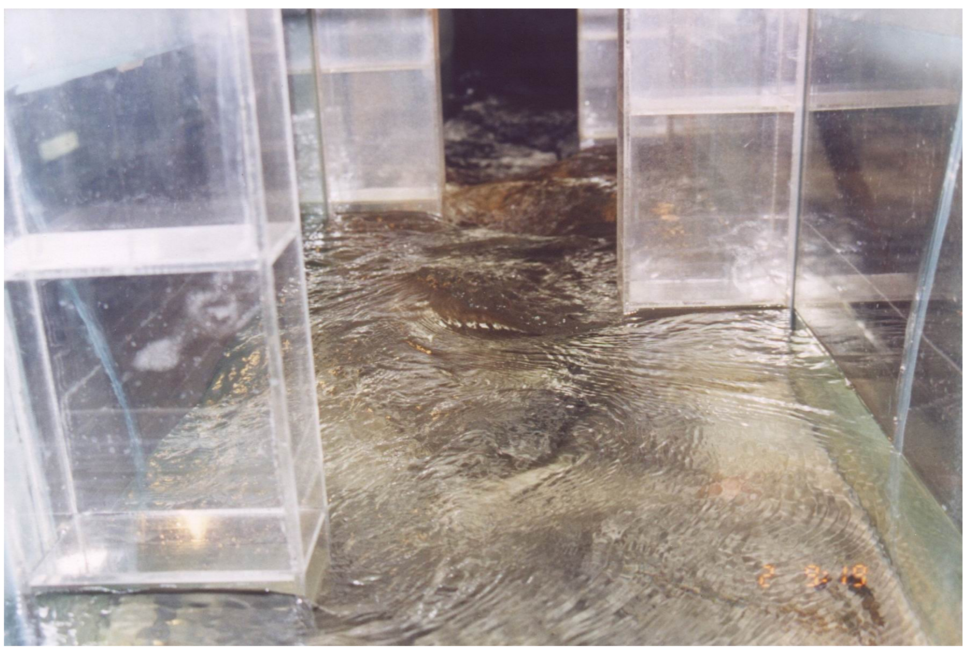

Figure A.4. Upstream view, Case B1

APPENDIX B

EXPERIMENTAL DATA

Experimental data collected following the order of Table 2.1. is presented as the water heights measured from bottom to the water surface. Data are given with their nodal locations where their metric location can be seen in Fig. 2.4.

Table B.1. Experimental data, Case A1

x (node)	1		2		3		4		5		6		7	
y (node)	**min (cm)**	**max (cm)**	**min (cm)**	**max (cm)**	**min (cm)**	**max (cm)**	**min (cm)**	**max (cm)**	**min (cm)**	**max (cm)**	**min (cm)**	**max (cm)**	**min (cm)**	**max (cm)**
1	10.39	12.27	10.4	11.79	8.71	9.88	8.46	9.7	8.63	9.44	9.15	9.68	9.54	10.24
2	10.14	11.71	10.05	11.25	8.57	9.82	8.54	9.48	8.4	9.1	9.12	9.73	9.6	10.22
3	9.77	11.4	9.68	11.04	8.87	9.72	8.6	9.29	8.6	9.12	8.99	9.6	9.79	10.11
4	9.24	10.57	9.36	10.47	8.82	9.72	8.63	9.39	8.42	9.01	8.84	9.43	9.38	9.9
5	8	8.95	8.32	9.35	8.6	9.44	8.37	9.28	8.18	8.8	8.66	9.28	9.4	9.88
6	7.54	8.18	8.38	9.15	8.74	9.47	8.21	9.03	8.05	8.86	8.83	9.28	9.38	9.78
7	6.78	7.29	8.53	9.51	8.81	9.33	8.22	8.72	8.22	9.29	9.02	9.53	9.28	9.68
8	6.39	7.03	8.62	9.6	9.12	9.91	8.3	9.15	8.19	9.31	8.97	9.55	9.05	9.63
9	5.92	6.78	8.95	9.61	9.17	9.86	8.02	9.11	8.47	9.14	9.03	9.67	9.11	9.88
10	5.65	6.26	9.39	10.14	10.15	10.75	8.7	9.32	8.7	9.35	8.99	9.74	8.21	8.7
11	5.46	6.13	9.67	10.2	10.35	11.1	9.44	10.37	9.01	9.87	9.37	10.49	7.66	8.53
12	4.66	5.64	9.99	10.58	10.59	11.5	9.81	10.78	10.24	11.02	10.01	10.88	8.05	8.65
13	4.37	5.22	10.28	10.86	10.94	12	10.67	11.41	10.95	12.14	10.9	12.32	8.72	9.55
14	3.16	4.11	10.66	11.56	11.62	12.6	11.08	11.73	11.73	12.78	11.7	12.62	9.41	10.14
15	1.5	2.29	11.56	12.34	12.32	13.14	11.67	12.31	11.88	12.81	12.11	13.67	9.93	10.58
16	0.55	1.04	13.04	13.91	12.1	13.63	11.87	12.82	12.27	13.25	12.98	14.12	10.59	11.37
17	0.29	0.39	13.51	14.31	12.54	13.69	12.2	13.45	12.42	13.41	13.17	14.43	11.61	12.39
18	0.3	0.45	13.68	14.67	13.62	14.31	12.61	13.58	12.41	13.37	13.1	14.29	11.97	12.83
19	0.3	0.5	13.88	14.77	13.23	14.15	12.93	14.28	12.74	13.52	13.27	14.38	12.15	13.18
20	0.34	0.6	14.05	14.81	13.51	14.27	13.13	14.31	12.95	13.82	13.55	14.19	12.64	13.67
21	0.34	0.56	14.04	14.79	13.92	14.64	13.61	14.7	13.37	14.09	13.13	14.04	12.87	13.72
22	0.28	0.5	13.87	15.09	13.75	14.62	13.71	14.57	13.49	14.08	13.28	14.04	12.84	13.92
23	0.26	0.56	13.91	15.19	13.76	14.66	13.53	14.49	13.2	14.11	13.45	14.15	13	13.98

Table B.1. (continued)

x (node)	8		9		10		11		12		13		14	
y (node)	**min (cm)**	**max (cm)**	**min (cm)**	**max (cm)**	**min (cm)**	**max (cm)**	**min (cm)**	**max (cm)**	**min (cm)**	**max (cm)**	**min (cm)**	**max (cm)**	**min (cm)**	**max (cm)**
1	15.31	15.63	15.03	15.53	15.05	15.59	14.99	15.28	14.81	15.12	14.55	14.93	14.13	14.59
2	15.13	15.74	15.04	15.54	15	15.56	14.9	15.18	14.86	15.11	14.58	14.9	14.19	14.69
3	15.42	15.9	14.95	15.48	14.99	15.38	14.87	15.13	14.83	15.12	14.73	15.01	14.13	14.77
4	15.39	15.91	14.79	15.32	14.96	15.27	14.84	15.11	14.76	15.13	14.67	15.1	14.34	14.65
5	15.33	15.84	14.73	15.18	14.88	15.2	14.76	15	14.77	15.12	14.61	14.97	14.2	14.65
6	15.18	15.72	14.53	15.13	14.76	15.19	14.42	14.85	14.58	14.95	14.43	14.9	14.22	14.53
7	14.49	14.99	14.41	15.04	14.6	15.05	14.02	14.47	14.55	15.01	14.29	14.68	14.17	14.45
8	13.42	14.28	14.32	14.83	14.54	15.02	13.66	14.1	14.5	14.87	14	14.31	14.08	14.38
9	11.88	12.53	13.91	14.48	14.33	14.76	13.16	13.65	14.3	14.64	13.61	14.18	13.86	14.16
10	11.11	12.06	13.71	14.17	13.84	14.78	12.98	13.37	13.89	14.21	13.17	13.43	13.77	14.05
11	10.83	11.67	13.27	13.66	13.77	14.47	12.7	13.15	13.3	13.67	12.62	13.1	13.69	13.92
12	11.37	11.72	12.76	13.32	13.08	14.12	12.44	12.77	12.54	13	12.41	13.06	13.57	13.78
13	11.27	11.64	12.2	12.87	12.47	13.46	12.14	12.63	12.34	12.8	12.22	12.97	13.53	13.83
14	11.32	11.6	11.96	12.43	12.06	12.81	12.08	12.48	12.41	12.68	12.37	12.78	13.64	13.9
15	11.19	11.61	11.67	12.15	12.08	12.67	12.28	12.61	12.38	12.67	12.36	12.68	13.8	14.15
16	11.37	12.2	11.81	12.21	11.94	12.43	12.11	12.47	12.25	12.57	12.18	12.6	14.01	14.2
17	11.57	12.61	11.7	12.31	11.74	12.47	12.12	12.43	12.18	12.5	12.3	12.55	15.58	15.76
18	11.69	12.88	11.82	12.51	12	12.4	12.18	12.51	12.27	12.46	12.29	12.63	15.84	16.05
19	12.07	12.96	11.82	12.44	12.01	12.29	12.1	12.53	12.27	12.56	12.2	12.54	15.89	16.07
20	12.05	13.24	11.68	12.47	11.86	12.35	12.16	12.54	12.29	12.64	12.34	12.64	15.88	16.09
21	12.16	13.19	11.72	12.51	11.7	12.42	12.11	12.58	12.17	12.58	12.31	12.7	15.89	16.05
22	12.4	13.33	11.77	12.48	11.84	12.45	12.16	12.52	12.28	12.57	12.27	12.7	15.74	16
23	12.15	13.66	11.63	12.58	11.7	12.54	12.13	12.61	12.23	12.66	12.22	12.71	15.71	15.93

Table B.1. (continued)

x (node)	15		16		17		18		19		20		21	
y (node)	**min (cm)**	**max (cm)**	**min (cm)**	**max (cm)**	**min (cm)**	**max (cm)**	**min (cm)**	**max (cm)**	**min (cm)**	**max (cm)**	**min (cm)**	**max (cm)**	**min (cm)**	**max (cm)**
1	13.66	14.15	13.67	13.88	13.69	13.97	13.99	14.21	14.19	14.42	16	16.13	15.89	16
2	13.71	14.12	13.54	13.93	13.82	14.07	14.08	14.3	14.22	14.45	16.05	16.14	15.97	16.05
3	13.7	14.3	13.72	14.06	13.85	14.2	14.14	14.4	14.25	14.44	16.13	16.22	16.04	16.17
4	13.91	14.39	13.83	14.03	13.9	14.2	14.15	14.42	14.21	14.46	16.18	16.31	16.06	16.15
5	13.91	14.44	13.95	14.11	13.99	14.22	14.16	14.4	14.2	14.39	16.13	16.29	16.04	16.13
6	13.94	14.43	13.98	14.24	13.93	14.24	14.08	14.4	14.13	14.42	16.06	16.19	16.03	16.12
7	14.05	14.42	13.92	14.33	14.01	14.31	14.24	14.57	14.27	14.41	15.78	15.99	15.95	16.07
8	14.1	14.4	14.07	14.42	13.87	14.41	14.21	14.57	14.18	14.42	14.68	14.9	15.79	15.91
9	14.18	14.48	14.15	14.53	14	14.54	14.23	14.58	14.3	14.57	14.76	15.05	15.73	15.89
10	14.32	14.53	14.35	14.6	14.27	14.59	14.29	14.66	14.55	14.71	15.05	15.2	15.69	15.82
11	14.41	14.63	14.65	14.85	14.38	14.74	14.66	14.86	14.69	15	15.16	15.34	15.68	15.79
12	14.57	14.76	14.74	14.95	14.74	14.93	14.61	14.9	14.87	15.09	15.28	15.39	15.62	15.75
13	14.77	14.92	14.9	15.08	14.93	15.16	14.77	15	14.96	15.12	15.37	15.49	15.62	15.73
14	15	15.17	14.9	15.09	14.99	15.25	15	15.16	15.08	15.21	15.39	15.5	15.61	15.71
15	15.2	15.36	15.16	15.27	15.16	15.3	15.09	15.23	15.18	15.29	15.44	15.55	15.64	15.7
16	15.35	15.49	15.22	15.41	15.21	15.4	15.19	15.38	15.2	15.4	15.46	15.59	15.61	15.69
17	15.51	15.68	15.3	15.51	15.29	15.44	15.3	15.44	15.31	15.45	15.42	15.6	15.59	15.69
18	15.62	15.74	15.41	15.59	15.3	15.5	15.37	15.52	15.33	15.49	15.45	15.58	15.62	15.7
19	15.64	15.81	15.46	15.65	15.37	15.54	15.37	15.53	15.35	15.53	15.5	15.6	15.62	15.71
20	15.71	15.89	15.49	15.61	15.39	15.52	15.38	15.53	15.36	15.53	15.5	15.6	15.6	15.72
21	15.64	15.8	15.48	15.6	15.35	15.51	15.39	15.5	15.34	15.5	15.51	15.61	15.54	15.63
22	15.6	15.7	15.41	15.54	15.34	15.44	15.28	15.44	15.39	15.5	15.44	15.58	15.48	15.58
23	15.56	15.69	15.35	15.54	15.31	15.42	15.22	15.4	15.32	15.48	15.38	15.54	15.42	15.57

Table B.1. (continued)

x (node)	22		23		24		25		26		27		28	
y (node)	min (cm)	max (cm)	min (cm)	max (cm)	min (cm)	max (cm)	min (cm)	max (cm)	min (cm)	max (cm)	min (cm)	max (cm)	min (cm)	max (cm)
1	15.79	15.88	15.79	15.86	15.87	15.97	15.84	15.95	15.68	15.8	15.75	15.91	15.65	15.83
2	15.85	15.92	15.82	15.9	15.88	15.97	15.86	15.98	15.72	15.85	15.78	15.92	15.74	15.87
3	15.87	15.96	15.88	15.94	15.9	16	15.89	16	15.78	15.9	15.84	15.96	15.84	15.93
4	15.92	16	15.86	15.96	15.9	16	15.9	16.01	15.81	15.94	15.87	16	15.85	15.95
5	15.92	16.01	15.86	15.99	15.88	15.98	15.87	16	15.84	15.96	15.85	15.96	15.89	15.98
6	15.91	15.99	15.9	15.98	15.87	15.96	15.88	15.98	15.84	15.94	15.85	15.95	15.92	15.99
7	15.92	15.99	15.87	15.94	15.86	15.95	15.85	15.95	15.83	15.95	15.86	15.96	15.92	16
8	15.84	15.95	15.81	15.92	15.8	15.93	15.83	15.95	15.81	15.95	15.85	15.97	15.93	16.02
9	15.79	15.89	15.78	15.89	15.79	15.92	15.8	15.93	15.78	15.93	15.84	15.97	15.89	15.99
10	15.73	15.85	15.74	15.88	15.76	15.91	15.77	15.91	15.76	15.9	15.82	15.96	15.89	15.98
11	15.75	15.82	15.76	15.89	15.76	15.9	15.76	15.9	15.76	15.88	15.84	15.95	15.9	16
12	15.71	15.81	15.74	15.83	15.76	15.89	15.74	15.89	15.78	15.9	15.86	15.95	15.92	15.98
13	15.68	15.78	15.71	15.85	15.73	15.86	15.76	15.89	15.8	15.91	15.85	15.95	15.9	15.98
14	15.72	15.79	15.72	15.84	15.73	15.86	15.74	15.9	15.78	15.91	15.85	15.96	15.9	16
15	15.67	15.76	15.69	15.81	15.73	15.87	15.74	15.89	15.78	15.91	15.83	15.95	15.92	16
16	15.61	15.78	15.71	15.8	15.76	15.88	15.75	15.92	15.78	15.93	15.85	15.95	15.93	16.02
17	15.61	15.74	15.71	15.79	15.72	15.86	15.73	15.89	15.79	15.91	15.86	15.97	15.95	16.04
18	15.65	15.73	15.68	15.76	15.74	15.86	15.73	15.89	15.78	15.9	15.84	15.97	15.9	16
19	15.6	15.72	15.68	15.77	15.77	15.88	15.72	15.88	15.76	15.89	15.83	15.95	15.91	16.01
20	15.58	15.69	15.67	15.74	15.76	15.87	15.74	15.89	15.7	15.83	15.79	15.91	15.88	15.95
21	15.56	15.66	15.63	15.74	15.75	15.89	15.71	15.87	15.64	15.77	15.74	15.86	15.82	15.92
22	15.46	15.59	15.57	15.74	15.7	15.86	15.66	15.81	15.56	15.67	15.68	15.82	15.74	15.82
23	15.41	15.59	15.55	15.69	15.69	15.85	15.62	15.77	15.49	15.64	15.65	15.78	15.73	15.8

Table B.2. Experimental data, Case A2

x (node)	1		2		3		4		5		6		7	
y (node)	**min (cm)**	**max (cm)**	**min (cm)**	**max (cm)**	**min (cm)**	**max (cm)**	**min (cm)**	**max (cm)**	**min (cm)**	**max (cm)**	**min (cm)**	**max (cm)**	**min (cm)**	**max (cm)**
1	15.56	16.67	15.11	15.9	14.17	15.21	14.03	14.99	14.42	15	14.64	15.26	14.78	15.31
2	15.63	16.52	14.85	15.87	14.13	15.07	13.99	14.73	14.28	14.92	14.61	15.18	14.7	15.4
3	15.51	16.37	15	15.81	14.21	14.97	14.09	14.78	14.28	14.78	14.47	15.19	14.88	15.48
4	15.4	16.14	14.73	15.61	14.3	14.9	14.06	14.67	14.19	14.76	14.4	15.07	14.65	15.23
5	14.83	15.96	14.62	15.48	14.43	15.03	14.01	14.74	14.11	14.62	14.56	15.07	14.84	15.28
6	14.58	15.79	14.36	15.41	14.35	14.98	13.92	14.58	14.12	14.56	14.34	14.91	14.71	15.23
7	14.22	15.65	14.33	15.1	14.39	14.92	14	14.64	14.22	14.7	14.41	14.99	14.58	15.2
8	13.63	14.87	14.09	14.91	14.08	15.12	14.01	14.67	14.17	14.8	14.51	15.04	14.54	15.11
9	13.29	14.34	13.92	14.53	14.28	15.08	14.19	14.95	13.97	14.78	14.41	14.98	14.45	15.26
10	12.92	14.47	14.08	14.61	14.48	15.24	14.3	14.99	14.19	14.85	14.56	15.15	14.62	15.43
11	12.57	14.11	14.17	14.67	14.85	15.54	14.46	15.27	14.21	15.04	14.6	15.31	14.82	15.51
12	12.95	14.07	14.29	15.04	15.28	15.9	15.06	15.68	14.76	15.5	14.9	15.64	14.75	15.56
13	13.38	14.34	14.69	15.36	15.46	16.26	15.6	16.27	14.96	15.72	15.47	16.11	15.03	15.8
14	13.66	14.27	14.69	15.43	15.92	16.65	15.82	16.67	15.34	16.16	15.83	16.52	15.6	16.44
15	13.61	14.23	15.33	15.86	16.34	17.15	16.07	16.82	15.46	16.48	15.9	16.76	16.03	17.11
16	13.57	14.21	16.33	17.15	16.56	17.34	16.28	16.93	15.92	17.07	15.87	16.88	16.19	17.3
17	13.76	14.19	17	17.72	16.87	17.47	16.58	17.4	16.45	17.36	16.12	16.93	16.36	17.38
18	13.78	14.16	17.3	18.28	16.9	17.85	16.71	17.61	16.76	17.45	16.29	17.1	16.43	17.39
19	13.81	14.21	17.2	18.34	17.16	17.93	17.04	17.69	16.86	17.44	16.59	17.24	16.56	17.32
20	13.8	14.14	17.15	18.28	17.14	17.97	17	17.81	16.83	17.55	16.81	17.6	16.67	17.39
21	13.76	14.16	17.34	18.26	17.21	17.92	17.26	17.84	17	17.53	16.93	17.63	16.72	17.51
22	13.59	14.12	17.28	18.33	17.12	17.94	16.9	17.77	16.93	17.69	16.86	17.6	16.7	17.43
23	13.63	14.04	17.41	18.31	17.19	17.95	17.08	17.84	17.12	17.65	17.07	17.64	16.73	17.54

Table B.2. (continued)

x (node)	8		9		10		11		12		13		14	
y (node)	min (cm)	max (cm)	min (cm)	max (cm)	min (cm)	max (cm)	min (cm)	max (cm)	min (cm)	max (cm)	min (cm)	max (cm)	min (cm)	max (cm)
1	18.03	18.49	17.91	18.6	18.08	18.5	17.97	18.3	17.86	18.19	17.53	18.08	17.35	17.88
2	17.96	18.68	18.02	18.48	18.13	18.49	18.05	18.37	17.88	18.16	17.51	18.1	17.3	17.88
3	18.04	18.73	17.77	18.46	18.04	18.4	17.9	18.24	17.79	18.14	17.68	18.21	17.3	17.96
4	18.29	18.76	17.79	18.49	17.98	18.36	17.89	18.27	17.88	18.2	17.7	18.24	17.47	18
5	18.21	18.68	17.73	18.44	17.74	18.34	17.85	18.25	17.7	18.22	17.78	18.22	17.5	18.12
6	18.01	18.63	17.43	18.06	17.79	18.26	17.83	18.17	17.68	18.15	17.63	18.14	17.57	17.96
7	17.58	18.31	17.33	18.02	17.53	18.09	17.66	18.13	17.51	18.07	17.62	18.02	17.4	17.91
8	16.42	17.05	17.25	17.82	17.43	18.06	17.4	17.97	17.17	17.71	17.55	17.97	17.33	17.78
9	15.44	16.31	17.22	17.8	17.51	17.97	17.18	17.74	17	17.43	17.47	17.91	17.3	17.76
10	14.7	15.82	17.13	17.62	16.97	17.81	17.12	17.53	16.71	17.27	17.27	17.72	17.3	17.68
11	14.61	15.83	16.86	17.31	16.63	17.41	16.61	17.21	16.6	17.03	17.17	17.57	17.05	17.47
12	15.2	15.91	16.57	17.11	16.33	17.12	16.42	16.93	16.4	16.87	16.91	17.46	17.03	17.36
13	15.18	15.81	16.17	16.73	16.11	16.79	16.19	16.75	16.18	16.64	16.47	17.01	16.8	17.15
14	15.29	16	15.98	16.62	16.19	16.67	16.11	16.68	16.28	16.7	16.27	16.8	16.7	17.09
15	15.61	16.32	15.88	16.51	16.04	16.58	16.09	16.58	16.31	16.67	16.26	16.62	16.77	17.25
16	15.89	16.5	15.97	16.49	15.93	16.46	16.19	16.57	16.35	16.85	16.29	16.67	18.01	18.26
17	16.2	16.71	15.9	16.45	15.73	16.32	16.21	16.52	16.34	16.71	16.32	16.73	18.37	18.71
18	16.09	16.83	15.82	16.41	15.83	16.36	15.91	16.43	16.22	16.73	16.3	16.82	18.59	18.88
19	16.14	16.89	15.98	16.49	15.87	16.26	16.01	16.38	16.29	16.73	16.26	16.75	18.63	18.95
20	16.39	16.92	15.94	16.63	15.83	16.27	16.17	16.51	16.34	16.69	16.44	16.82	18.65	18.94
21	16.19	16.96	15.72	16.46	15.86	16.33	15.97	16.54	16.39	16.73	16.51	16.85	18.62	18.89
22	16.15	17	15.91	16.51	15.81	16.34	15.95	16.54	16.18	16.7	16.41	16.91	18.59	18.78
23	16.3	17.05	16.08	16.6	15.73	16.41	16.07	16.52	16.28	16.71	16.3	16.9	18.48	18.81

Table B.2. (continued)

x (node)	15		16		17		18		19		20		21	
y (node)	**min (cm)**	**max (cm)**	**min (cm)**	**max (cm)**	**min (cm)**	**max (cm)**	**min (cm)**	**max (cm)**	**min (cm)**	**max (cm)**	**min (cm)**	**max (cm)**	**min (cm)**	**max (cm)**
1	17.12	17.47	16.9	17.27	17.1	17.39	17.31	17.67	17.55	17.83	18.63	18.97	18.73	18.93
2	17.1	17.54	17.15	17.36	17.22	17.46	17.32	17.64	17.45	17.81	18.83	19.08	18.78	19
3	17.2	17.6	17.22	17.49	17.33	17.57	17.44	17.72	17.41	17.74	18.84	19.09	18.87	19.06
4	17.28	17.81	17.24	17.55	17.36	17.62	17.42	17.67	17.55	17.83	18.9	19.13	18.9	19.11
5	17.28	17.77	17.36	17.67	17.46	17.65	17.46	17.74	17.42	17.79	18.88	19.17	18.91	19.12
6	17.23	17.81	17.29	17.71	17.51	17.74	17.46	17.79	17.43	17.72	18.9	19.06	18.92	19.07
7	17.38	17.86	17.23	17.79	17.44	17.78	17.55	17.85	17.51	17.83	18.74	18.96	18.81	19.03
8	17.4	17.89	17.34	17.82	17.41	17.75	17.52	17.88	17.54	17.75	18.02	18.41	18.17	18.72
9	17.49	17.87	17.49	17.84	17.44	17.76	17.56	17.88	17.58	17.79	18.16	18.28	18.25	18.61
10	17.62	17.86	17.54	17.92	17.58	17.83	17.59	17.95	17.59	17.87	18.2	18.37	18.29	18.59
11	17.66	17.97	17.74	18.04	17.69	18.04	17.73	17.98	17.78	17.97	18.18	18.45	18.28	18.54
12	17.79	18.01	17.87	18.19	17.85	18.09	17.79	18.12	17.87	18.08	18.27	18.5	18.35	18.57
13	17.85	18.11	18.07	18.28	18.05	18.26	17.99	18.27	17.99	18.28	18.3	18.53	18.38	18.6
14	18.02	18.3	18.09	18.31	18.07	18.31	18.1	18.3	18.08	18.29	18.32	18.58	18.41	18.65
15	18.21	18.42	18.19	18.35	18.19	18.41	18.21	18.49	18.19	18.36	18.4	18.59	18.45	18.67
16	18.37	18.6	18.19	18.45	18.25	18.46	18.25	18.45	18.27	18.4	18.45	18.65	18.53	18.71
17	18.43	18.63	18.31	18.57	18.26	18.54	18.32	18.51	18.32	18.5	18.4	18.68	18.48	18.73
18	18.41	18.78	18.39	18.6	18.31	18.57	18.34	18.61	18.33	18.53	18.44	18.67	18.51	18.75
19	18.4	18.82	18.52	18.69	18.39	18.6	18.39	18.58	18.31	18.56	18.41	18.64	18.47	18.73
20	18.47	18.77	18.42	18.68	18.39	18.59	18.38	18.57	18.35	18.57	18.37	18.61	18.45	18.7
21	18.49	18.74	18.38	18.67	18.29	18.54	18.36	18.53	18.34	18.5	18.39	18.58	18.39	18.65
22	18.34	18.62	18.27	18.55	18.27	18.51	18.22	18.43	18.33	18.53	18.39	18.56	18.4	18.61
23	18.29	18.64	18.27	18.55	18.25	18.45	18.22	18.41	18.25	18.5	18.39	18.54	18.37	18.6

Table B.2. (continued)

x (node)	22		23		24		25		26		27		28	
y (node)	min (cm)	max (cm)	min (cm)	max (cm)	min (cm)	max (cm)	min (cm)	max (cm)	min (cm)	max (cm)	min (cm)	max (cm)	min (cm)	max (cm)
1	18.61	18.83	18.63	18.83	18.7	18.91	18.61	18.85	18.51	18.72	18.57	18.83	18.47	18.74
2	18.65	18.9	18.65	18.86	18.73	18.92	18.66	57.98	18.59	18.77	18.61	18.81	18.54	18.75
3	18.72	18.96	18.69	18.9	18.75	18.93	18.73	18.93	18.63	18.8	18.67	18.84	18.65	18.8
4	18.76	18.99	18.73	18.93	18.77	18.95	18.77	18.93	18.69	18.81	18.71	18.84	18.69	18.8
5	18.78	19.02	18.73	18.98	18.79	18.95	18.78	18.9	18.75	18.88	18.73	18.84	18.77	18.86
6	18.75	18.98	18.72	18.96	18.78	18.93	18.75	18.9	18.74	18.87	18.73	18.87	18.8	18.9
7	18.73	18.93	18.71	18.92	18.75	18.9	18.72	18.9	18.71	18.86	18.68	18.87	18.75	18.91
8	18.28	18.74	18.48	18.85	18.6	18.86	18.62	18.89	18.68	18.86	18.66	18.84	18.73	18.87
9	18.29	18.69	18.4	18.74	18.5	18.78	18.53	18.81	18.63	18.8	18.67	18.81	18.77	18.9
10	18.38	18.65	18.39	18.73	18.48	18.75	18.54	18.79	18.65	18.78	18.68	18.85	18.79	18.93
11	18.36	18.63	18.4	18.66	18.44	18.71	18.52	18.75	18.62	18.76	18.67	18.84	18.74	18.91
12	18.35	18.6	18.42	18.64	18.45	18.69	18.53	18.71	18.67	18.78	18.71	18.86	18.77	18.92
13	18.37	18.62	18.45	18.63	18.49	18.69	18.55	18.72	18.7	18.8	18.74	18.86	18.77	18.9
14	18.4	18.62	18.48	18.67	18.52	18.72	18.58	18.74	18.7	18.77	18.73	18.85	18.8	18.91
15	18.44	18.63	18.5	18.66	18.55	18.72	18.58	18.75	18.68	18.81	18.7	18.87	18.78	18.91
16	18.48	18.65	18.51	18.69	18.59	18.77	18.61	18.79	18.71	18.81	18.71	18.89	18.81	18.94
17	18.46	18.67	18.49	18.71	18.57	18.79	18.59	18.8	18.68	18.84	18.73	18.9	18.83	18.98
18	18.46	18.67	18.5	18.72	18.61	18.79	18.6	18.8	18.7	18.85	18.74	18.9	18.78	18.94
19	18.43	18.65	18.49	18.71	18.61	18.8	18.58	18.77	18.65	18.86	18.73	18.88	18.79	18.95
20	18.4	18.61	18.47	18.69	18.6	18.8	18.57	18.81	18.64	18.77	18.66	18.85	18.73	18.89
21	18.41	18.59	18.49	18.69	18.6	18.81	18.56	18.77	18.56	18.72	18.64	18.82	18.68	18.85
22	18.37	18.53	18.48	18.65	18.6	18.8	18.54	18.72	18.44	18.65	18.57	18.76	18.58	18.76
23	18.32	18.51	18.44	18.61	18.55	18.79	18.48	18.72	18.37	18.62	18.49	18.72	18.53	18.74

Table B.3. Experimental data, Case B1

x (node)	1		2		3		4		5		6		7	
y (node)	min (cm)	max (cm)	min (cm)	max (cm)	min (cm)	max (cm)	min (cm)	max (cm)	min (cm)	max (cm)	min (cm)	max (cm)	min (cm)	max (cm)
1	16.12	18.31	15.96	18.49	13.02	14.88	12.67	14.02	13.15	14.2	12.7	14.37	12.39	14.22
2	15.71	17.32	15.16	16.52	13.17	14.77	12.71	14.11	13.17	14.01	12.69	14.08	12.6	14.11
3	14.81	16.21	14.31	16.22	12.82	14.76	12.66	14.2	12.82	13.77	13.04	13.93	13.01	14.2
4	13.25	14.94	13.45	15.62	12.73	13.93	12.5	13.94	12.93	13.55	12.97	13.85	12.65	14.15
5	12.04	13.38	12.65	14.5	12.63	13.82	12.54	13.68	12.79	13.44	12.81	13.74	13.21	14.38
6	11.22	12.72	12.59	14.04	12.45	13.81	12.54	13.46	12.7	13.72	12.74	13.67	13.02	13.9
7	10.91	11.83	13.34	14.31	12.63	13.92	12.74	13.87	12.43	13.59	12.9	13.84	12.95	14.06
8	11.04	11.98	13.67	14.64	12.65	13.88	12.73	13.97	12.66	13.77	12.88	13.68	12.78	14.67
9	10.81	11.52	14.19	15.15	13.11	14.33	12.32	14.38	12.42	13.86	13	13.82	13.05	14.45
10	10.7	11.27	14.61	15.69	14.69	15.65	12.84	14.33	12.76	14.44	12.71	14.28	12.85	14.74
11	9.8	10.81	15.49	16.35	15.37	16.67	13.33	16.62	13.88	15.91	12.4	14.2	12.63	14.54
12	9.49	10.58	15.99	17.16	15.94	17.44	15.42	17.71	14.42	16.65	13.12	15.13	12.13	13.76
13	9.21	10.42	16.86	17.93	16.95	18.18	16.73	18.17	15.5	17.58	12.91	15.71	12.72	13.89
14	7.38	8.98	17.53	18.37	17.29	18.72	17.92	19.29	16.73	19.07	13.21	17.27	13.54	14.36
15	2.28	3.41	18.71	19.91	18.03	19.52	18.41	19.52	18.53	20.32	14.51	17.87	14.07	15.05
16	1.45	2.67	20.35	21.44	18.6	20.51	18.86	19.74	19.54	20.56	15.91	19.41	14.83	15.75
17	0.59	1.19	20.98	21.99	19.49	20.81	19.31	20.07	19.35	20.71	17.49	19.38	15.52	16.61
18	0.52	0.93	21.11	22.5	19.56	20.9	19.47	20.4	19.86	20.88	18.16	20.41	16.73	18.01
19	0.5	0.91	21.51	22.58	19.6	21.14	19.62	20.46	19.69	20.86	19.19	20.74	17.9	19.59
20	0.7	1.03	21.85	22.64	20.3	21.22	19.66	20.93	19.63	20.47	19.85	20.93	19.26	20.8
21	0.66	1.28	21.12	22.69	20.92	21.67	20.27	21.46	19.88	20.81	19.63	20.86	19.51	20.71
22	0.6	1.22	20.99	22.7	20.37	21.77	20.35	21.53	19.74	21	19.77	21.2	19.66	21.1
23	0.56	1.37	20.73	22.8	20.81	21.79	20.59	21.54	20	21.48	19.76	21.13	19.5	21.11

Table B.3. (continued)

x (node)	8		9		10		11		12		13		14	
y (node)	**min (cm)**	**max (cm)**	**min (cm)**	**max (cm)**	**min (cm)**	**max (cm)**	**min (cm)**	**max (cm)**	**min (cm)**	**max (cm)**	**min (cm)**	**max (cm)**	**min (cm)**	**max (cm)**
1	22.44	23.59	22.1	22.51	22.06	22.89	21.74	22.14	21.52	22.03	21.12	21.9	20.69	21.43
2	22.49	23.53	21.97	23.06	22.02	22.78	21.79	22.2	21.4	22.03	20.96	21.78	20.6	21.36
3	22.6	23.71	21.97	22.89	21.95	22.69	21.56	22.01	21.18	21.73	21.22	21.93	20.85	21.49
4	22.52	23.8	21.55	22.57	21.85	22.63	21.71	22	21.29	21.93	21.27	21.92	20.66	21.45
5	22.52	23.78	21.73	22.45	21.49	22.38	21.37	21.71	21.34	21.9	20.86	21.62	20.62	21.37
6	22.13	23.46	20.87	22.31	21.36	22.26	20.79	21.65	21.17	21.73	20.48	21.6	20.57	21.19
7	21.51	22.88	20.81	22.02	20.89	22.01	20.67	21.32	20.9	21.86	19.93	20.87	20.41	21
8	19.9	21.42	20.54	21.8	20.58	21.85	20.34	21.3	20.9	22.2	19.26	20.07	20.11	20.75
9	18.38	19.71	20.04	21.41	19.69	21.58	20.05	20.77	20.59	21.85	18.81	19.52	19.96	20.57
10	16.78	18.5	19.93	20.99	18.88	21.01	19.64	20.56	20	21.22	18.2	19.01	19.81	20.35
11	16.1	18.11	19.76	20.61	18.3	20.12	19.1	19.94	18.67	19.86	17.6	18.23	19.9	20.26
12	15.01	17.73	19.3	20.31	17.59	18.9	18.5	19.33	18.02	18.87	17.11	17.69	19.52	20.1
13	16.01	17.44	18.99	19.9	17.2	18.12	17.42	17.83	17.64	18.28	16.97	17.61	18.66	20.3
14	16.46	17.79	18.53	19.36	17.22	18.16	17.28	17.72	17.62	18.15	17.11	17.95	18.7	20.23
15	16.8	17.9	18.32	19.25	17.38	18.43	17.58	17.84	17.69	18.05	17.25	17.87	20.39	21.15
16	16.89	17.68	17.85	18.79	17.22	17.97	17.13	17.64	17.65	17.89	17.5	18	22.1	22.48
17	16.77	17.91	17.36	18.54	17.25	17.77	17.21	17.72	17.71	17.98	17.69	18.07	22.59	23.13
18	16.92	17.92	16.94	18.45	16.94	17.76	17.08	17.41	17.73	17.99	17.692	18.09	23.17	23.49
19	17.23	18.47	17.12	18.35	16.89	17.69	17.32	17.78	17.68	18.13	17.68	18.09	23.17	23.44
20	17.33	19.37	16.97	18.28	16.79	17.72	17.46	17.86	17.38	17.96	17.7	18.31	23.14	23.59
21	18.16	19.92	17.27	18.36	17.11	18.08	17.37	17.89	17.63	18.04	17.6	18.13	23.01	23.4
22	18.01	19.85	17.17	18.72	17.3	18.34	16.89	17.83	17.61	17.97	17.6	18.21	22.99	23.19
23	18.59	20.36	17.19	19.21	16.79	18.6	17.16	17.92	17.65	17.99	17.74	18.12	22.92	23.29

Table B.3. (continued)

x (node)	15		16		17		18		19		20		21	
y (node)	**min (cm)**	**max (cm)**	**min (cm)**	**max (cm)**	**min (cm)**	**max (cm)**	**min (cm)**	**max (cm)**	**min (cm)**	**max (cm)**	**min (cm)**	**max (cm)**	**min (cm)**	**max (cm)**
1	19.95	20.99	19.7	20.67	20.26	20.66	20.59	20.83	20.71	21.24	23.42	23.58	23.26	23.52
2	20.15	21.07	19.93	20.67	20.22	20.68	20.48	20.84	20.75	21.17	23.43	23.69	23.28	23.6
3	20.22	21.06	20.08	20.7	20.29	20.81	20.62	20.96	20.85	21.21	23.47	23.74	23.38	23.62
4	20.24	21.15	20.2	20.74	20.42	20.8	20.62	20.94	20.73	21.11	23.5	23.82	23.34	23.63
5	20.22	21.02	20.37	20.88	20.38	20.8	20.7	20.92	20.71	21.11	23.49	23.83	23.4	23.64
6	20.16	21	20.24	20.85	20.54	20.85	20.63	20.97	20.68	21.04	23.38	23.8	23.3	23.56
7	20.32	20.95	20.44	20.92	20.64	20.98	20.69	21.03	20.7	21.12	23.25	23.55	23.29	23.51
8	20.28	20.98	20.61	21.14	20.73	21.01	20.7	21.12	20.59	20.96	21.87	22.99	23.16	23.44
9	20.41	20.99	20.82	21.23	20.65	21.01	20.75	21.17	20.77	21.19	21.48	21.92	23.12	23.35
10	20.78	21.19	20.95	21.43	20.92	21.18	20.83	21.27	21.13	21.57	21.37	22.07	22.99	23.17
11	20.91	21.38	21.34	21.77	21.1	21.48	21.02	21.36	21.35	21.83	21.79	22.39	22.93	23.19
12	21.08	21.58	21.57	22.02	21.46	21.75	21.32	21.67	21.46	21.86	22.27	22.49	22.81	23.11
13	21.49	21.98	21.78	22.17	21.56	21.82	21.61	21.93	21.7	21.94	22.34	22.66	22.84	23.04
14	21.81	22.17	22.04	22.36	21.77	22.11	21.91	22.17	21.92	22.3	22.47	22.75	22.8	23.08
15	22.07	22.38	22.14	22.45	22.04	22.3	22.15	22.43	22.1	22.38	22.49	22.71	22.8	23.04
16	22.34	22.79	22.31	22.59	22.16	22.44	22.22	22.49	22.22	22.46	22.52	22.78	22.78	23
17	22.52	22.99	22.46	22.77	22.38	22.62	22.19	22.53	22.28	22.51	22.58	22.76	22.71	22.95
18	22.6	23.07	22.64	22.9	22.5	22.71	22.37	22.6	22.3	22.55	22.57	22.81	22.76	22.94
19	22.7	23.11	22.75	23	22.59	22.77	22.54	22.78	22.4	22.64	22.6	22.8	22.74	23
20	22.6	23.14	22.77	23.04	22.61	22.82	22.46	22.72	22.45	22.67	22.61	22.89	22.78	22.98
21	22.65	23.09	22.78	23.05	22.64	22.83	22.43	22.63	22.4	22.58	22.6	22.92	22.75	22.97
22	22.42	22.85	22.68	22.94	22.58	22.8	22.34	22.56	22.42	22.7	22.48	22.76	22.68	22.85
23	22.59	22.96	22.59	22.91	22.61	22.79	22.38	22.56	22.44	22.7	22.53	22.73	22.67	22.89

Table B.3. (continued)

x (node)	22		23		24		25		26		27		28	
y (node)	min (cm)	max (cm)	min (cm)	max (cm)	min (cm)	max (cm)	min (cm)	max (cm)	min (cm)	max (cm)	min (cm)	max (cm)	min (cm)	max (cm)
1	23.46	23.66	23.38	23.5	23.45	23.61	23.34	23.48	23.1	23.22	23.28	23.44	23.31	23.45
2	23.41	23.63	23.45	23.57	23.48	23.6	23.36	23.48	23.18	23.32	23.26	23.44	23.38	23.56
3	23.5	23.66	23.48	23.62	23.5	23.61	23.38	23.52	23.21	23.33	23.34	23.49	23.39	23.58
4	23.36	23.64	23.5	23.63	23.52	23.61	23.42	23.56	23.26	23.42	23.44	23.59	23.43	23.57
5	23.42	23.61	23.49	23.68	23.46	23.58	23.38	23.5	23.29	23.43	23.43	23.53	23.47	23.64
6	23.32	23.54	23.45	23.64	23.4	23.57	23.4	23.53	23.34	23.5	23.38	23.54	23.46	23.62
7	23.31	23.51	23.44	23.61	23.41	23.54	23.41	23.59	23.34	23.48	23.4	23.52	23.44	23.58
8	23.23	23.45	23.44	23.56	23.39	23.51	23.41	23.55	23.33	23.49	23.44	23.54	23.49	23.63
9	23.1	23.32	23.36	23.53	23.4	23.52	23.42	23.56	23.33	23.49	23.41	23.55	23.49	23.63
10	23.08	23.3	23.3	23.48	23.42	23.53	23.35	23.53	23.35	23.47	23.4	23.51	23.42	23.54
11	23.1	23.28	23.38	23.5	23.42	23.55	23.32	23.46	23.36	23.45	23.44	23.56	23.47	23.61
12	23.04	23.22	23.3	23.46	23.43	23.52	23.3	23.48	23.36	23.49	23.45	23.53	23.46	23.59
13	23	23.16	23.3	23.42	23.4	23.48	23.27	23.43	23.37	23.49	23.45	23.53	23.44	23.59
14	22.98	23.12	23.28	23.42	23.37	23.5	23.35	23.48	23.35	23.49	23.45	23.57	23.51	23.66
15	22.91	23.05	23.27	23.4	23.34	23.48	23.31	23.45	23.35	23.49	23.45	23.55	23.48	23.62
16	22.9	23.08	23.25	23.39	23.33	23.49	23.38	23.5	23.32	23.51	23.42	23.54	23.56	23.66
17	22.85	23.03	23.21	23.38	23.33	23.46	23.35	23.49	23.3	23.48	23.47	23.59	23.55	23.67
18	22.8	23.02	23.18	23.34	23.33	23.45	23.32	23.53	23.34	23.5	23.49	23.61	23.52	23.64
19	22.84	23.05	23.17	23.33	23.32	23.46	23.35	23.48	23.38	23.52	23.42	23.59	23.5	23.62
20	22.83	23.04	23.2	23.4	23.41	23.56	23.35	23.51	23.29	23.44	23.4	23.55	23.4	23.54
21	22.81	23.02	23.22	23.35	23.37	23.49	23.32	23.44	23.23	23.37	23.35	23.45	23.37	23.52
22	22.81	22.99	23.08	23.36	23.29	23.53	23.24	23.36	23.16	23.26	23.28	23.46	23.34	23.49
23	22.57	22.85	23.02	23.28	23.31	23.45	23.2	23.34	23.1	23.25	23.24	23.38	23.26	23.38

Table B.4. Experimental data, Case B2

x (node)	1		2		3		4		5		6		7	
y (node)	**min (cm)**	**max (cm)**	**min (cm)**	**max (cm)**	**min (cm)**	**max (cm)**	**min (cm)**	**max (cm)**	**min (cm)**	**max (cm)**	**min (cm)**	**max (cm)**	**min (cm)**	**max (cm)**
1	25.96	27.58	25.2	26.86	24.29	26.1	24.36	25.39	24.6	25.93	24.77	25.88	25.18	26.01
2	25.71	27.31	24.98	26.19	24.22	26.08	24.27	25.58	24.68	25.61	25.28	25.72	25.31	26.1
3	25.79	27.21	24.61	26.28	24.15	25.56	24.33	25.5	24.59	25.36	24.92	25.58	25.14	26.12
4	25.8	27.26	24.62	26.18	24.14	25.42	24.2	25.3	24.53	25.27	24.71	25.68	25.31	26.01
5	25.64	27.1	24.31	25.87	24.4	25.35	24.37	25.34	24.41	25	24.78	25.68	24.99	26
6	24.89	27.05	24.04	25.5	24.15	25.32	24.43	25.28	24.46	24.94	24.74	25.66	25.03	25.81
7	24.13	26.44	23.6	25.43	24.16	25.33	24.33	25.29	24.23	24.96	25.03	25.59	24.96	25.62
8	23.11	25.28	23.43	25.05	24.01	25.35	24.34	25.12	24.46	25.05	25	25.72	24.76	25.66
9	22.99	24.87	23.68	25.09	24.51	25.37	24.08	25.12	24.37	25.18	25	25.75	24.95	25.75
10	22.9	24.69	23.99	25.22	24.93	25.91	24.27	25.43	24.48	25.41	24.88	25.64	25.16	26.11
11	22.6	24.46	24.19	25.21	25.33	26.04	24.42	25.54	24.62	25.49	24.9	25.61	25.17	26.41
12	22.94	24.15	24.56	25.39	25.84	26.86	24.91	25.87	24.92	25.7	25.5	26.3	25.3	26.2
13	22.51	24.5	24.86	25.94	26.37	27.51	25.58	26.95	25.56	26.53	25.87	26.9	24.92	26
14	23.63	24.65	24.87	26.18	26.43	27.7	26.38	27.21	26.37	27.23	26.62	27.56	25.44	26.97
15	23.65	24.74	25.82	26.92	27.18	28.05	26.97	27.94	26.57	27.46	27.14	28.18	26.14	27.63
16	23.83	24.44	26.93	28.09	27.4	28.55	27.47	28.45	26.94	27.82	26.92	28.01	26.82	28.49
17	24.01	24.55	27.87	28.99	27.93	28.65	27.77	28.51	27.35	28.31	27.03	28.07	27.14	28.52
18	24.01	24.53	27.95	29.12	28.15	28.92	27.78	28.72	27.46	28.26	27.36	28.27	27.57	28.52
19	24.03	24.66	28.48	29.37	28.21	28.96	28.08	28.8	27.56	28.42	27.62	28.59	27.48	28.4
20	24.05	24.64	28.52	29.5	28.35	29.21	27.91	29.08	27.9	28.82	27.88	28.91	27.27	28.76
21	23.89	24.64	28.56	29.6	28.21	29.22	27.93	29.1	28.03	28.79	27.79	28.7	27.5	28.77
22	23.88	24.57	28.99	29.84	28.23	29.14	28.14	29.12	28.13	28.82	27.91	28.76	27.53	28.55
23	23.88	24.65	28.78	29.91	28.12	29.24	28.39	29.23	27.89	28.9	27.92	28.96	27.7	28.77

Table B.4. (continued)

x (node)	8		9		10		11		12		13		14	
y (node)	**min (cm)**	**max (cm)**	**min (cm)**	**max (cm)**	**min (cm)**	**max (cm)**	**min (cm)**	**max (cm)**	**min (cm)**	**max (cm)**	**min (cm)**	**max (cm)**	**min (cm)**	**max (cm)**
1	29.11	30.23	29.22	29.85	29.09	29.66	28.98	29.45	28.81	29.36	28.6	29.21	28.12	28.76
2	29.52	30.23	29.06	29.68	28.96	29.54	28.86	29.29	28.71	29.29	28.51	29.05	28.1	28.81
3	29.33	30.27	29.05	29.75	28.97	29.51	28.86	29.27	28.61	29.29	28.63	29.2	28.27	28.84
4	29.52	30.26	28.77	29.68	28.87	29.47	28.71	29.47	28.73	29.3	28.66	29.17	28.27	28.88
5	29.4	30.21	28.53	29.78	28.78	29.4	28.76	29.43	28.78	29.48	28.58	29.17	28.29	28.86
6	29.31	30.18	28.33	29.46	28.4	29.38	28.67	29.25	28.49	29.15	28.49	29.08	28.03	28.95
7	28.92	29.63	28.06	29.15	28.61	29.35	28.6	29.29	28.37	29.01	28.44	29.03	28.1	28.87
8	27.51	28.78	28.1	28.9	28.26	29.18	28.54	29.28	28.06	28.67	28.28	28.97	27.99	28.65
9	26.78	27.58	27.83	28.81	28.28	28.94	28.23	29.02	27.85	28.4	28.09	28.83	27.93	28.47
10	25.7	26.61	27.51	28.48	27.74	28.49	27.61	28.63	27.51	28	27.87	28.56	27.9	28.33
11	25.41	26.27	27.6	28.17	27.33	28.27	27.16	28	27.37	27.9	27.51	28.28	27.75	28.26
12	25.2	26.37	27.4	28.05	27.13	27.68	26.76	27.5	26.97	27.64	27.4	28.12	27.48	27.91
13	25.28	26.41	27.27	27.87	26.66	27.56	26.69	27.23	26.87	27.34	26.77	27.81	27.06	27.89
14	25.66	26.61	26.82	27.56	26.4	27.34	26.56	27.25	26.86	27.36	26.82	27.41	27.19	27.8
15	25.82	26.5	26.88	27.52	26.54	27.18	26.62	27.18	26.95	27.32	26.76	27.27	27.65	28.32
16	26.18	27.12	26.5	27.32	26.54	27.13	26.45	27.13	26.78	27.19	26.79	27.31	29.01	29.28
17	26.12	27.51	26.51	27.35	26.55	27.14	26.71	27.1	26.66	27.26	26.63	27.31	29.42	29.85
18	26.52	27.45	26.6	27.43	26.34	27.06	26.61	27.14	26.73	27.36	26.66	27.34	29.7	30.09
19	26.87	27.78	26.44	27.3	26.4	27.05	26.52	27.09	26.77	27.36	26.68	27.29	29.7	30.13
20	26.72	27.76	26.31	27.3	26.36	27.06	26.42	27.1	26.66	27.28	26.71	27.54	29.77	30.11
21	26.79	28	26.56	27.42	26.41	27.11	26.59	27.17	26.57	27.3	26.71	27.69	29.77	30.16
22	26.63	27.88	26.24	27.52	26.41	27.19	26.47	27.26	26.6	27.37	26.72	27.72	29.59	30.08
23	26.69	27.96	26.67	27.59	26.24	27.3	26.35	27.4	26.74	27.37	26.6	27.73	29.6	30.12

Table B.4. (continued)

x (node)	15		16		17		18		19		20		21	
y (node)	**min (cm)**	**max (cm)**	**min (cm)**	**max (cm)**	**min (cm)**	**max (cm)**	**min (cm)**	**max (cm)**	**min (cm)**	**max (cm)**	**min (cm)**	**max (cm)**	**min (cm)**	**max (cm)**
1	27.93	28.49	27.49	28.2	27.96	28.29	28	28.61	28.38	28.83	29.83	30.28	29.86	30.1
2	27.73	28.42	27.77	28.16	27.85	28.26	28.01	28.49	28.34	28.83	29.94	30.26	29.92	30.11
3	27.87	28.62	27.87	28.38	28.09	28.45	28.27	28.6	28.45	28.83	29.95	30.31	30.04	30.19
4	28.06	28.65	28.01	28.57	28.11	28.48	28.2	28.55	28.39	28.78	30.08	30.28	29.99	30.26
5	28	28.63	28.18	28.67	28.23	28.6	28.11	28.65	28.38	28.72	30.09	30.37	30.02	30.34
6	27.94	28.72	27.94	28.53	28.22	28.69	28.17	28.61	28.42	28.79	29.99	30.36	30.04	30.21
7	28.08	28.64	28.31	28.67	28.04	28.73	28.1	28.67	28.32	28.68	29.86	30.16	29.85	30.25
8	28.17	28.77	27.96	28.65	28.11	28.67	28.33	28.72	28.25	28.67	28.75	29.11	29.82	30.08
9	28.3	28.82	28.22	28.68	28.12	28.86	28.07	28.86	28.42	28.71	28.99	29.29	29.62	30.02
10	28.31	28.79	28.42	28.91	28.43	28.91	28.38	28.89	28.5	28.9	29.15	29.39	29.64	30.02
11	28.39	28.86	28.47	28.98	28.53	28.94	28.55	29.04	28.47	28.9	29.18	29.57	29.67	29.96
12	28.42	28.98	28.79	29.11	28.68	29.04	28.84	29.1	28.76	29.27	29.3	29.55	29.59	29.88
13	28.68	29.05	28.97	29.21	28.9	29.17	28.87	29.28	28.98	29.3	29.27	29.5	29.71	29.92
14	28.9	29.3	28.95	29.49	28.98	29.35	29.06	29.27	28.98	29.35	29.31	29.6	29.59	29.88
15	29.11	29.55	29.13	29.49	29.16	29.4	29.23	29.45	29.13	29.49	29.29	29.68	29.55	29.82
16	29.08	29.61	29.26	29.57	29.21	29.55	29.28	29.51	29.24	29.53	29.42	29.68	29.58	29.82
17	29.22	29.81	29.41	29.7	29.32	29.8	29.3	29.59	29.27	29.57	29.49	29.75	29.61	29.82
18	29.11	29.89	29.46	29.72	29.39	29.76	29.31	29.7	29.24	29.59	29.46	29.78	29.61	29.78
19	29.24	29.94	29.49	29.84	29.44	29.71	29.42	29.67	29.34	29.65	29.59	29.8	29.55	29.81
20	29.28	29.97	29.45	29.82	29.44	29.7	29.37	29.64	29.37	29.66	29.4	29.87	29.58	29.82
21	29.44	29.91	29.51	29.84	29.35	29.66	29.36	29.6	29.35	29.62	29.43	29.73	29.37	29.73
22	29.52	29.87	29.35	29.76	29.36	29.56	29.23	29.66	29.37	29.63	29.32	29.72	29.31	29.73
23	29.41	29.9	29.22	29.79	29.37	29.66	29.23	29.65	29.39	29.64	29.4	29.68	29.5	29.72

Table B.4. (continued)

x (node)	22		23		24		25		26		27		28	
y (node)	**min (cm)**	**max (cm)**	**min (cm)**	**max (cm)**	**min (cm)**	**max (cm)**	**min (cm)**	**max (cm)**	**min (cm)**	**max (cm)**	**min (cm)**	**max (cm)**	**min (cm)**	**max (cm)**
1	29.29	29.66	29.3	29.63	29.43	29.68	29.39	29.6225	29.24	29.455	29.33	29.5275	29.25	29.43
2	29.33	29.73	29.39	29.7	29.49	29.73	29.455	29.6975	29.3	29.545	29.325	29.5725	29.26	29.51
3	29.46	29.73	29.48	29.71	29.52	29.73	29.49	29.7	29.37	29.58	29.39	29.6	29.35	29.56
4	29.52	29.73	29.41	29.76	29.49	29.73	29.4825	29.715	29.385	29.61	29.4175	29.635	29.38	29.59
5	29.49	29.81	29.41	29.73	29.45	29.63	29.4325	29.6225	29.385	29.585	29.3775	29.5875	29.38	29.6
6	29.49	29.77	29.53	29.81	29.43	29.65	29.42	29.6325	29.37	29.575	29.38	29.5775	29.41	29.6
7	29.55	29.79	29.44	29.74	29.42	29.72	29.4075	29.6825	29.375	29.625	29.3925	29.6175	29.43	29.63
8	29.44	29.68	29.42	29.71	29.44	29.69	29.4325	29.675	29.405	29.64	29.4075	29.635	29.43	29.65
9	29.26	29.51	29.38	29.63	29.38	29.64	29.3825	29.62	29.375	29.59	29.4175	29.61	29.46	29.63
10	29.32	29.61	29.34	29.68	29.48	29.65	29.4575	29.6125	29.435	29.575	29.4625	29.5875	29.49	29.6
11	29.28	29.54	29.4	29.67	29.37	29.58	29.36	29.565	29.35	29.55	29.4	29.595	29.45	29.64
12	29.2	29.57	29.35	29.62	29.3	29.62	29.305	29.595	29.33	29.59	29.405	29.635	29.47	29.67
13	29.21	29.49	29.42	29.68	29.3	29.54	29.3125	29.55	29.315	29.55	29.3575	29.59	29.39	29.62
14	29.26	29.53	29.38	29.61	29.41	29.62	29.4	29.6125	29.38	29.595	29.42	29.6375	29.45	29.67
15	29.21	29.43	29.37	29.61	29.35	29.58	29.345	29.5675	29.37	29.585	29.425	29.6325	29.49	29.69
16	29.17	29.48	29.25	29.57	29.36	29.58	29.345	29.5675	29.35	29.575	29.395	29.6225	29.46	29.69
17	29.17	29.4	29.35	29.61	29.32	29.54	29.3225	29.525	29.365	29.55	29.4475	29.615	29.54	29.69
18	29.2	29.42	29.34	29.61	29.27	29.52	29.2675	29.505	29.295	29.52	29.3725	29.585	29.43	29.63
19	29.21	29.48	29.31	29.55	29.37	29.61	29.3325	29.5575	29.355	29.565	29.4275	29.6225	29.5	29.68
20	29.16	29.5	29.36	29.53	29.39	29.68	29.3575	29.615	29.325	29.55	29.4225	29.615	29.49	29.65
21	29.08	29.45	29.33	29.63	29.36	29.6	29.3025	29.5325	29.245	29.465	29.3575	29.5675	29.43	29.63
22	28.99	29.39	29.28	29.58	29.31	29.59	29.21	29.4975	29.08	29.375	29.21	29.5125	29.22	29.53
23	29.06	29.41	29.35	29.6	29.31	29.58	29.2225	29.5075	29.085	29.385	29.2275	29.5425	29.27	29.6

Table B.5. Experimental data, Case C1

x (node)	1		2		3		4		5		6		7	
y (node)	min (cm)	max (cm)	min (cm)	max (cm)	min (cm)	max (cm)	min (cm)	max (cm)	min (cm)	max (cm)	min (cm)	max (cm)	min (cm)	max (cm)
1	19.62	21.81	19.03	20.6	14.89	18.02	14.6	16.5	15.17	16.94	15.6	16.85	15.59	17.3
2	18.16	20.41	18.22	19.55	16.04	17.37	14.69	16.37	15.4	16.51	15.49	16.58	15.44	17.01
3	17.41	19.6	17.19	18.73	15.69	17.17	14.72	16.29	15.32	16.32	15.61	16.6	15.52	16.81
4	17.01	18.64	16.62	18.17	15.39	16.92	14.6	16.05	15.1	16.22	15.28	16.45	15.58	16.84
5	15.17	16.91	15.2	17.12	14.79	16.6	13.96	15.98	15	16.21	15.36	16.34	15.99	17.1
6	14.21	15.44	14.79	16.33	14.75	16.32	14.84	16.12	14.94	16.15	15.56	16.5	15.88	17.01
7	14.28	15.13	15.44	16.53	14.02	16.53	14.93	16.39	14.92	16.08	15.37	16.43	15.58	16.68
8	14.45	15.4	16.4	17.57	14.15	16.39	14.5	16.18	15.27	16.2	15.42	16.45	15.66	16.75
9	14.52	15.26	17.42	18.28	15.71	17.48	14.42	16.48	15.25	16.42	15.39	16.41	15.41	16.81
10	14.23	15.37	18.25	19.38	17.99	19.65	15.51	17.89	15.11	16.91	14.59	15.98	16.45	17.61
11	13.89	15.34	19.02	20.03	19.48	20.77	17.32	20.01	16.02	17.83	13.29	15.36	16.8	17.86
12	13.68	14.9	19.69	20.96	20.47	21.58	19.89	21.39	16.26	18.41	13.78	15.09	16.32	17.75
13	13.34	15.27	20.45	21.98	21.32	22.41	21.4	22.94	17.65	20.46	13.67	15.2	16.12	17.53
14	11.36	13.44	21.95	23.13	22.29	23.53	22.42	23.71	20.28	21.85	14.79	16.18	16.09	17.5
15	2.36	2.87	22.98	24.19	23.01	24.3	22.91	23.97	21.92	23.83	15.67	16.74	16.62	18.14
16	0.55	1.35	24.15	25.44	23.5	25.03	23.21	24.76	22.82	24.63	17.11	20.62	17.49	18.4
17	0.64	1.37	24.9	26.53	24.13	25.54	23.57	24.87	23.44	24.71	19.6	22.26	18.22	19.48
18	0.68	1.36	25.17	27.12	24.33	25.82	23.74	25.17	23.32	24.58	21.09	23.91	18.99	20.98
19	0.7	1.3	25.66	27.28	24.43	26.07	23.95	25.2	23.84	24.75	23.2	24.48	20.8	22.09
20	0.69	1.38	25.35	27.15	24.47	26.2	23.98	25.51	23.93	24.78	23.35	25.05	22.67	24.69
21	0.67	1.37	25.33	27.25	24.72	26.19	24.29	25.71	23.85	24.95	23.75	25.02	23.4	24.85
22	0.6	1.3	25.29	27.2	24.89	26.09	24.22	25.75	23.81	24.97	23.78	25.08	23.45	25.03
23	0.57	1.26	25.09	27.38	24.81	26.1	24.52	25.92	24.12	25.23	23.95	25.32	23.69	25.41

Table B.5. (continued)

x (node)	8		9		10		11		12		13		14	
y (node)	min (cm)	max (cm)	min (cm)	max (cm)	min (cm)	max (cm)	min (cm)	max (cm)	min (cm)	max (cm)	min (cm)	max (cm)	min (cm)	max (cm)
1	26.9	28.16	26.51	27.32	26.56	27.43	26.34	27.22	26.14	26.93	25.9	26.93	25.3	26.49
2	26.86	28.03	26.5	27.39	26.72	27.51	26.31	27.1	26.13	26.97	25.88	27.1	25.4	26.41
3	27	28.17	26.53	27.36	26.74	27.29	26.22	27.07	26.14	26.98	26.19	27.1	25.41	26.58
4	27.12	28.24	26.31	27.34	26.51	27.27	26.36	27.14	26.07	26.86	25.83	26.9	24.97	26.59
5	27.06	28.42	25.87	27.18	26.01	27.21	25.97	26.9	25.94	26.83	25.57	26.68	24.92	26.12
6	26.69	28.02	25.03	27.04	25.87	27.03	25.89	26.91	25.84	26.68	24.93	26.22	24.55	25.87
7	26.02	27.21	24.84	26.55	25.62	26.66	26.02	26.9	25.5	26.3	23.72	24.95	24.57	25.17
8	25.28	26.23	24.63	26.24	25.13	26.22	26	26.88	24.46	26.19	22.89	23.79	24.36	24.8
9	23.55	25.08	24.14	25.9	24.01	26.04	25.35	27.05	23.39	25.41	22.49	23	24.39	24.86
10	21.93	23.49	23.81	25.48	23.33	25.06	24.62	26.26	21.9	24.71	21.91	22.51	24.44	24.89
11	20.41	22.8	23.2	24.99	22.54	23.8	23.54	25.1	21.66	23.41	21.36	22.17	24.23	25.11
12	20.07	22.13	22.5	24.22	21.57	22.91	22.22	23.6	21.14	22.35	20.77	21.53	24.2	25.09
13	20.22	21.93	21.67	23.43	20.9	22.02	21.32	22.46	21.26	22.17	20.19	21.27	23.58	25.05
14	20.09	21.69	21.46	22.95	20.27	21.36	20.78	21.57	21.08	22	20.4	21.67	24.17	25.36
15	19.83	21.5	20.56	22.24	20.57	21.55	20.78	21.55	21.18	21.9	21.31	21.91	25.49	26.29
16	19.7	21.11	20.44	21.86	20.34	21.63	20.43	21.37	20.95	21.58	21.37	21.89	27.44	27.86
17	19.77	21.39	20.21	21.54	20.25	21.23	20.23	21.42	20.99	21.71	21.5	22.12	27.84	28.55
18	19.76	21.57	20.33	21.76	20.39	21.45	20.37	21.4	21.12	21.93	21.33	22.23	28.16	28.92
19	20.33	22.35	20.24	21.72	20.43	21.24	20.43	21.36	21.16	21.97	21.31	22.2	28.36	28.94
20	20.76	22.53	20.48	22.21	20.33	21.32	20.6	21.49	21.11	22	21.52	22.35	28.41	28.93
21	21.9	23.47	20.62	22.21	20.52	21.51	20.81	21.72	21.07	22.08	21.45	22.34	28.25	28.82
22	22.43	23.84	20.39	22.32	20.27	21.59	20.8	21.78	21.04	22.2	21.51	22.36	28.11	28.8
23	22.38	24.29	20.66	22.6	20.33	21.68	20.89	22.03	21.08	22.21	21.38	22.4	28.19	28.82

Table B.5. (continued)

x (node)	15		16		17		18		19		20		21	
y (node)	**min (cm)**	**max (cm)**	**min (cm)**	**max (cm)**	**min (cm)**	**max (cm)**	**min (cm)**	**max (cm)**	**min (cm)**	**max (cm)**	**min (cm)**	**max (cm)**	**min (cm)**	**max (cm)**
1	24.64	25.76	24.59	25.3	24.4	25.69	24.86	25.62	25.12	25.9	28.57	29.13	28.46	28.8
2	24.71	25.73	24.77	25.46	24.65	25.55	24.89	25.55	25.21	25.81	28.66	29.15	28.43	28.86
3	24.93	25.74	24.77	25.45	24.79	25.44	25.03	25.53	25.3	25.93	28.79	29.27	28.53	28.89
4	25.01	25.77	24.73	25.54	25.12	25.56	24.9	25.52	25.23	25.88	28.72	29.23	28.64	28.94
5	24.65	25.78	24.68	25.6	24.97	25.61	25.04	25.52	25.27	25.76	28.78	29.28	28.6	28.84
6	24.83	25.71	24.79	25.52	25.11	25.56	24.95	25.46	25.25	25.72	28.57	29.08	28.54	28.88
7	24.96	25.72	24.82	25.61	25.07	25.63	25.08	25.59	25.3	25.78	28.27	28.79	28.43	28.78
8	25.21	26	24.76	25.57	25.04	25.74	25.17	25.69	25.28	25.81	27.18	27.82	28.33	28.61
9	25.51	26.06	25.33	25.82	25.06	25.8	25.14	25.63	25.3	25.87	27.12	27.56	28.11	28.55
10	25.9	26.32	25.64	26.05	25.55	26.1	25.48	25.92	25.57	26.1	27.07	27.54	28.06	28.35
11	26.3	26.71	25.97	26.35	25.81	26.17	25.89	26.28	25.49	26.03	27.18	27.52	28	28.27
12	26.42	26.89	26.09	26.56	25.98	26.29	26.41	26.79	25.78	26.21	27.23	27.55	27.87	28.11
13	26.68	27.18	26.41	26.77	26.37	26.71	26.55	27.11	26.32	26.65	27.29	27.57	27.8	28.1
14	26.81	27.3	26.57	26.97	26.87	27.24	26.68	27.05	26.72	27.04	27.3	27.56	27.85	28.08
15	27.1	27.57	27.07	27.39	27.09	27.4	26.8	27.15	26.81	27.08	27.3	27.6	27.87	28.09
16	27.57	27.89	27.27	27.66	27.27	27.57	26.89	27.21	26.98	27.3	27.28	27.68	27.85	28.03
17	27.71	28.21	27.56	27.89	27.33	27.7	27.01	27.45	27.16	27.43	27.32	27.69	27.77	27.94
18	27.86	28.27	27.7	28.04	27.5	27.79	27.12	27.52	27.24	27.53	27.35	27.75	27.8	28.04
19	27.7	28.34	27.87	28.18	27.58	27.97	27.24	27.57	27.35	27.66	27.4	27.76	27.79	28.08
20	27.88	28.37	27.97	28.29	27.74	28.06	27.27	27.59	27.26	27.63	27.45	27.77	27.8	28.1
21	27.93	28.36	27.95	28.25	27.69	28.05	27.23	27.61	27.25	27.66	27.53	27.8	27.68	28.01
22	27.79	28.33	27.96	28.14	27.68	28.01	27.18	27.59	27.28	27.64	27.52	27.85	27.6	27.91
23	27.78	28.43	27.9	28.13	27.71	28.02	27.1	27.57	27.24	27.7	27.39	27.87	27.65	27.95

Table B.5. (continued)

x (node)	22		23		24		25		26		27		28	
y (node)	**min (cm)**	**max (cm)**	**min (cm)**	**max (cm)**	**min (cm)**	**max (cm)**	**min (cm)**	**max (cm)**	**min (cm)**	**max (cm)**	**min (cm)**	**max (cm)**	**min (cm)**	**max (cm)**
1	28.39	28.66	28.26	28.52	28.26	28.55	28.17	28.45	27.99	28.21	28.13	28.4	28.15	28.39
2	28.39	28.71	28.31	28.53	28.26	28.51	28.24	28.43	28.05	28.28	28.2	28.45	28.17	28.4
3	28.46	28.74	28.4	28.56	28.32	28.54	28.25	28.46	28.11	28.3	28.22	28.48	28.25	28.5
4	28.46	28.76	28.4	28.59	28.36	28.56	28.26	28.5	28.13	28.34	28.22	28.46	28.26	28.49
5	28.45	28.75	28.42	28.58	28.36	28.52	28.27	28.46	28.2	28.36	28.25	28.42	28.31	28.58
6	28.41	28.67	28.42	28.61	28.36	28.55	28.29	28.51	28.18	28.36	28.23	28.46	28.38	28.59
7	28.31	28.59	28.41	28.58	28.39	28.54	28.28	28.51	28.16	28.38	28.24	28.47	28.35	28.59
8	28.25	28.57	28.26	28.58	28.27	28.51	28.26	28.53	28.22	28.41	28.24	28.47	28.35	28.55
9	28.18	28.45	28.22	28.54	28.23	28.51	28.24	28.48	28.2	28.38	28.27	28.47	28.38	28.57
10	28.12	28.38	28.21	28.5	28.23	28.48	28.25	28.49	28.21	28.44	28.28	28.49	28.39	28.57
11	28.07	28.28	28.16	28.39	28.24	28.42	28.22	28.43	28.17	28.42	28.28	28.49	28.39	28.59
12	28.06	28.27	28.15	28.35	28.16	28.42	28.25	28.44	28.24	28.43	28.33	28.49	28.37	28.57
13	28.09	28.29	28.13	28.34	28.19	28.37	28.21	28.43	28.24	28.43	28.3	28.48	28.3	28.53
14	28.04	28.26	28.09	28.32	28.21	28.39	28.11	28.41	28.24	28.41	28.32	28.51	28.34	28.56
15	27.99	28.26	28.06	28.3	28.15	28.38	28.14	28.41	28.28	28.46	28.33	28.52	28.38	28.58
16	27.94	28.18	28.01	28.29	28.17	28.41	28.19	28.41	28.23	28.48	28.3	28.55	28.41	28.59
17	27.88	28.11	28.03	28.24	28.12	28.39	28.17	28.41	28.2	28.46	28.29	28.54	28.46	28.63
18	27.89	28.1	28.04	28.3	28.11	28.39	28.2	28.41	28.2	28.46	28.28	28.53	28.4	28.58
19	27.87	28.09	28.02	28.24	28.13	28.36	28.15	28.41	28.19	28.5	28.29	28.52	28.4	28.62
20	27.84	28.09	28.02	28.26	28.12	28.37	28.15	28.43	28.12	28.4	28.28	28.47	28.3	28.59
21	27.8	28.05	28	28.23	28.09	28.39	28.11	28.41	28.05	28.35	28.22	28.44	28.23	28.51
22	27.69	28.03	27.94	28.21	28.04	28.36	28.05	28.4	27.94	28.29	28.14	28.38	28.13	28.44
23	27.69	28.01	27.86	28.16	28.03	28.33	28.09	28.5	27.91	28.27	28.11	28.45	28.13	28.46

Table B.6. Experimental data, Case C2

x (node)	1		2		3		4		5		6		7	
y (node)	min (cm)	max (cm)	min (cm)	max (cm)	min (cm)	max (cm)	min (cm)	max (cm)	min (cm)	max (cm)	min (cm)	max (cm)	min (cm)	max (cm)
1	28.16	30.5	27.16	29.46	25.78	28.23	25.76	27.59	26.03	27.92	26.29	27.87	26.73	28.42
2	28.44	30.41	26.32	28.57	25.62	27.73	25.62	27.32	25.97	27.62	26.34	27.66	26.48	28.02
3	27.7	29.81	26.17	28.64	25.89	27.34	25.66	27.06	25.89	27.37	26.34	27.66	26.61	28
4	27.04	29.53	26.27	28.45	25.66	27.29	25.67	26.96	25.93	27.22	26.37	27.51	26.49	27.88
5	25.8	28.73	25.59	27.91	25.25	27.5	25.84	27.16	25.78	27.22	26.27	27.44	26.78	27.93
6	25.03	27.74	25.35	27.34	25.21	27.55	25.54	27.07	25.53	27.11	26.34	27.42	26.63	27.78
7	24.11	27.68	24.43	26.45	25.49	27.42	25.61	27.2	25.29	27.25	26.38	27.53	26.6	27.67
8	23.71	26.52	25.11	26.93	25.63	27.68	25.4	27.36	25.43	27.12	26.29	27.57	26.19	27.75
9	23.72	25.98	25.52	27.14	25.71	27.69	25.5	27.41	25.74	27.21	26.26	27.57	26.18	27.71
10	23.21	25.6	25.78	28.04	26.09	28.06	25.77	27.55	25.69	27.38	26.49	27.6	25.71	27.86
11	22.97	25.03	26.29	28.19	27.14	29	26.01	27.8	26.16	27.94	26.9	27.99	25.51	27.6
12	23.43	25.28	26.35	28.6	28.16	29.67	26.92	28.63	26.95	28.64	26.88	28.28	25.3	27.32
13	23.4	25.47	27.08	29.28	28.71	30.42	27.96	29.66	28.08	29.67	27.28	28.47	25.69	27.24
14	23.85	25.87	28.15	29.6	29.29	30.91	28.68	30.36	28.83	30.37	28.3	30.04	26.09	27.5
15	24.47	26.06	29.25	30.84	30.1	31.39	29.05	30.97	29.41	30.99	29.73	31.47	27.03	28.32
16	24.84	25.9	30.5	32.03	30.16	31.73	29.6	31.32	29.85	31.47	30.07	31.99	27.39	29.8
17	25.01	26.12	31.18	32.84	30.64	32.13	30.27	31.74	29.83	31.54	30.79	32.31	28.13	29.97
18	25.08	26.05	31.63	33.28	30.94	32.51	30.78	32.28	29.94	31.77	30.43	32.36	29.04	30.9
19	25.23	26.07	31.78	33.37	31.19	32.9	30.94	32.53	30.28	31.88	30.48	32.36	30.01	31.65
20	25.18	26.23	31.68	33.4	31.33	33	31.02	32.61	30.46	32.12	30.47	32.25	29.89	31.75
21	25.12	26.2	31.8	33.46	31.42	33.07	31.29	32.8	30.77	32.42	30.63	32.04	30.1	31.68
22	25.1	26.17	31.89	33.6	31.28	33.04	31.23	32.76	30.94	32.43	30.68	32.07	30.1	31.65
23	24.91	26.34	31.74	33.55	31.32	33.04	31.29	32.84	30.98	32.55	30.76	32.39	30.08	32.08

Table B.6. (continued)

x (node)	8		9		10		11		12		13		14	
y (node)	**min (cm)**	**max (cm)**	**min (cm)**	**max (cm)**	**min (cm)**	**max (cm)**	**min (cm)**	**max (cm)**	**min (cm)**	**max (cm)**	**min (cm)**	**max (cm)**	**min (cm)**	**max (cm)**
1	32.84	33.92	32.64	33.7	32.87	33.6	32.48	33.46	32.41	33.42	32.37	33.26	31.91	32.82
2	32.97	33.89	32.85	33.67	32.59	33.61	32.69	33.55	32.48	33.36	32.33	33.15	31.89	32.86
3	33.03	34.02	32.83	33.71	32.67	33.59	32.69	33.49	32.44	33.29	32.32	33.22	31.97	32.92
4	33.09	34.1	32.63	33.67	32.7	33.58	32.6	33.34	32.54	33.35	32.26	33.3	31.99	32.97
5	32.89	33.98	32.44	33.35	32.72	33.6	32.47	33.39	32.4	33.3	32.33	33.26	31.79	32.86
6	32.73	33.81	32	33.2	32.53	33.49	32.09	33.27	32.35	33.18	32.09	33.22	31.66	32.72
7	32.1	33.48	31.33	32.8	32.36	33.27	31.76	32.91	32.48	33.29	31.79	32.93	31.67	32.52
8	30.98	32.45	31.13	32.77	32.13	33.06	31.15	32.36	32.49	33.56	31.5	32.45	31.5	32.28
9	29.68	32.08	31.03	32.55	31.96	32.94	30.57	31.64	32.31	33.65	30.81	31.82	31.35	32.11
10	28.6	30.46	30.95	31.97	31.51	32.68	30.46	31.31	31.78	32.9	30.37	31.22	31.39	31.99
11	27.74	29.81	30.77	31.79	30.62	32.28	30.21	31.13	30.9	31.86	30.04	30.9	31.26	31.9
12	28.1	29.37	30.67	31.51	29.68	31.72	29.83	30.74	30.13	31.04	29.41	30.55	31.23	31.81
13	27.88	29.51	30.08	30.97	29.16	30.81	29.62	30.43	29.76	30.47	29.3	30.32	30.61	31.76
14	27.95	29.26	29.52	30.35	29.59	30.67	29.59	30.42	29.74	30.4	29.38	30.47	30.73	31.5
15	28.06	29.43	28.85	29.92	29.3	30.04	29.56	30.31	29.61	30.43	29.57	30.45	31.58	32.25
16	27.74	29.67	28.56	29.82	29.34	30.33	29.48	30.17	29.66	30.44	29.56	30.34	32.91	33.54
17	28.29	30.27	28.71	30.23	29.24	30.12	29.42	30.11	29.67	30.35	29.69	30.42	33.52	34.1
18	28.59	30.75	29.03	30.3	29.07	30.05	29.38	30.09	29.73	30.32	29.67	30.48	33.66	34.16
19	28.95	30.83	28.93	30.24	29.14	30.1	29.39	30.1	29.68	30.42	29.59	30.48	33.89	34.35
20	29.14	30.9	28.8	30.02	29.29	30.19	29.31	30.28	29.77	30.48	29.73	30.56	33.88	34.39
21	29.26	30.98	28.84	30.07	29.29	30.24	29.37	30.24	29.53	30.61	29.71	30.59	33.82	34.33
22	29.41	31.2	29.17	30.47	29.24	30.26	29.35	30.37	29.5	30.58	29.51	30.63	33.72	34.32
23	29.33	31.46	29.08	30.5	29.1	30.24	29.31	30.33	29.6	30.58	29.48	30.53	33.71	34.42

Table B.6. (continued)

x (node)	15		16		17		18		19		20		21	
y (node)	**min (cm)**	**max (cm)**	**min (cm)**	**max (cm)**	**min (cm)**	**max (cm)**	**min (cm)**	**max (cm)**	**min (cm)**	**max (cm)**	**min (cm)**	**max (cm)**	**min (cm)**	**max (cm)**
1	31.35	32.34	31.16	32.09	31.22	32.01	31.79	32.25	31.82	32.53	34	34.56	33.95	34.47
2	31.54	32.32	31.32	32.13	31.37	32.15	31.78	32.26	31.9	32.66	34.08	34.66	34	34.55
3	31.4	32.25	31.43	32.1	31.58	32.2	31.87	32.43	31.92	32.61	34.11	34.61	34.09	34.53
4	31.57	32.64	31.43	32.2	31.69	32.2	31.83	32.4	31.94	32.57	34.14	34.63	34.14	34.59
5	31.59	32.62	31.47	32.27	31.78	32.24	31.9	32.46	32.02	32.47	34.22	34.76	34.11	34.61
6	31.63	32.58	31.54	32.31	31.65	32.33	31.78	32.46	32.02	32.45	34.08	34.62	34.15	34.63
7	31.68	32.54	31.7	32.43	31.56	32.46	31.85	32.55	31.83	32.4	33.85	34.44	34.04	34.47
8	31.78	32.57	31.75	32.52	31.71	32.41	31.87	32.54	31.9	32.57	32.77	33.75	33.94	34.31
9	31.66	32.65	31.89	32.5	31.73	32.54	31.98	32.61	31.99	32.59	32.88	33.6	33.89	34.21
10	31.93	32.75	32.01	32.62	31.86	32.65	32.09	32.72	32.21	32.79	33.09	33.68	33.72	34.13
11	32.28	32.84	32.24	32.9	32.32	33.03	32.19	32.7	32.48	33	33.14	33.6	33.7	34.05
12	32.45	33.08	32.49	33.05	32.48	33.1	32.42	32.96	32.66	33.04	33.16	33.65	33.63	34.03
13	32.59	33.09	32.83	33.27	32.67	33.22	32.77	33.21	32.79	33.28	33.28	33.7	33.62	34.03
14	32.82	33.3	33.01	33.49	32.79	33.31	32.81	33.32	32.83	33.29	33.37	33.78	33.6	33.98
15	33.07	33.51	33.08	33.6	32.97	33.49	32.98	33.42	32.94	33.41	33.36	33.75	33.6	33.95
16	33.31	33.82	33.29	33.75	33.09	33.61	33.08	33.62	33.06	33.54	33.41	33.88	33.56	34.01
17	33.33	33.93	33.46	33.9	33.27	33.75	33.2	33.68	33.15	33.57	33.42	33.89	33.5	33.96
18	33.58	34.16	33.5	34.01	33.3	33.78	33.21	33.7	33.23	33.59	33.46	33.83	33.56	33.93
19	33.7	34.19	33.58	34.15	33.36	33.92	33.29	33.78	33.26	33.71	33.46	33.87	33.58	33.98
20	33.52	34.22	33.59	34.09	33.38	33.91	33.28	33.78	33.38	33.85	33.42	33.92	33.62	33.94
21	33.7	34.19	33.62	34.1	33.36	33.92	33.23	33.75	33.32	33.82	33.4	33.89	33.59	33.88
22	33.59	34.18	33.51	34.04	33.37	33.88	33.18	33.75	33.23	33.74	33.35	33.82	33.47	33.87
23	33.55	34.2	33.51	33.96	33.45	33.85	33.12	33.73	33.29	33.86	33.35	33.87	33.42	33.85

Table B.6. (continued)

x (node)	22		23		24		25		26		27		28	
y (node)	**min (cm)**	**max (cm)**	**min (cm)**	**max (cm)**	**min (cm)**	**max (cm)**	**min (cm)**	**max (cm)**	**min (cm)**	**max (cm)**	**min (cm)**	**max (cm)**	**min (cm)**	**max (cm)**
1	33.92	34.26	33.8	34.3	33.95	34.34	33.76	34.23	33.69	34.11	33.81	34.26	33.72	34.21
2	33.94	34.3	33.93	34.27	33.83	34.26	33.78	34.26	33.7	34.13	33.82	34.25	33.8	34.18
3	34.04	34.39	34.01	34.38	33.94	34.33	33.84	34.26	33.75	34.19	33.86	34.26	33.93	34.19
4	33.98	34.41	33.96	34.35	34.04	34.43	33.87	34.26	33.84	34.25	33.9	34.27	33.98	34.29
5	33.99	34.43	33.99	34.34	33.97	34.35	33.82	34.28	33.85	34.29	33.92	34.29	33.98	34.33
6	33.94	34.35	34.02	34.34	33.9	34.3	33.86	34.24	33.85	34.26	33.99	34.35	34.04	34.37
7	33.87	34.38	34.03	34.33	33.92	34.29	33.86	34.22	33.88	34.24	33.96	34.3	34.05	34.4
8	33.82	34.31	33.93	34.3	33.92	34.3	33.88	34.26	33.88	34.25	34.01	34.31	34.03	34.39
9	33.78	34.3	33.89	34.29	33.89	34.28	33.85	34.22	33.84	34.24	33.98	34.31	34.03	34.4
10	33.75	34.17	33.88	34.22	33.9	34.31	33.83	34.21	33.84	34.25	33.93	34.32	34.01	34.41
11	33.72	34.11	33.87	34.21	33.82	34.23	33.85	34.24	33.85	34.23	33.92	34.35	34.03	34.4
12	33.69	34.06	33.83	34.19	33.9	34.28	33.84	34.23	33.84	34.24	33.91	34.32	33.96	34.36
13	33.72	34.03	33.79	34.2	33.83	34.32	33.82	34.2	33.86	34.24	33.92	34.3	33.96	34.34
14	33.68	33.95	33.8	34.17	33.81	34.27	33.85	34.19	33.86	34.27	33.97	34.34	33.99	34.33
15	33.64	33.97	33.72	34.15	33.79	34.22	33.85	34.2	33.86	34.23	33.98	34.37	34.02	34.39
16	33.72	34.04	33.73	34.12	33.78	34.19	33.88	34.21	33.89	34.26	33.96	34.31	34.01	34.37
17	33.61	33.97	33.75	34.11	33.81	34.2	33.88	34.17	33.91	34.26	34	34.37	34.04	34.41
18	33.58	33.96	33.73	34.13	33.83	34.18	33.86	34.23	33.86	34.25	33.93	34.38	33.97	34.33
19	33.54	33.9	33.69	34.13	33.84	34.28	33.81	34.26	33.87	34.26	33.95	34.32	34	34.39
20	33.51	33.91	33.7	34.11	33.87	34.29	33.88	34.29	33.85	34.22	33.93	34.3	34.01	34.38
21	33.53	33.85	33.68	34.15	33.85	34.27	33.79	34.21	33.8	34.13	33.83	34.31	33.97	34.32
22	33.42	33.8	33.61	34.11	33.78	34.21	33.74	34.2	33.66	34.06	33.79	34.27	33.9	34.22
23	33.33	33.77	33.65	34.12	33.85	34.33	33.74	34.21	33.59	34.09	33.78	34.24	33.87	34.25